ANL-IFR-85

Integral Fast Reactor

Studies of Prefailure Fuel Extrusion in Metal Fuel Pins with Extrus

by H. H. Hummel and P. A. Pizzica

Argonne National Laboratory, Argonne, Illinois 60439
operated by The University of Chicago
for the United States Department of Energy under Contract W-31-109-Eng-38

February 1988

ANL-IFR-85

STUDIES OF PREFAILURE FUEL EXTRUSION IN METAL FUEL PINS WITH EXTRUS

by

H. H. Hummel and P. A. Pizzica

Applied Physics Division
Argonne National Laboratory
9700 South Cass Avenue
Argonne, Illinois 60439

IFR TECHNICAL MEMORANDUM NO. 85

Results reported in the IFR-TM series of memoranda frequently are preliminary and subject to revision. Consequently they should not be quoted or referenced.

DISCLAIMER

TABLE OF CONTENTS

TABLE OF CONTENTS (Contd.)

LIST OF FIGURES

LIST OF TABLES

LIST OF TABLES (Contd.)

Blank Page

STUDIES OF PREFAILURE FUEL EXTRUSION IN METAL FUEL PINS WITH EXTRUS

by

H. H. Hummel and P. A. Pizzica

ABSTRACT

1. A SAS4A module, EXTRUS, available in a special version of SAS4A, has been prepared to deal with prefailure metal fuel extrusion in a slow TOP accident, as an alternative to the PINACLE module. "Extrusion" in the present case refers to the movement of molten fuel under fission gas pressure rather than to solid fuel extrusion. In EXTRUS pressure equilibrium between a molten fuel pin cavity and the fission gas plenum is assumed to be maintained continuously. The potential for fuel extrusion is provided by the higher pressure in closed porosity as compared to that in open porosity, and also by the larger temperature rise in the fuel from the steady state compared to that for the plenum. Calculation of closed porosity volume in reference cases has followed suggestions by R. Sevy. Clad attack by eutectic penetration has been modeled as suggested by T. Bauer, with a high rate of penetration occurring when the fuel-clad interface temperature reaches 1353 K.

2. Results of calculation of prefailure fuel extrusion for the TREAT M4 experiment as calculated in SAS4A by PINACLE and by EXTRUS have been compared. The purpose of this comparison is to determine whether hydrodynamic effects, taken into account by PINACLE, influence significantly the calculated extrusion for metal fuel. Comparison with experiment indicates that the equilibrium model gives adequate results for relatively slow TOP transients as represented by the M-series experiments. Threshold effects associated with the onset of melting at the top of the fuel do not seem to be important in delaying the initiation of extrusion in these experiments. However, there could be a problem in extrapolating these results to full length prototypical pins.

It would be expected that with PINACLE parameters set so that the equilibrium condition is approximately maintained, similar results would be obtained for PINACLE and EXTRUS. However, it was found that, because of differences in detailed modeling assumptions and calculation methods between PINACLE and EXTRUS, it was difficult to compare the two modules on a completely consistent basis. A major problem is that, because of differences in methods of calculating heat transfer between the

molten fuel cavity and the solid pin fuel, the cavity fuel mass for a given total energy input is usually 20-30% greater for EXTRUS than for PINACLE. Extrusion results were found to be sensitive to this and to other inconsistencies between the two calculations. Fuel thermal conductivity is an important parameter because of its effect on fuel melting. It was found that for the same assumed fuel thermal conductivity, extrusion calculated by EXTRUS for M4 Pin 3 at a given time was considerably larger than that obtained from PINACLE, mainly because of the difference in calculated cavity fuel mass. For M4 Pin 2, however, the various inconsistencies approximately counter-balanced each other so that extrusion results for the two codes agreed fairly well. A fuel thermal conductivity 55 to 60% of that for unirradiated U-5% Fs appears to give reasonable results for extrusion. The assumption of 5 μmols/gm fuel for retained fission gas gives reasonable results, as does assumption of 0.3 for the SAS4A parameter FNMELT. Calculation of M2 Pins 1 and 3 also indicated that top fuel melting threshold effects are not large. EXTRUS results were in reasonable agreement with experiment for Pin 1, but there is uncertainty in the analysis. Because of the preliminary current state of utilization of PINACLE in SAS4A, problems were encountered in application of the code to the low burnup, low porosity Pin 1. For Pin 3 the amount of extrusion calculated by both codes was too small.

3. The questions of the importance for metal fuel of inpin axial fuel distribution on fuel motion reactivity effects and of dynamic effects on prefailure molten fuel extrusion have been investigated using the PINACLE and EXTRUS modules of SAS4A. A full length prototypical pin was assumed, with only a single radial zone. Calculations were carried out for a single subassembly, with power histories of 10¢/sec and 50¢/sec for PINACLE. Only the 50¢/sec case was considered for EXTRUS. Results for the different cases were compared on the basis of a given molten pin cavity fuel mass. It was concluded that the assumption of uniform cavity fuel smear density made in EXTRUS gives results of adequate accuracy. The question of whether or not there are dynamic effects on fuel extrusion, particularly at the 50¢/sec ramp rate, is still somewhat open, but it appears that these effects if present could not exceed about 15% in mass of extruded fuel.

4. Calculations with the EXTRUS module have been performed for the 1.9% burnup pin in the F2 M5 TREAT experiment to try to understand the low molten fuel extrusion of only 1-2% observed. Kalimullah's SSCOMP SAS4A module has been applied to approximate the three-zone structure found in irradiated ternary alloys. This approximation was not too close because the temperature criteria assumed for zone radius location do not reproduce the observed zone configurations very successfully. However, it was found that the amount of fuel extrusion was not very sensitive to zone configuration, so that zone formation does not seem to be a possible explanation for low extrusion. The amount of fuel extrusion is sensitive to the amount of fuel melting and to the

amount of retained fission gas. It is likely that the reference assumption of 5 μmols/gm of retained gas is too high for the prototypical fuel. However, it was found that while 10% extrusion was calculated for a reference case, an extrusion of 2% was still obtained even with zero retained fission gas, because of the heating of open porosity released gas assumed in EXTRUS to be trapped in the fuel during the transient.

Another approach to reducing the calculated fuel extrusion besides reducing the assumed retained gas is to alter the modeling by abandoning the assumption that open porosity gas remains trapped in the fuel during the transient. Taking this course, which represents a departure from usual fuel modeling assumptions, it is possible to calculate fuel extrusions as low as those measured in M5 while still retaining some closed porosity gas. Another possibility for reducing the trapped open porosity gas while retaining the original modeling is to reduce the open porosity. However, the required reduction to remove the discrepancy between calculated and measured fuel extrusion seems extreme. Because less fuel melting at peak power is calculated to occur in M5 F2 than in previous M-series experiments, it is possible that extrusion is being inhibited by flow blockage not accounted for in the EXTRUS modeling.

5. The M6 experiment showed extrusion of 3-5%, considerably larger than that in M5. Calculations of fuel extrusion in M6 using EXTRUS showed best agreement with experiment assuming zero retained gas, with the pressure for extrusion coming from expansion during the transient of open porosity gas, assumed trapped in the fuel. More extrusion is calculated for M6 than for M5 because of the higher peak power. However, use of the measured retained gas gave far too much extrusion, particularly for Pin 1, which had 1.9% maximum burnup. A sharp radial variation in retained fission gas is a possible explanation for this discrepancy. Another factor that would reduce extrusion is retention of part of the gas in large closed pores. Parallel calculations were carried out with the actual TREAT power history, with no zone formation, and with a power history altered to have a prototypical steady-state power, with zone formation calculated with the SSCOMP module of SAS4A. After adjustments to the zoned calculations to eliminate inconsistencies with the non-zoned cases, little difference in calculated extrusions was found between the two. All cases in which SSCOMP was used had to be corrected for an error in transient fuel porosity caused by the current inability to use DEFORM with SSCOMP in SAS4A. Slightly larger extrusions were found for M6 with a TREAT power coupling factor (PCF) of 5.2 than with 4.9. Failure conditions were found to be attained for Pin 2, with maximum burnup 5.3%, with a PCF of 5.2 but not with 4.9. Failure was not approached for Pin 1, with much lower pressure, in agreement with experiment.

An alternate model to the pin cavity model in EXTRUS, used by T. Bauer, assumes that extrusion is caused by open porosity gas trapped in the total fuel volume. For M6 this model was found to give slightly less extrusion than EXTRUS cases with

zero retained gas, still agreeing well with experiment. The larger gas volume in the Bauer model, which increases extrusion, is offset by a lower average gas temperature. The model variation applied in M5 analysis in which open porosity gas was assumed not trapped in the fuel during the transient was not helpful in explaining the results for M6 Pin 1.

6. Fuel clad failure conditions and prefailure fuel extrusion for prototypical SAFR metal fuel pins have been investigated for a programmed power history typical of a 10¢/sec transient overpower accident. The SSCOMP module of SAS4A has been used for zone formation calculations, and EXTRUS has been used for calculation of fuel extrusion. A four-batch fuel management scheme has been assumed, with a peak discharge burnup of 14.8%. Peak burnups at BOEC for the first three batches have been assumed to be 0.0%, 3.7%, and 7.4%, with corresponding peak linear powers 14.1, 13.1, and 12.1 kw/ft respectively. Coolant flow rate has been adjusted to give a peak subassembly outlet temperature for fresh fuel of 813 K (1003 F), with the corresponding peak clad temperature calculated to be 845 K (1061 F). Calculations have not been carried out for higher burnups, for which the linear power is lower, because clad failure would occur sooner in lower burnup fuel, and there would be too little fuel melting for any fuel extrusion to occur in the higher burnup fuel prior to clad failure in lower burnup fuel.

Clad failure in a slow TOP accident with metal fuel will usually occur as a result of rapid eutectic attack, assumed to begin at a fuel/clad interface temperature of 1353 K. Gas pressures are too low for failure to occur before extensive clad thinning has taken place, and the time scale of events is too short for slow eutectic attack to be significant. It was found that for the Batch 1 fuel at BOEC, rapid eutectic penetration began at a normalized power of 3.6, with clad failure occurring at a power of 3.9. Rapid attack for the Batch 2 fuel at BOEC starts at a power of 3.9, when failure is already occurring in the Batch 1 fuel. These results were found not to be sensitive to the degree of zone formation.

Fuel extrusion for the prototypical pins has been calculated with EXTRUS assuming a low retained fission gas content of 0.8 μmol/gm fuel, so that most fuel extrusion is coming from fission gas and fill gas trapped in fuel open porosity. In M5 this gas content gave an extrusion slightly larger than observed. The fuel reactivity feedback calculated with EXTRUS at the 3.6 power level is -74¢. Reduction of the retained gas to essentially zero combined with a parametric reduction in cavity fuel, which for M5 gave an extrusion well within the measured range, reduced the total extrusion feedback in the present case to -36¢ at the 3.6 normalized power level. This does not take account of the large extrusion expected in fuel with a few tenths of a percent burnup and observed in M2 and M3 but not in M5. A definitive treatment of fuel extrusion in prototypical fuel is not really possible until the low extrusion observed in M5 is understood.

1. EXTRUS CODE FOR CALCULATION OF MOLTEN FUEL EXTRUSION

A. Introduction

A SAS4A module, EXTRUS, has been programmed to calculate prefailure molten fuel motion in metal-fueled reactors. This module is currently available only in a special version of SAS4A and not in a released version. EXTRUS represents an alternative to the PINACLE module. In EXTRUS, pressure equilibrium is continuously maintained between the fuel region and the fission gas plenum. No hydrodynamics calculation is performed. This assumption has been incorporated into the FP1N2 metal fuel version,[1-1] and has also been recommended by T. Bauer and by R. Sevy[1-2] on the basis of analysis of TREAT M-series results.

B. Modeling Assumptions

The fuel is assumed to contain both open and closed porosity. The total porosity is determined by the amount of fuel swelling from the original unirradiated pin dimensions, reduced by the volume of solid fission products. This latter swelling has been assumed to be 2.2% of the original fuel volume per percent burnup.

Closed porosity volume in reference cases has been calculated as recommended by Sevy.[1-2] Bubble radius is assumed to be 0.1 μm, corresponding to a pressure of 200 atm under steady-state irradiation conditions. In the code, an input temperature may be substituted for the steady-state temperatures if desired. This is useful in analysis of TREAT experiments, in which the steady-state fuel temperature is the same as the inlet sodium temperature. The total closed porosity volume is then obtained from the total gas retained in closed porosity as specified in the input in μgm mols/gm fuel. The open porosity volume is then the difference between the total porosity and the sum of closed porosity and the volume of the solid fission products. The possibility exists in the code of obtaining negative open porosity with large solid fission product swelling, so that care has to be exercised at high burnups to avoid inconsistent conditions.

The released fission gas, the difference between the total generated and that retained in closed porosity, is assumed to be distributed at steady state between the open porosity and the plenum according to the available volume and the local temperature at a uniform pressure. At the start of the transient, the fuel is assumed sealed off from the plenum. The calculated pressure until fuel melting starts is simply that of the plenum, at fixed volume and at the plenum temperature at the given time. Once fuel melting starts, pressure equilibrium is maintained between the molten fuel pin cavity, assumed sealed off from the solid fuel, and the plenum by extruding fuel, even though melting may not yet have started at the top. This assumption in the calculations may require further consideration, and it is probably reasonable in reactor calculations to ignore feedback from fuel extrusion in a given channel until some fuel melting criterion for the top node is satisfied. Note that the SAFR axial power distribution is more asymmetric at earlier times in the cycle than in TREAT experiments because of partial control rod insertion. This tends to cause more delay in top node fuel melting relative to melting in the rest of the fuel than there is in the TREAT M-series.

As the molten pin cavity is formed, it is assumed to contain the gas originally present in open porosity in the cavity region plus that in the closed porosity in the fuel melting into the cavity. The closed porosity volume in this fuel is also added to the cavity porosity volume.

Pin failure in EXTRUS is calculated using the DiMelfi-Kramer clad stress-strain algorithms programmed into FPIN2.[1-3] The failure criterion currently used is attainment of a clad plastic strain of 1%. A life fraction is also calculated using the Dorn parameter correlation developed by HEDL for HT-9 clad,[1-4] which is applicable for pins with this cladding. Eutectic thinning of clad is calculated as recommended by Bauer.[1-5] The essential feature of this for present purposes is that rapid clad attack occurs when the fuel-clad interface temperature reaches 1353 K. Clad failure in a slow TOP accident tends to occur fairly rapidly after this rapid eutectic attack occurs. The intact cladding is usually strong enough to resist failure at lower temperatures.

C. Equation for Pressure Equilibrium

A system of notation has been adopted here in which quantities relating to fuel and gas mass or volume are given a three- or four-letter name, as follows:

Letter		
1	M or V	mass or volume
2	F or G	fuel or gas
3	F,C,P,T	total fuel pin, cavity, plenum, total
4	O,C,T	open, closed, total

Following this scheme, the following quantities are defined:

MFT	Total pin fuel mass, gms
MFC	Mass fuel in cavity, gms
VFT	Total fuel volume, cc
MGTO	Total mass released fission gas plus fill gas, gm mols x 10^6
MGFO	Total open porosity gas in fuel, fission gas plus fill gas, gm mols x 10^6
MGP	Total plenum gas, gm mols x 10^6
MGCT	Total gas in cavity, gm mols x 10^6
MGCO	Total gas in cavity from open porosity, gm mols x 10^6
MGCC	Total gas in cavity from closed porosity, gm mols x 10^6
VGFO	Total open porosity volume in pin at steady state, cc
VGFC	Total closed porosity volume in pin at steady state, cc
VGCT	Total gas volume in cavity before pressure equilibration, cc
VGP	Gas volume available in plenum at steady state, cc

Additional definitions are as follows:

ΔV	Fuel extrusion on equilibration, cc
TP1,TF1	Steady state plenum and average fuel temperature, K
TF2	Cavity temperature at time t_2, K

$\overline{TF2}$	Average fuel temperature at time t_2, K
R	Gas constant, 83.14 cc-bar
TP2	Plenum temperature at time t_2, K

With these definitions, at steady state the partition of gas between fuel open porosity and plenum by pressure equilibration is as follows:

$$MGP = MGTO - MGFO \tag{1}$$

$$\frac{MGFO \times TF1}{VGFO} = \frac{MGP \times TP1}{VGP} \tag{2}$$

$$MGP = MGFO \times \frac{TF1}{TP1} \times \frac{VGP}{VGFO} \tag{3}$$

$$MGFO = \frac{MGTO}{1 + \frac{TF1}{TP1} \times \frac{VGP}{VGFO}} \tag{4}$$

At time t_2, pressure equilibration between pin cavity and plenum yields:

$$\frac{(MGCT)\ TF2}{VGCT + \Delta V} = \frac{MGP \times TP2}{VGP - \Delta V} \tag{5}$$

Solving for ΔV,

$$\Delta V = \frac{VGP \times r - VGCT}{1 + r} \tag{6}$$

where $r \equiv \frac{MGCT}{MGP} \times \frac{TF2}{TP2}$

This is the equation used by EXTRUS to obtain the extrusion ΔV at time t_2

The equilibrium pressure at time t_2 is

$$P = \frac{MGP \times R \times TP2}{VGP - \Delta V} \tag{7}$$

The pressure required for fuel extrusion comes both from the pressues of the retained gas entering the molten fuel cavity, as emphasized by Sevy[1-2], and also from the increasing temperature difference between the cavity gas and the plenum gas during the transient.

pressues of the retained gas entering the molten fuel cavity, as emphasized by Sevy[1-2], and also from the increasing temperature difference between the cavity gas and the plenum gas during the transient.

Information on EXTRUS input and output is given in the Appendix.

For the model applied by Bauer[1-6] to M6, in which all pressure for extrusion is assumed to come from heating of gas trapped in the open porosity during the transient, Eq. 6 is altered by the substitutions

$$\text{VGCT} \rightarrow \text{VGFO}$$
$$\text{MGCT} \rightarrow \text{MGFO}$$
$$TF_2 \rightarrow \overline{TF_2}$$

and becomes, using (2) with TF1 = TP1 for a TREAT transient,

$$\Delta V = \text{VGFO} \frac{\text{VGFO}\left(\frac{\overline{TF_2}}{\overline{TP_2}} - 1\right)}{1 + \frac{\text{VGFO}}{\text{VGP}} \times \frac{\overline{TF_2}}{\overline{TP_2}}} \qquad (8)$$

D. References

1-1. T. H. Hughes, "FPIN2 Analysis of Metal Fueled Pins," ANL-IFR-23, (September 1985).

1-2. R. H. Sevy, unpublished information (1986).

1-3. J. M. Kramer, unpublished information (1985).

1-4. M. L. Hamilton and N. S. Cannon, "HT-9 Transient Data Base and Failure Correlation," HEDL-TC-2681, (October 1985).

1-5. T. H. Bauer, unpublished information (1984).

1-6. T. H. Bauer, private communication (March 1987).

2. APPLICATION OF PINACLE AND EXTRUS SAS4A MODULES TO TREAT M2 AND M4 EXPERIMENTS

A. Introduction

The PINACLE module of SAS4A[2-1,2-2] provides a hydrodynamic treatment of prefailure inpin fuel motion for both oxide and metal fuel. It was felt to be of interest to compare PINACLE results for prefailure metal fuel extrusion with those from EXTRUS (Section I.) to check the validity of the pressure equilibrium assumption made in the latter code. In this section application of these codes to the TREAT M2 and M4 experiments is discussed. The pressure equilibrium assumption is expected to be most applicable for such relatively slow transients.

It is planned eventually that irradiated metal fuel properties, including swelling, retained fission gas distribution, and porosity distribution will be described by the DEFORM4 module of SAS4A. Because this module is still under development, it was not used at all in the PINACLE calculations. Instead, a temporary subroutine named FAILUR, not actually a part of the PINACLE code, was used to supply needed fuels characterization information. Some modifications to this subroutine were made for the purposes of the present calculations. In EXTRUS the DEFORM module was used only for heat transfer and fuel expansion calculations, with fuels characterization information supplied by EXTRUS itself.

B. Parameter Choices

Parameter assumptions common to both PINACLE and EXTRUS, some of which were varied in the calculations, are given in the following with SAS4A input locations.

1. FNMELT, Bl. 13, Loc 1169. This is the fraction of the heat of fusion that must be attained by fuel entering the molten fuel pin cavity. A value of 0.3 for this parameter has been found to be reasonable in previous TREAT analyses and was used in most cases here. Because this choice is rather arbitrary, some calculations were also made with a value of 0.5.

2. Fuel thermal conductivity, K_{fu}, Bl. 13, loc. 420-599. The table of values assumed in the original M-series analyses with PINACLE is listed as Mod 1 in Table 2-1. A series of higher values, which correspond to about 0.65 of the values for unirradiated U-5 wt % Fs available up to 900°C (1173 K)[2-3] (this factor is slightly below the value of 0.7 recommended in ANL-IFR-29[2-3] for irradiated fuel) is designated as Mod 2 in Table 2-1. The Mod 1 values are about 0.57 of the unirradiated U-5 Fs ones. Above the solidus (1283 K) the value used in Ref. 2-1 of 56.0 watts/m-K has been used in the Mod 2 set. A third choice of fuel thermal conductivity, designated as Mod 3, was obtained by assuming that the conductivity in the Mod 2 table stays constant at 34.0 watts/m-K above 1240 K.

3. Fission gas retained in closed porosity. In EXTRUS this can be specified in μmols/gm of fuel in Bl. 65, loc. 65. In the FAILUR routine used to supply data to PINACLE it is varied by updating the FORTRAN. Values of 5.0, recommended by Sevy,[2-5] and 7.0 μmols/gm were used.

4. Fuel porosity volume. In EXTRUS the closed porosity volume was about 9% of the total in the M4 calculations, varied by varying the temperature at which 0.1 μm radius bubbles exert a pressure of 200 atm, Bl. 65, loc. 57. In a modification of the FAILUR routine used with PINACLE the closed porosity volume was varied by FORTRAN update. The closed porosity volume in this case also was about 9% of the total in the M4 calculations. Total porosity was determined by the specified fabricated porosity, PRSTY, Bl. 13, loc. 1073, which was adjusted to account for fuel swelling, since DEFORM was not used for this purpose. The fuel was assumed to have swollen to the clad, except for M2 Pin 1, and to have a pin length as given in Table 2-2. For EXTRUS the total porosity was reduced by solid fission product swelling amounting to 2.2% of the original fuel volume per percent burnup. Resultant initial total and closed fuel porosity fractions for PINACLE and for EXTRUS are given in Table 2-2. As is discussed later, because the current SAS4A computational scheme involving PINACLE does not provide for alteration of the radial mesh in the course of the transient, cavity fuel porosity decreases 5-6% in the course of the transient compared to 1% for EXTRUS, which uses DEFORM to calculate radial mesh spacing.

5. Pin average burnup, BURNFU. This is given in Table 2-2 and was used in the calculations. It was assumed to be 10% less than the maximum burnup, given in the figures.

6. Gas plenum pressure. This is a sensitive parameter for TREAT experiments because of the short plenum length compared to that for prototypical fuel. Parameter selections were such that reasonable consistency was obtained for plenum pressure between the PINACLE and EXTRUS calculations.

7. Pin radial power distribution. Because of the thermal flux in TREAT there is a radial variation of the pin power, which can be specified in Bl. 62, loc. 30-44. The distribution used in this report is given in Table 2-3. Because it was found that this distribution differs slightly from that recommended in ANL-IFR-9,[2-6] a case was run with the latter radial power distribution. No significant change in fuel extrusion was found to result from this variation.

Input assumptions peculiar to PINACLE are the following:

FPINAC, Bl. 65, loc. 22. This is the minimum axial melt fraction which must be attained in the peak node before PINACLE can be initiated. Because of the manner in which initial cavity conditions are handled in PINACLE it is desirable to keep it small. It was fixed at 0.06 in the present calculations.

CIPNTP, Bl. 13, loc. 1287. This controls the peak radial temperature at the top of the fuel which must be attained before fuel ejection into the upper plenum can occur. For CIPNTP = 1.0 the fuel solidus temperature must be attained in the top fuel node. For CIPNTP = 0.5 the average of the peak temperature in the top fuel node and of the peak temperature of the next node above must reach the fuel solidus temperature, introducing a considerable delay in fuel ejection. Because the cavity must extend to the top fuel node before ejection can begin, if FNMELT >0 an additional requirement for fuel ejection is that the central radial node of the top fuel node must have reached a temperature between the solidus and liquidus corresponding to the specified value of FNMELT.

C. Differences in Modeling Assumptions Between PINACLE and EXTRUS

In both codes at the initiation of a transient the fission gas released in steady state is assumed distributed between the fission gas plenum and the fuel open porosity. The fuel is subsequently assumed sealed off from the plenum, the pressure of which varies according to the temperature of the plenum gas and to eventual diminution of the plenum gas volume by upward movement of molten fuel. No mixture of plenum and cavity gas occurs in either code as a result of this movement. In EXTRUS fuel movement to maintain static gas pressure equilibrium between the plenum and the pin cavity begins at the start of fuel melting. In PINACLE, molten fuel movement begins when the top node melting criteria is satisfied that corresponds to the selected value of CIPNTP, provided that the cavity has been extended to this node. Before this condition is reached, cavity pressure buildup occurs as fuel containing closed porosity gas melts into the cavity. After satisfaction of the top node melting criterion, a hydrodynamic calculation is used to calculate the movement of the upper fuel plug resulting from the pressure difference between cavity and plenum. In this calculation pressure, temperature, mass of fuel, and mass of fission gas are obtained at each axial node as a function of time. Extruded fuel is described by an additional cavity node. The temperature of this fuel tends to be considerably less than that of the remaining cavity fuel. In EXTRUS, on the other hand, a single cavity gas pressure, temperature, fuel mass, and gas mass are obtained. In EXTRUS, no heat transfer calculations are performed beyond what was already available in SAS4A. Cavity molten fuel content is obtained from the purely static calculation in DEFORM by simply adding up the calculated molten fuel in the appropriate region. In PINACLE, a new cavity heat transfer calculation is performed in which the cavity fuel is assumed to be radially homogenized, with a flowing heat transfer coefficient calculated between cavity fuel and surrounding solid fuel.

D. Results of M4 Calculations

1. Comparison of PINACLE and EXTRUS

Results of calculations of fuel extrusion for M4 Pin 2 in comparison with experiment[2-7] are given in Figs. 2-1 to 2-3 and results for Pin 3 are

given in Figs. 2-4 to 2-6. "Extrusion" here is used to refer to molten fuel motion under fission gas pressure rather than to creep of solid fuel, which has been found to be small for the time scale of interest here. In these figures, PINACLE cases are those denoted by "P", and EXTRUS cases are denoted by "E". PINACLE and EXTRUS results are compared for a reference set of parameters with the Mod 1 choice of K_{fu}, with FNMELT = 0.3, with retained fission gas set at 5.0 μmols/gm fuel, and with CIPNTP in PINACLE set at 1.0. Cases with variations in these parameters are also presented. Parameter choices are summarized in Tables 2-4 and 2-5.

A point of special interest in these comparisons is whether or not significant premature fuel extrusion is being caused by the assumption in EXTRUS that pressure equilibration is maintained between pin cavity and fission gas plenum as soon as fuel melting starts anywhere in the pin even though the fuel is still solid at the top. Although it seems reasonable that this might be a problem, comparison of EXTRUS results with experiment does not show excess early extrusion. Furthermore, the calculated time dependence of extrusion from EXTRUS is similar to that obtained from PINACLE with CIPNTP = 1.0. Choice of a value of 0.5 for CIPNTP, which averages the temperature of the fuel in the top node and of the sodium above, introduces far too much delay in extrusion, as is evident in Fig. 2-1.

With a choice of 0.5 for CIPNTP in PINACLE, there is a considerable buildup of pin cavity pressure prior to fuel ejection. At the time of ejection the cavity pressure blows down to approximate equilibrium with the plenum in a few milliseconds, with rapid fuel ejection as shown in Fig. 2-1. With CIPNTP = 1.0, on the other hand, pressures do not build up greatly, the cavity pressure stays in near equilibrium with the plenum pressure over practically the entire transient, and fuel ejection is much more gradual. Because this time dependence of ejection agrees better with experiment, the implication is that the hydrodynamic treatment of prefailure inpin fuel motion provided by PINACLE is not necessary for calculating this ejection for metal fuel undergoing a slow power transient. For M4 Pin 2 there is indicated to be a period of rapid fuel ejection, but it does not appear possible to reproduce the reported fuel ejection history by parameter adjustment in PINACLE. It is noted that the quality of the data for Pin 2 is regarded by the experimenters as inferior to that for Pin 3.

It can be argued that the modeling in EXTRUS can be improved by taking account in some way of the threshold effect from the delayed melting at the top of the pin. However, failure to do so does not seem to be causing a serious problem in obtaining agreement of calculated and experimental results. The threshold effect might be more important for full-length pins because of a possibly greater length of unmelted fuel at the top. Counterbalancing this is the existence of a lower-melting middle zone in prototypical fuel, which should aid early extrusion.

Because PINACLE with CIPNTP = 1.0 is essentially maintaining the pressure equilibration assumed in EXTRUS, it might be supposed that the results of the two codes for fuel extrusion would be in close agreement. The fact that this is not always true arises from a number of other differences in modeling assumptions and in computational algorithms that complicated the problem of obtaining a completely consistent comparison between the two codes, as given in the following:

(a) Because of the different ways of calculating heat transfer between the pin cavity and solid fuel, the calculated amount of molten fuel for the same total energy input to the system tends to be 20-30% larger for EXTRUS than for PINACLE. It is difficult to tell which is more correct: possibly the right value is somewhere in between.

(b) A coalescence time constant of 60 ms (CIRTFS, Bl. 13, loc. 1070) was assumed in PINACLE for closed porosity gas entering the cavity. No delay was assumed in EXTRUS. This generally reduced the available free gas in PINACLE by several percent.

(c) In EXTRUS, available porosity is reduced by buildup of solid fission products, not taken into account in PINACLE.

(d) At the time of initiation of PINACLE, the process of equilibrating pressure between plenum and cavity results in discarding some cavity gas. This process has no counterpart in EXTRUS, and is an important reason for keeping FPINAC small, to minimize the amount of discarded gas.

(e) Cavity porosity is reduced 5-6% between the steady state and transient conditions in the PINACLE calculations because it is not possible without use of DEFORM correctly to account for fuel volume increase on melting.

In retrospect, some reduction of these inconsistencies would be possible by adjustment of input parameters. In spite of these differences, extrusion results for PINACLE with CIPNTP = 1.0 and for EXTRUS are fairly close for Pin 2 for the same values of the parameters given in the figures. It appears that the effects of other discrepancies have about counterbalanced that of the most important one, the difference in amount of molten fuel. For Pin 3, on the other hand, late in the transient there is about 20% more extrusion with EXTRUS for the same parameter set. The relative discrepancy is much larger earlier in the transient. The main reason for the different relative extrusions for the two codes between Pins 2 and 3 appears to be that the ratio of cavity gas to fuel increases by about 16% for EXTRUS compared to PINACLE in going from Pin 2 to Pin 3, from about 0.92 for Pin 2 to about 1.08 for Pin 3. All the reasons for the differences in ratio of cavity gas to fuel between the two codes have not been identified, and to accomplish this identification would probably require more complete edits than are now available to obtain complete gas inventories during the transient. It is noted that the effects of changes in parameters affecting cavity gas volume tend to be magnified in calculating fuel extrusion, which reflects the difference in gas volume before and after expansion to achieve pressure equilibration.

2. Effect of fuel thermal conductivity, K_{fu}.

It is seen in Figs. 2-2 and 2-5 that the extrusions with the Mod 1 values of K_{fu} are 20-30% greater than those with the Mod 3 values, with the ratio being larger earlier in the transient. The further increase in K_{fu} represented by the Mod 2 values causes a further reduction in extrusion from results with the Mod 3 values by a comparable amount, as seen in Fig. 2-2.

Although the sensitivity of calculated extrusion to modeling details and parameter choices makes caution in interpretation of the results of these

calculations advisable, the present results imply that the Mod 3 and certainly the Mod 2 values for K_{fu} are too high. In fact, with PINACLE the calculated values fall below the experimental ones for Pin 3 even with the Mod 1 choice for K_{fu}.

3. Effect of retained fission gas.

Assumption of a closed porosity gas content of 7.0 μmols/gm fuel instead of 5.0 raises the fuel extrusion. Agreement with experiment seems somewhat worse with the higher value because the variation of extrusion with time becomes too rapid, and values of extrusion late in the transient tend to become considerably too high.

4. Effect of variations of FNMELT.

Increasing FNMELT from 0.3 to 0.5 delays the development of extrusion slightly and increases its time rate of change. However, this makes agreement with experiment slightly poorer. Retention of a value of 0.3 seems appropriate.

5. Relative effect of retained gas and cavity/plenum differential temperature in producing extrusion.

In auxiliary calculations, it was found for Pin 3 case M4P307 that about 60% of the extrusion was produced by retained gas melting into the cavity, the balance being produced by cavity/plenum differential temperature. For Pin 2, which had higher burnup and for which the effect of retained gas, assumed constant at 5 μmols/gm, was less important, the retained gas effect was only about 40% of the total.

E. M2 Results

The analysis of the low burnup Pin 1 in M2 involves special problems because of the open fuel/clad gap and because of the low fuel porosity, the exact amount of which is uncertain. The open fuel/clad gap creates the possibility that molten fuel could run down into the gap instead of moving up

above the pin. This possibility has been ignored in the present calculation, implying that the entrance to the gap will be blocked by frozen fuel before any significant amount of fuel trickles down.

Choices made for fuel porosity are given in Table 2-6, representing variations in the PRSTY variable, loc. 1073 in Bl. 13. Differences in computational algorithms between EXTRUS and PINACLE have made it particularly difficult to make a meaningful comparison of the effect of porosity variations in the two codes. The difference between the codes for porosity change between steady state and transient conditions is evident in Table 2-6.

In PINACLE, all porosity for this low burnup case is assumed to be closed. It is not convenient to make this assumption in EXTRUS in its present form. However, little difference in extrusion was found between cases E10 and E12 (Table 2-4 and Fig. 2-7) in which the steady state open porosity fraction varied from 0.086 to 0.015 while closed porosity fraction remained at 0.019.

In the PINACLE cases, because of the larger porosity reduction in going from the steady state to transient conditions, fuel porosity is completely squeezed out if PRSTY = 0.06 or less, leading to overcompaction. This unphysical result is due to the current inability to use DEFORM. Small spurious hydrodynamics effects appear to be present in Case P9, with slight overcompaction. This case certainly gives an upper limit for fuel extrusion for PINACLE. Use of a lower value of PRSTY leads to larger overcompaction and larger spurious hydrodynamics effects.

The most reasonable PINACLE case to compare with the EXTRUS results seems to be one with a cavity porosity of about 2%. This would be bracketed by Cases P6 and P9, and indicates that the PINACLE results lie below the EXTRUS results and also below experiment.[2-8] As for the M4 cases, fuel melting at a given time in the transient is greater for EXTRUS than for PINACLE, which probably contributes to the discrepancy. However, a more important factor in the present case is the cavity gas discarded to achieve pressure equilibration at PINACLE initiation. Retaining this gas would remove most of the discrepancy between EXTRUS and PINACLE results. This is not an important effect at higher burnups.

It is concluded that there does not seem to be an obvious disagreement between experiment and calculation for M2 Pin 1 and the assumption of continuous equilibration seems to be justified in this case also. However, there is considerable uncertainty in the calculated results. Also, the preliminary state of the current utilization of PINACLE within SAS4A makes comparison of PINACLE results with experiment or with EXTRUS calculations of limited usefulness for this low burnup, low porosity case. In any case, although the large amount of extrusion observed for Pin 1 is gratifying for the safety analyst, this is of limited significance because it can hardly be assumed that there will be such low burnup fuel present at the time an accident occurs.

For M2 Pin 3 there is again more cavity fuel for EXTRUS than for PINACLE, the ratio being about 1.3. However, the calculated fuel extrusion for both codes is too low. A factor reducing fuel extrusion for EXTRUS relative to PINACLE is the effect of solid fission product swelling, which reduces cavity porosity considerably for the high burnup fuel. CIPNTP = 0.5 in PINACLE is clearly inappropriate here, as shown in Fig. 8. Assumption of 7.0 μmols/gm retained gas instead of 5.0 in PINACLE calculations did not give a significant difference in calculated extrusion.

F. Conclusions

1. For M2 and M4, the assumption of continuous pressure equilibrium between pin cavity and fission gas plenum, as represented by the modeling in EXTRUS and approximated in PINACLE with CIPNTP = 1.0, gives reasonable results for the time dependence of prefailure fuel extrusion.

2. The normalization of the calculated results is sensitive to modeling details and choices of parameters, especially of fuel thermal conductivity. With the methods and parameters used here, fuel thermal conductivity values 0.55 to 0.60 of those for unirradiated U-5% Fs give best agreement with experiment.

3. The amount of molten fuel calculated by EXTRUS is greater than that calculated by PINACLE for the same total energy input. This causes a significant difference in calculated extrusion for M4 Pin 3 and M2 Pin 1.

4. A closed porosity gas content of 5 μmols/gm fuel gives reasonable results for the time variations of extrusion for M4 using either EXTRUS or PINACLE. Use of a higher gas content gives too much extrusion late in the transient.

5. A value of FNMELT of 0.3 gives better results for the time dependence of prefailure extrusion than a value of 0.5.

A question not dealt with in this section is that of the axial distribution of fuel within the cavity. EXTRUS assumes that the fuel smear density is uniform in the cavity, while PINACLE calculates an axial distribution of smear density using compressible hydrodynamics. For a fast transient with fuel ejection occurring, it is reasonable to suppose that there would be a gradient of smear density within the cavity. Whether smear density variations have an important reactivity effect will be discussed in Section 3 for fuel length pins.

G. References

2-1. A. M. Tentner and D. J. Hill, Trans. Am. Nucl. Soc., 49 275 (1985).

2-2. Kalimullah, K. J. Miles, Jr., A. M. Tentner, and D. P. Weber, "Advancements in the Modeling of Metallic and Oxide Fuels in the SAS4A Codes," ANL/RAS 85-19 (October 1985).

2-3. G. L. Hofman, et al., "Metallic Fuels Handbook," ANL-IFR-29 (November 1985).

2-4. T. H. Hughes, "FPIN2 Analysis of Metal Fueled Pins," ANL-IFR-23 (September 1985).

2-5. R. H. Sevy, unpublished information (1986).

2-6. T. H. Bauer, et al., "TREAT Tests M2 and M3: Experiment Information and Pretest Analysis," ANL-IFR-9 (April 1985).

2-7. T. H. Bauer, et al., "Update of Safety Testing in TREAT on U-5s Fuel: Data from Test M4 and Combined Analysis of Test M2, M3 and M4," ANL-IFR-69, Appendix E.

2-8. W. R. Robinson., et al, "IFR Safety Tests M2 and M3 in TREAT: Data and Analysis," ANL-IFR-18 (June 1985).

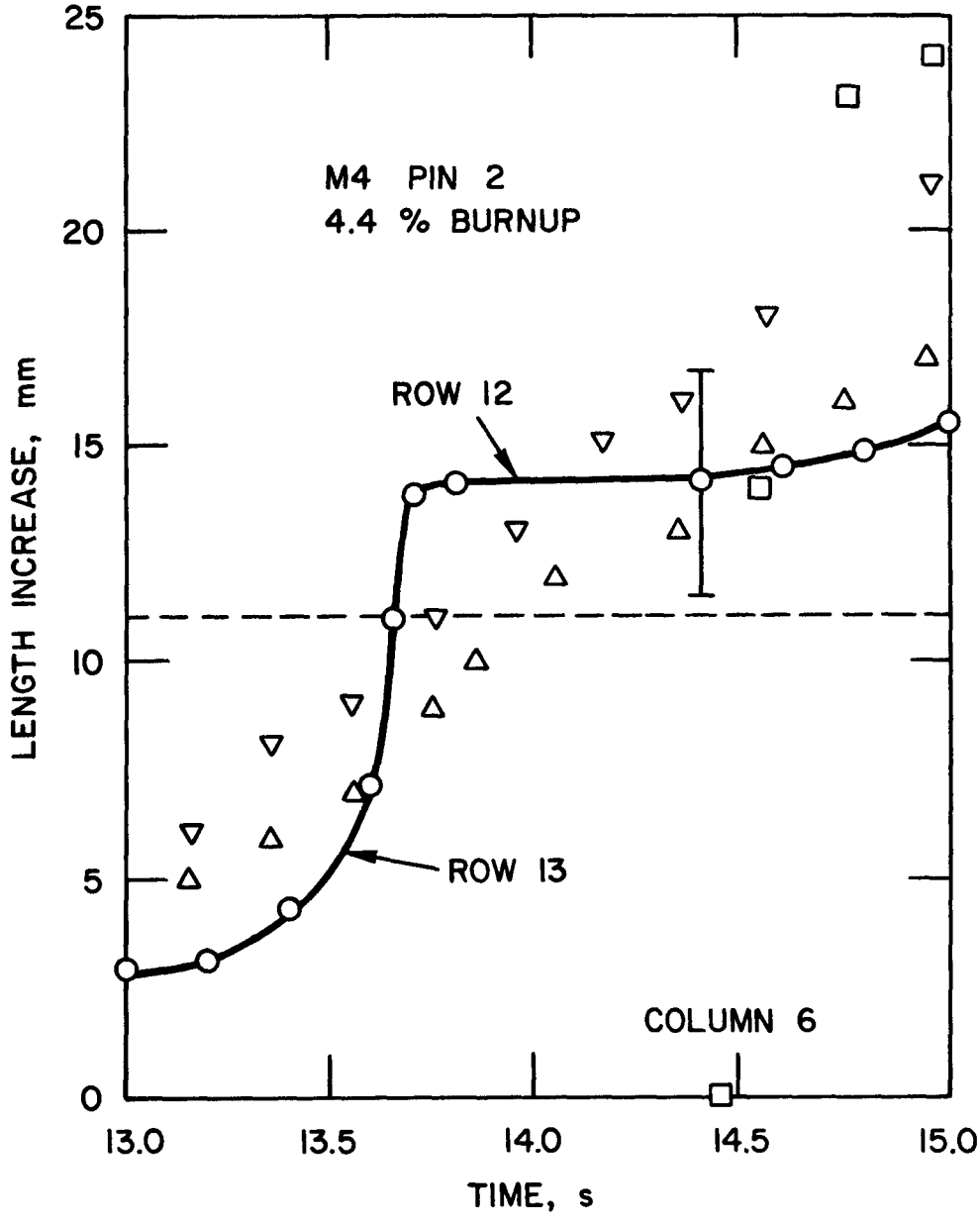

	Case	K_{fu}	Retained Gas, µmols/gm	FNMELT	CIPNTP
X	P1	1	7.0	0.3	1.0
•	P2	1	7.0	0.3	0.5
•	P3	1	5.0	0.3	1.0
•	Experiment				

Fig. 2-1. M4 Pin 2. Effect of varying retained fission gas and CIPNTP

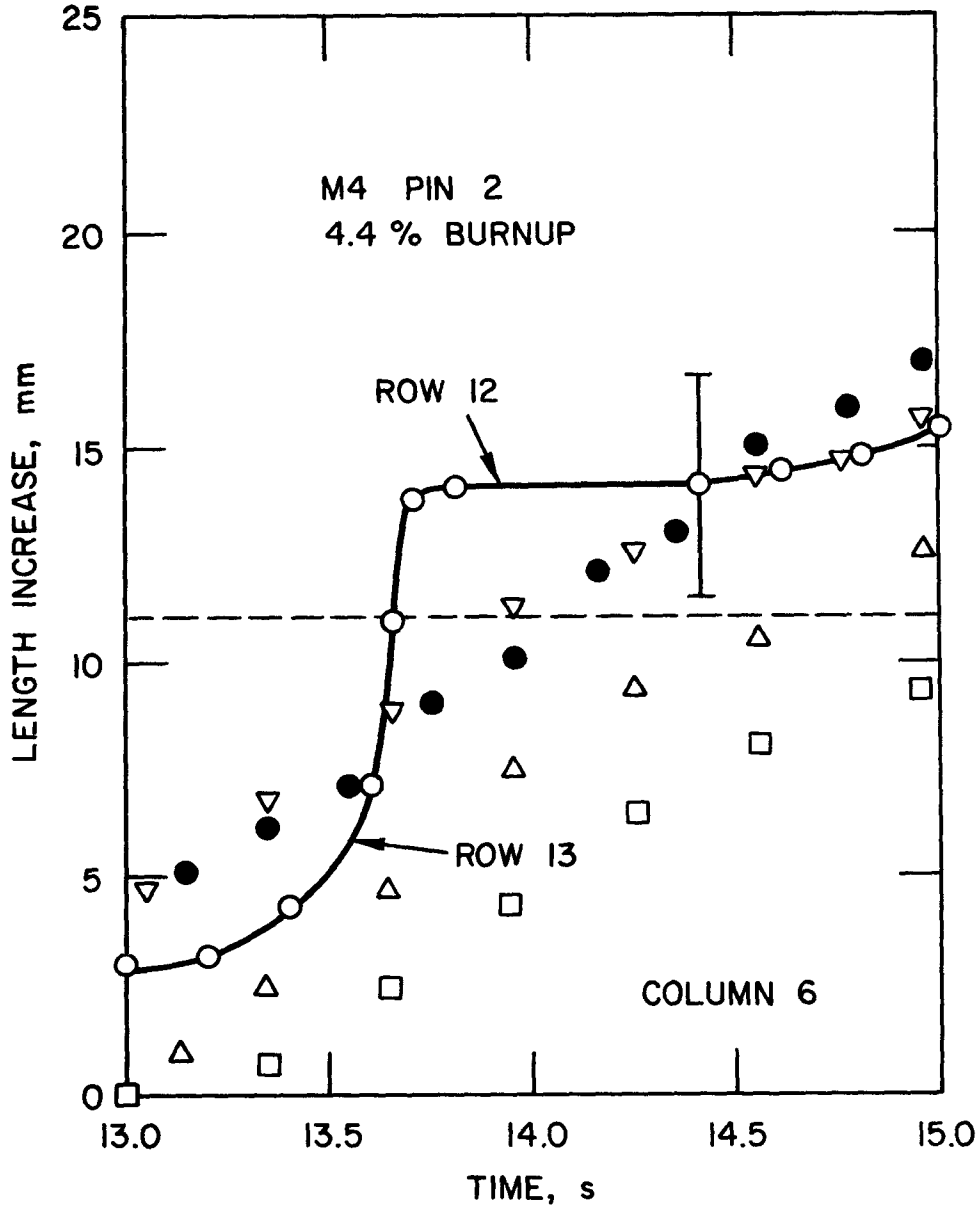

	Case	K_{fu}	Retained Gas, μmols/gm	FNMELT	CIPNTP
X	P3	1	5.0	0.3	1.0
•	E1	2	5.0	0.3	
•	E2	1	5.0	0.3	
•	E5	3	5.0	0.3	
	Experiment				

Fig. 2-2. M4 Pin 2. PINACLE vs. EXTRUS. Effect of varying K_{fu}

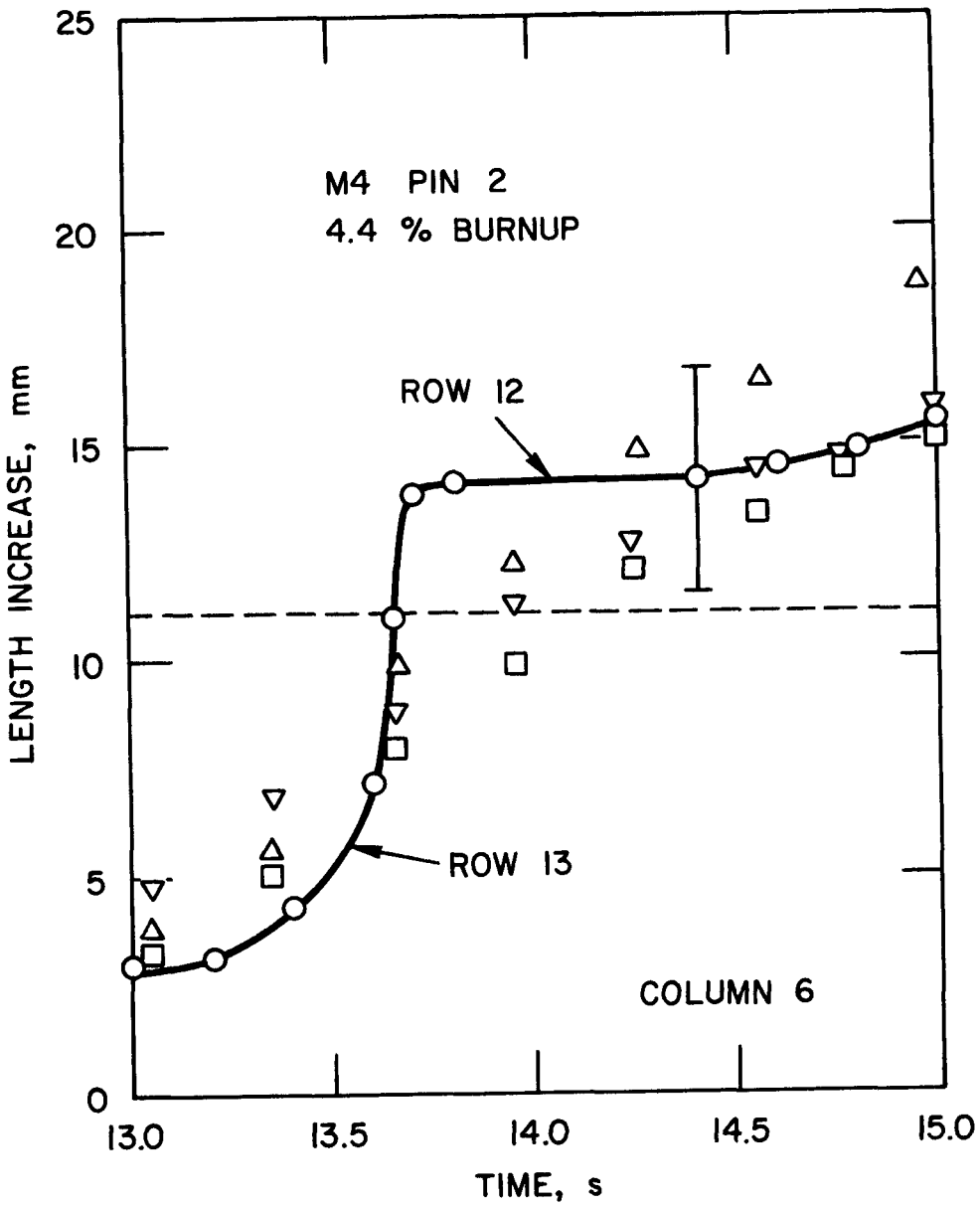

	Case	K_{fu}	Retained Gas, μmols/gm	FNMELT
•	E2	1	5.0	0.3
X	E3	1	7.0	0.5
•	E4	1	5.0	0.5
•	Experiment			

Fig. 2-3. M4 Pin 2. Effect of varying retained fission gas and FNMELT

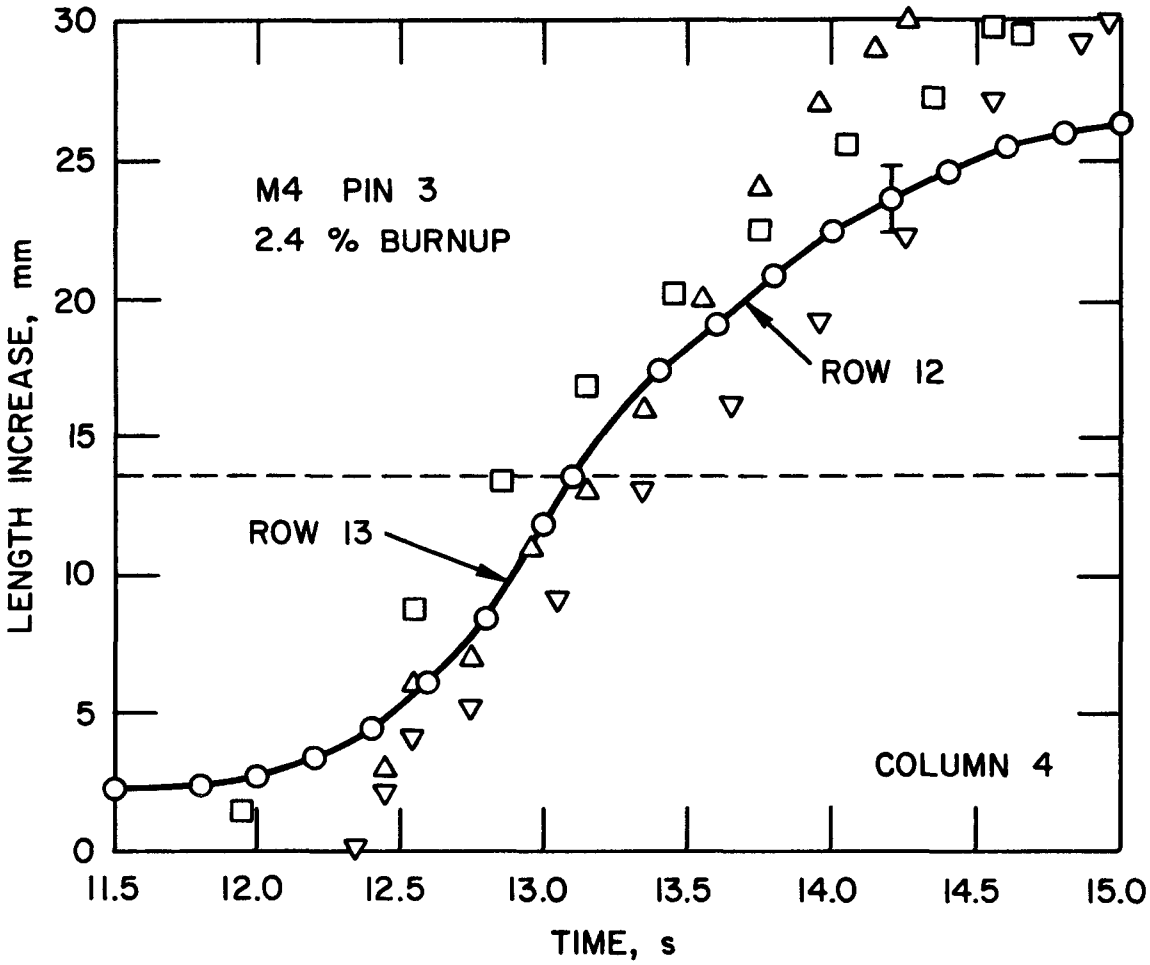

	Case	K_{fu}	Retained Gas, μmols/gm	FNMELT	CIPNTP
X	P4	1	5.0	0.3	1.0
•	P5	1	7.0	0.3	1.0
•	E6	1	5.0	0.3	
•	Experiment				

Fig. 2-4. M4 Pin 3. PINACLE vs. EXTRUS. Effect of varying retained fission gas

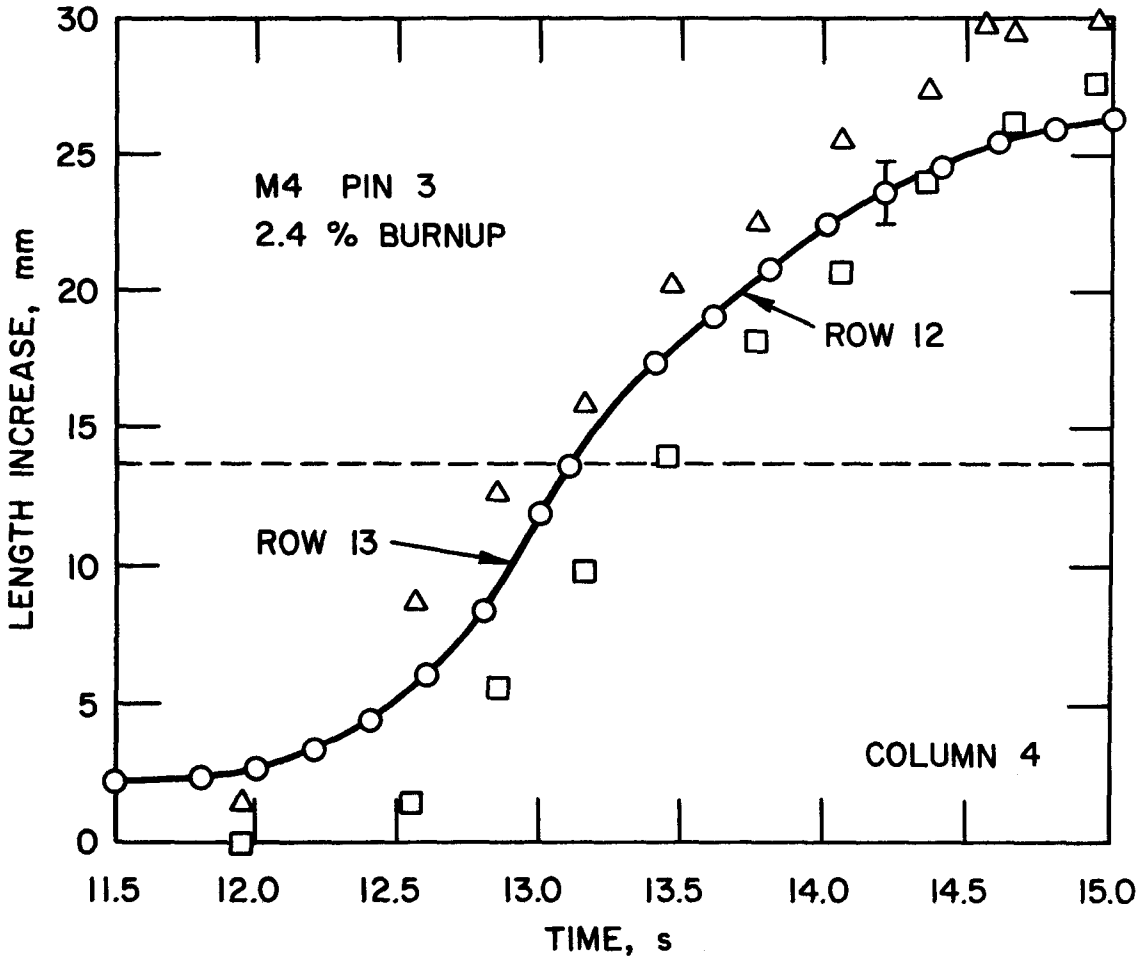

	Case	K_{fu}	Retained Gas, μmols/gm	FNMELT
X	E6	1	5.0	0.3
•	E7	3	5.0	0.3
•	Experiment			

Fig. 2-5. M4 Pin 3. Effect of varying K_{fu}.

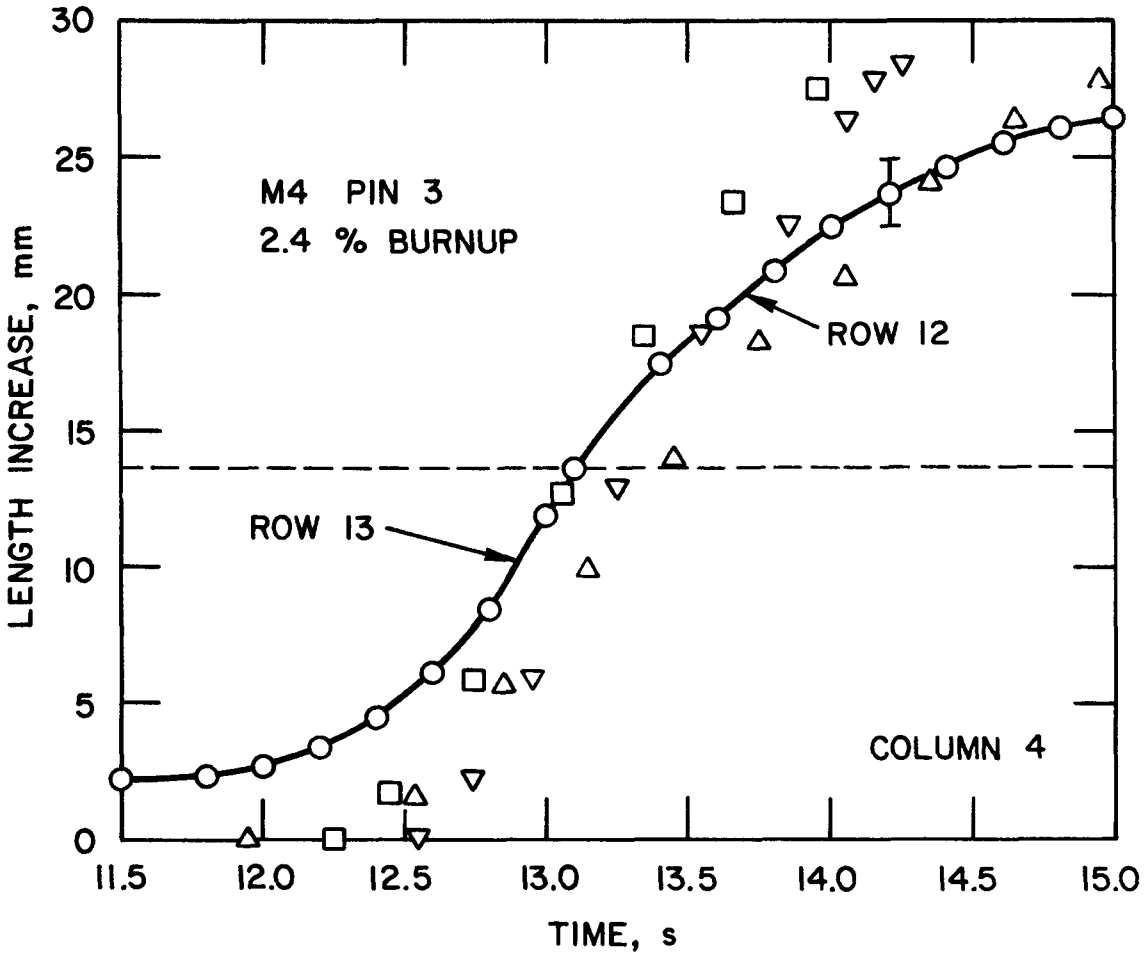

	Case	K_{fu}	Retained Gas, μmols/gm	FNMELT
•	E7	3	5.0	0.3
•	E8	3	7.0	0.3
X	E9	3	7.0	0.5
•	Experiment			

Fig. 2-6. M4 Pin 3. Effect of varying retained fission gas and FNMELT

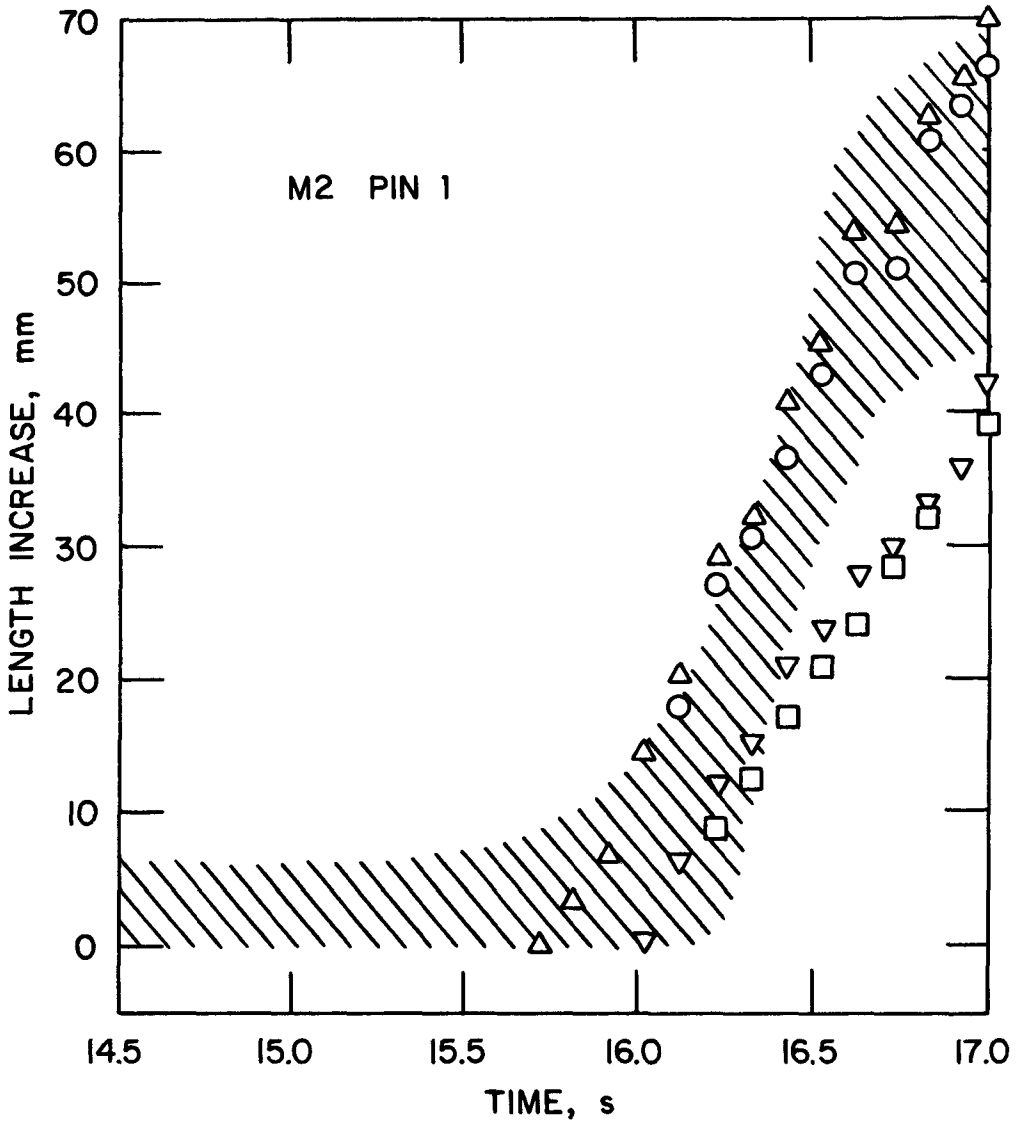

	Case	K_{fu}	Retained Gas, μmols/gm	FNMELT	CIPNTP	PRSTY
•	P6	1	2.7	0.3	1.0	0.11
X	P9	1	2.7	0.3	1.0	0.06
•	E10	1	2.7	0.3		0.11
•	E12	1	2.7	0.3		0.04

Fig. 2-7. M2 Pin 1. Effect of varying fuel porosity. Shaded area shows estimated/uncertainty in experimental results

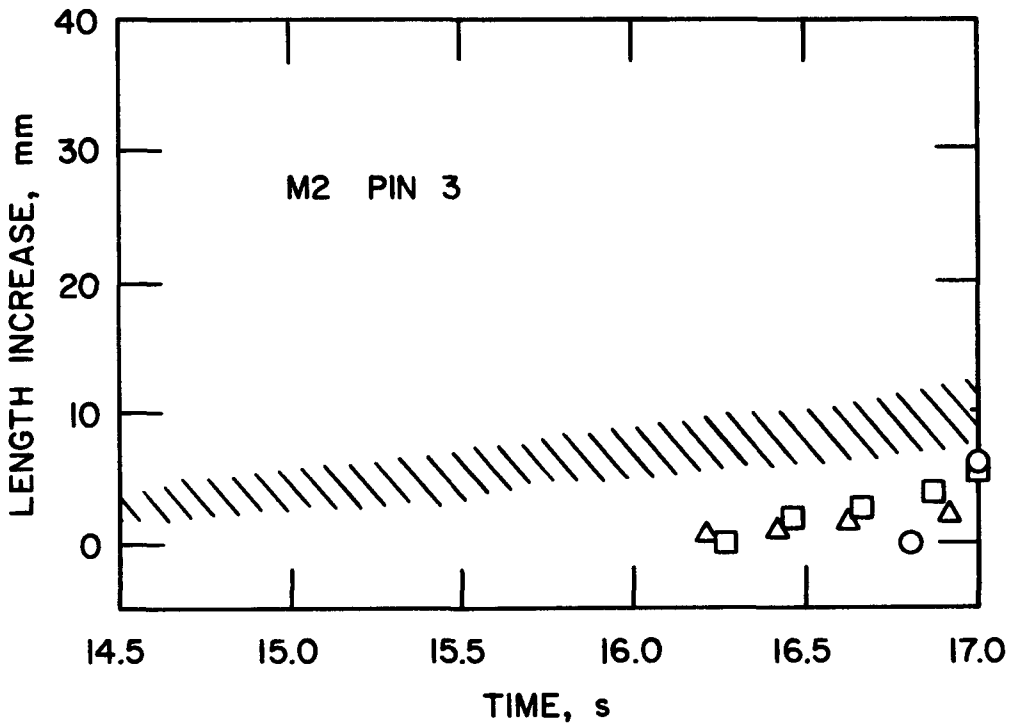

	Case	K_{fu}	Retained Gas, μmols/gm	FNMELT	CIPNTP
X	P7	1	5.0	0.3	0.5
•	P8	1	5.0	0.3	1.0
•	E11	1	5.0	0.3	

Fig. 2-8. M2 Pin 3. Effect of varying CIPNTP. Shaded area shows estimated uncertainty in experimental results

TABLE 2-1. Values of Fuel Thermal Conductivity, K_{fu}, Used in Extrusion Calculations, watts/m-K[a]

T,K	Mod 1	Mod 2
580	15.0	17.0
620	15.0	17.8
700	16.0	18.6
740	17.0	18.6
780	18.0	18.8
820	18.0	20.3
840	19.0	21.1
900	20.0	22.7
920	20.0	23.1
960	21.0	23.5
1000	21.0	25.1
1040	22.0	25.9
1080	23.0	26.7
1120	24.0	27.6
1160	24.0	28.4
1200	25.0	32.4
1240	26.0	34.0
1283	27.0	56.0
1373	29.0	56.0
2000	29.0	56.0

[a]Mod 3 values are formed from Mod 2 by keeping K_{fu} constant at 34.0 above 1240 K.

TABLE 2-2. Pin Parameters Used in Fuel Extrusion Calculations

Case	Ave. BU, %	Power Coupling Factor[a]	Pin Length, cm	Pin Fuel Volume, cm^3	Steady State Plenum Gas Volume, cc	Coolant Inlet Temp., K	Coolant Flow, Gms/sec	Initial Fuel Total Porosity		Initial Fuel Closed Porosity Fraction	
								PINACLE	EXTRUS	PINACLE	EXTRUS
M4 Pin 3	2.18	5.86	35.3	4.05	1.89	596	75.6	0.289	0.255	0.026	0.020
M4 Pin 2	4.00	5.74	36.3	4.17	1.70	596	83.5	0.308	0.247	0.028	0.023
M2 Pin 1	0.27	5.29	34.3	3.23	2.27	629	56.3	0.110	0.104	0.110	0.018
				3.04	2.27	629	56.3	0.006		0.060	0.019
				2.98	2.27	629	56.3	0.040	0.034	0.040	0.019
M2 Pin 3	7.18	5.33	37.0	4.24	1.41	629	58.9	0.307	0.214	0.028	0.021

[a]Watts/gm fuel/MW TREAT power. Maximum TREAT power for M2 178.7 MW; for M4 221.0 MW.

TABLE 2-3. Pin Radial Flux Distribution Assumed in TREAT

Radial Node[a]	Relative Specific Power for Uniform Radial Composition
1	0.62
2	0.66
3	0.71
4	0.79
5	0.83
6	0.96
7	1.04
8	1.23
9	1.50
10	1.75

[a]Nodes 1 (innermost) and 10 (outermost) each contain 1/18 of pin volume; others each have 1/9.

TABLE 2-4. EXTRUS Cases

Case	Job Name	K_{fu}, Fuel Thermal Cond.	Retained Fission Gas μmols/gm	FNMELT	PRSTY
		M4 Pin 2			
E1	M4 P2 09	2	5.0	0.3	0.308
E2	M4 P2 10	1	5.0	0.3	0.308
E3	M4 P2 11	1	7.0	0.5	0.308
E4	M4 P2 13	1	5.0	0.5	0.308
E5	M4 P2 14	3	5.0	0.3	0.308
		M4 Pin 3			
E6	M4 P3 07	1	5.0	0.3	0.289
E7	M4 P3 11	3	5.0	0.3	0.289
E8	M4 P3 13	3	7.0	0.3	0.289
E9	M4 P3 14	3	7.0	0.5	0.289
		M2 Pin 1			
E10	M2 P1 06	1	2.7	0.3	0.11
E12	M2 P1 08	1	2.7	0.3	0.04
		M2 Pin 3			
E11	M2 P3 03	1	5.0	0.3	0.307

TABLE 2-5. PINACLE Cases

Case	Job Name	K_{fu}, Fuel Thermal Cond.	Retained Fission Gas µmols/gm	FNMELT	CIPNTP	PRSTY
			M4 Pin 2			
P1	PI2 M4 14	1	7.0	0.3	1.0	0.308
P2	PI2 M4 08	1	7.0	0.3	0.5	0.308
P3	PI2 M4 15	1	5.0	0.3	1.0	0.308
			M4 Pin 3			
P4	PI3 M4 11	1	5.0	0.3	1.0	0.289
P5	PI3 M4 12	1	7.0	0.3	1.0	0.289
			M2 Pin 1			
P6	PI1 M2 09	1	2.7	0.3	1.0	0.11
P9	PI1 M2 13	1	2.7	0.3	1.0	0.06
			M2 Pin 3			
P7	PI3 M2 05	1	5.0	0.3	0.5	0.307
P8	PI3 M2 07	1	5.0	0.3	1.0	0.307

TABLE 2-6. Fuel Porosity Fractions for M2 Pin 1

Case	Job Name	PRSTY	Steady State Total Porosity	Steady State Closed Porosity	Cavity Porosity Before Extrusion	Cavity Pressure Before Extrusion, bars (@ 16.04 sec)	Cavity Pressure After Extrusion, bars (@ 16.52 sec)
E10	M2 P1 06	0.110	0.105	0.019	0.094	50	4.9
E12	M2 P1 08	0.040	0.034	0.019	0.023	211	5.2
P6	P11 M2 09	0.110	0.110	0.110	0.051	15 (91)[a]	5.0
P9	P11 M2 13	0.060	0.060	0.060	0.0005	288	5.0

[a]Pressure with no gas discarded from cavity on PINACLE initiation.

3. EFFECT OF INPIN FUEL DISTRIBUTION AND OF RATE OF POWER RISE ON THE REACTIVITY EFFECT OF PREFAILURE FUEL EXTRUSION IN METAL FUEL

A. Introduction

In Section 2, the PINACLE[3-1] and EXTRUS (Section 1) models of SAS4A were applied to calculations of the amount of prefailure fuel extrusion in TREAT experiments M2 and M4. The question of the reactivity effect of such extrusions was not dealt with, however. In this section, reactivity effects from prefailure fuel extrusion are studied for a full-length prototypical pin with 6.25% average burnup. As before, the term "fuel extrusion" refers to motion of molten fuel under fission gas pressure rather than to solid fuel extrusion. The three-zone structure observed in irradiated prototypical pins has not been taken into account; only a single radial zone has been assumed as SAS4A code development does not as yet allow PINACLE to be applied to the three-zone configuration. TOP accidents with power rises corresponding to 10¢/sec and 50¢/sec have been calculated for a single subassembly with assumed power histories.

B. Cases Considered

The PINACLE module has been applied to TOP cases with power histories as shown in Table 3-1. Energy inputs in full power seconds are also shown. The most reasonable basis for comparing the results of the 10¢/sec and 50¢/sec transients seem to be on the basis of equal mass of molten pin cavity fuel, calculated with the FNMELT parameter set at 0.3. The significance of FNMELT and of the other parameters specified in Table 3-1 is discussed in Section 2. The cavity fuel mass as a function of time[3-1] is also given in Table 3.1. The 50¢/sec transient has also been calculated with the EXTRUS module. As found in Section 2, the cavity fuel mass at a given time in the transient is considerably greater with EXTRUS than with PINACLE. The assumed axial power distribution in the core is given in Table 3-2.

In order to study the effect of axial distribution of molten fuel smear density in PINACLE on fuel motion reactivity, an additional edit has been provided in PINACLE giving the axially averaged molten fuel smear density and also the fuel motion reactivity resulting if the same amount of cavity fuel as

originally calculated has a uniform smear density instead of the smear density distribution calculated by PINACLE. The ratios of the former of these reactivities to the latter during the transients are given in Table 3-1. It is seen that these ratios are always near unity, so that the assumption of constant cavity smear density gives adequate accuracy. However, as seen in Fig. 3-1, there is a systematic difference in reactivity for a given cavity fuel mass, the values for the 50¢/sec case being about 15% less than those for the 10¢/sec case, implying some dynamic effect on fuel extrusion, at least at the higher ramp rate. The same effect is evident in Fig. 3.2, in which the extruded fuel masses are plotted against cavity fuel mass.

This question was further explored by running the 50¢/sec case also with EXTRUS, in which dynamic effects are not taken into account. Comparison of both extruded fuel masses and reactivities gives equivocal results: at lower extrusions agreement of the EXTRUS results is better with the 10¢/sec PINACLE case, while at higher extrusions agreement between the EXTRUS values and those from the 50¢/sec PINACLE case is quite close. PINACLE values for the 10¢/sec case are not available at higher extrusions because clad failure has occurred before these higher values are attained.

The magnitudes of the reactivity effects shown from prefailure molten fuel extrusion are typical of what would be obtained for the extrusions obtained in M4, with U-5 Fs fuel. In M5, with prototypical fuel, extrusions were down by a factor of 5 to 10 from these, for reasons not yet understood.

C. Conclusions

It appears that if dynamic effects really exist in metal fuel extrusion, they cannot be very large at least up to ramp rates of 50¢/sec. In any case, the assumption that the molten pin cavity has a constant smear density appears to be satisfactory.

D. References

3-1. Kalimullah, et al., "Advancements in the Modeling of Metallic and Oxide Fuels in the SAS4A Code," ANL/RAS 85-19 (October 1985).

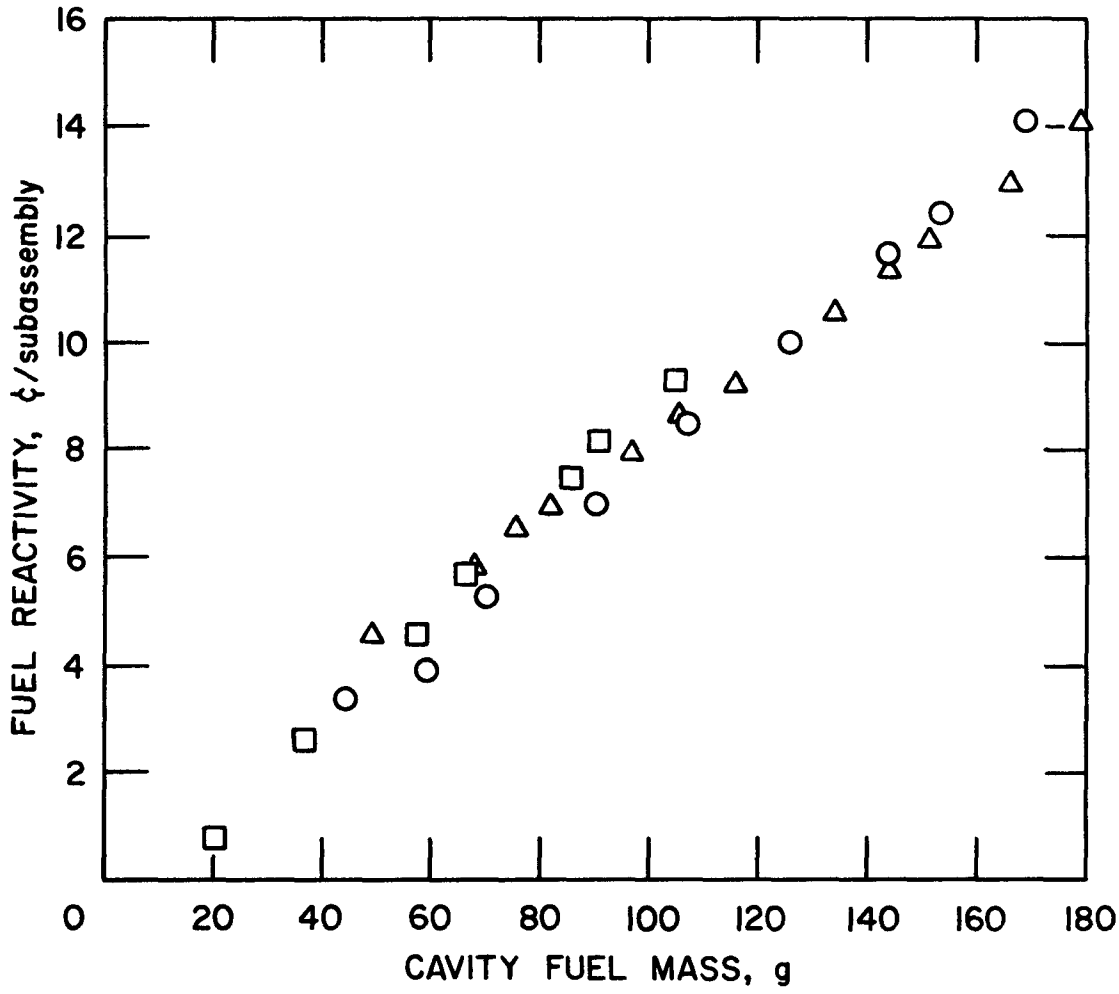

Fig. 3-1. Comparison of Extrusion Reactivity between PINACLE and EXTRUS for Full Length Pins

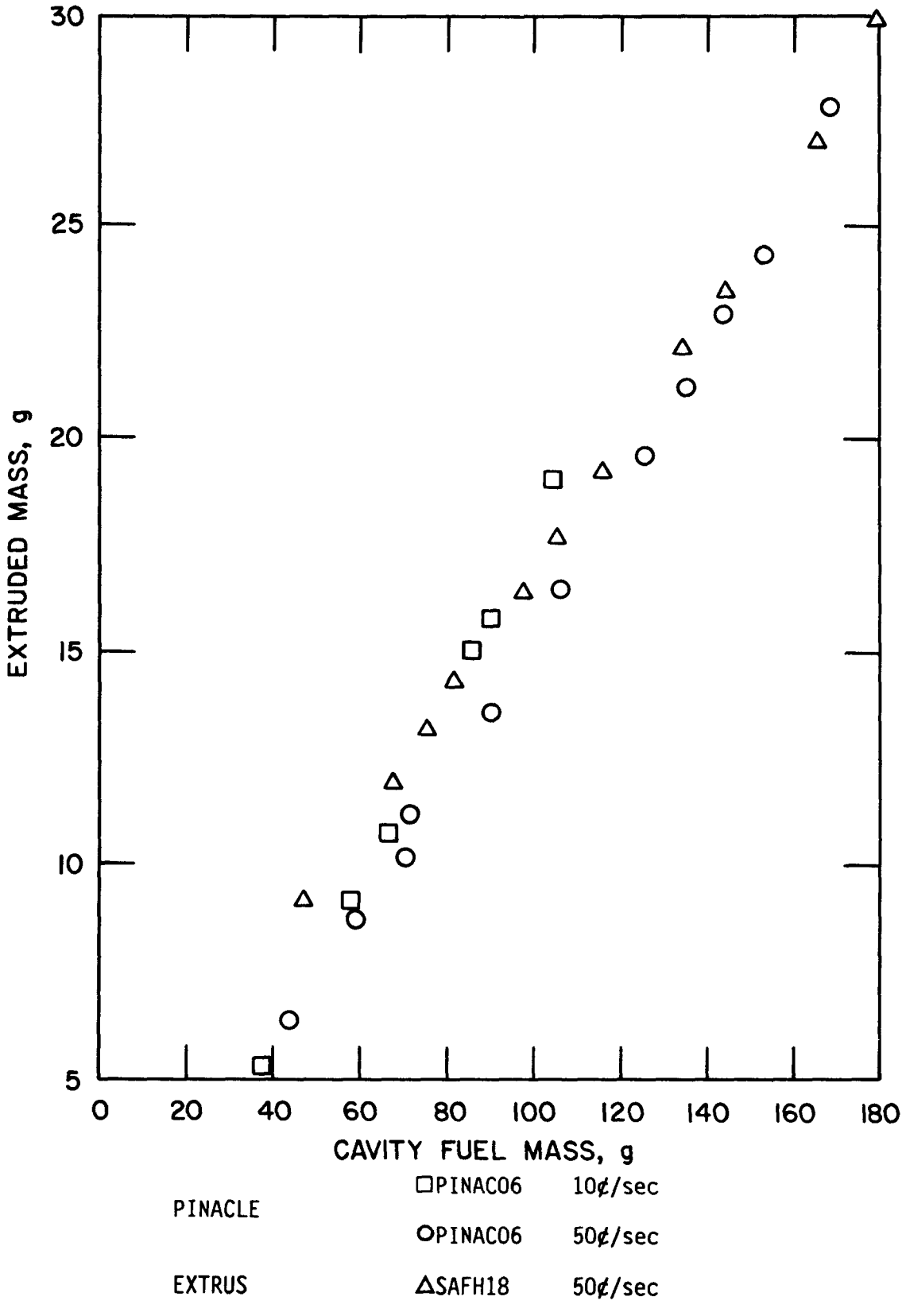

Fig. 3-2. Comparison of Extruded Fuel Mass between PINACLE and EXTRUS for Full Length Pins

TABLE 3-1. Power and Energy Histories for TOP Calculations[a]

10¢/sec TOP

Time, sec.	Normalized Power	Energy, Full Power Second	Cavity Fuel gms PINACLE PINAC06	Fuel Motion Reactivity, Uniform PINACLE
6.60	3.49	12.60	20.7	1.07
7.00	3.76	14.05	37.3	1.05
7.54	4.10	16.18	66.6	1.02
8.14	4.15	18.66	90.7	1.01
8.70	4.19	20.99	104.6	1.01

50¢/sec TOP

Time, sec.	Normalized Power	Energy Full Power Seconds	Cavity Fuel Mass, gms PINACLE PINAC07	Cavity Fuel Mass, gms EXTRUS SAFH18	Fuel Motion Reactivity, Uniform PINACLE
2.15	4.15	5.71	44.1	75.3	1.00
2.55	5.62	7.73	106.5	150.3	1.01
2.65	6.03	8.45	125.3	179.0	1.00
2.75	6.36	8.92	143.1		1.00
2.90	6.73	10.11	168.0		1.00

[a]Average burnup 6.25% FNMELT = 0.3 FPINAC = 0.06
CIPNTP = 1.0.
Single radial zone.
Retained fission gas 5μ mol/gm fuel.
Coolant steady-state inlet temperature 630°K.
Coolant steady-state outlet temperature 810°K.
Steady-state peak linear power 11.4 kW/ft.
Core height 91.44 cm.
Clad inner radius 0.3061 cm.
Clad outer radius 0.3619 cm.
Fuel smear density 11.85 g/c.

TABLE 3-2. Axial Power Distribution in SAFR (End of Cycle)

Core Axial Node[a]	Relative Nodal Power
3	0.660
4	0.725
5	0.794
6	0.859
7	0.875
8	0.922
9	0.961
10	0.989
11	0.993
12	1.000
13	0.997
14	0.984
15	0.978
16	0.943
17	0.899
18	0.845
19	0.824
20	0.751
21	0.673
22	0.595

[a]Each node is approximately 4.6 cm in length as fabricated.

4. APPLICATION OF SSCOMP THREE-ZONE MODEL TO ANALYSIS OF TREAT M5 EXPERIMENT

A. Introduction

The M5 TREAT test, the first on prototypical metal fuel, unexpectedly showed little molten fuel extrusion.[4-1] The extrusion of 1-2% in the F2 M5 transient was much less than the values calculated by Wright et al of 15% for the 0.8% maximum burnup pin and 7% for the 1.9% burnup pin.[4-1] Because these calculations were performed for a model with a single radial zone instead of the three-zone structure typical of irradiated prototypical fuel, it seemed to be of interest to see how use of a model that takes account of the three radial zones would affect the extrusion calculations, particularly with regard to the amount of fuel melting. An obvious possibility for calculation of too much extrusion is overprediction of the amount of fuel melting, to which extrusion is closely tied. Accordingly, calculations for the F2 transient of M5 have been carried out for the 1.9% maximum burnup pin, designated here as Pin 2, to determine the effect of taking the three radial zones into account.

A problem encountered in these calculations was caused by the inability to use DEFORM in the current version of SAS4A for three-zone metal pin calculations. EXTRUS (Section 1) depends on DEFORM to calculate changes in fuel mesh intervals corresponding to transient fuel expansion. Without use of DEFORM, no transient changes in mesh intervals occur, but EXTRUS is nevertheless calculating thermal expansion of fuel contained in a fuel node. The result of this is a spurious reduction in cavity porosity and an overestimate of fuel extrusion which for the present M5 calculations amounts to about 1% of the fuel in volume. This problem was not present in M2 and M4 calculations (Section 2) for which use of DEFORM was possible, but, as discussed in Section 2 was a problem in applying PINACLE to metal fuel because of an inability to use DEFORM. Estimated corrections for this inconsistency have been made for the present calculations, as discussed in the Appendix.

B. Calculation Methods and Data for Radial Zone Formation

The formation of the three radial zones during irradiation has been calculated using the SSCOMP module of SAS4A developed by Kalimullah.[4-2] In

this model, the radii of the zones are determined by input interface temperature TCM, which determines the boundary between central and middle zones, and TMO, which does the same for the middle and outer zones. The compositions of the zones are determined by input equilibrium coefficients CICM and CIMO, which determine the ratios of concentrations of constituent I for the central and middle zones and for the middle and outer zones respectively. Three chemical constituents are involved: plutonium, zirconium, and uranium, but assigning coefficients for only two of these completely defines the system. Coefficients for plutonium (P) and zirconium (Z) will be specified for this purpose.

In order to apply Kalimullah's model to the ternary alloy, it is necessary to have available values of several properties of the ternary system. These properties include solidus and liquidus temperatures, latent heat of fusion, specific heat, density, and thermal conductivity. The amount of data available for these properties is limited, so that Kalimullah found it necessary to develop correlations for them based on what data are available.

It is also necessary to determine the interface temperature and equilibrium coefficients by analysis of radial zone radii and compositions in irradiated ternary alloy fuel. At the time of Kalimullah's initial work on this problem, the available irradiation data on ternary alloys were limited in extent and dated from the initial ANL work on metal fuel development in the 1960's.[4-3] More irradiation data are now becoming available,[4-4] including data from examination of sibling pins of the U-19 Pu-10 Zr pins used in the M5 transients. The data for the 1.9% peak burnup pins for which transient calculations are presented in this section indicate that the central zone is conical in shape, with the base of the cone at the bottom of the pin and the tip at the top. At the bottom the radius of the central zone is about half the total fuel radius, at the core midplane this fractional radius is about 0.30, and at the top it is about 0.20. The middle zone has fractional radial thickness of 0.15 to 0.20 over the entire pin.

In the calculations, 10 radial pin mesh intervals (nodes) have been used. These are of equal volume except that the inner and outer intervals have half the volume of the interior intervals, so that interior intervals

each have 1/9 of the total pin volume and the innermost and outermost intervals 1/18 each. Within this framework, the data from irradiated pin examination indicates that at the bottom of the pin there should be 3 central zone intervals and 2 middle zone intervals, at the midplane there should be 1 to 2 central zone intervals and 1 to 2 middle zone intervals, and at the top of the pin 1 central zone interval and 1 to 2 middle zone intervals. Unfortunately, this pattern is quite different from what is obtained by using temperature criteria for zone formation. Pin temperatures increase with axial height, so that application of these criteria will yield more central and middle zone formation in the upper part of the pin than in the lower. Apparently no explanation for this discrepancy has been advanced so far. It is noted that in the current state of LIFE-METAL development[4-5] no attempt is made to calculate zone formation; rather, radial composition distributions are input based on experimental results.

In spite of this problem, Kalimullah's model has been applied to the M5 experiment in the hope that at least a qualitative indication of the effect of zone formation on fuel melting and extrusion could be obtained. Little fuel melting would be expected to occur in the lower part of the pin in M5, so that a reasonable indication of the effect of zone formation on extrusion may be obtained if this formation is simulated reasonably well in the upper part of the pin.

Zonal compositions used in evaluation of the equilibrium coefficients were obtained from the analysis by M. C. Billone[4-6] of G. L. Hofman's electron microprobe data[4-4] taken at 0.67 of the core height in Pin T179 of EBR-II Subassembly X419. Zonal porosities, required as SSCOMP input, were obtained from Billone's LIFE-METAL calculations for this pin.[4-7] These data are all summarized in Table 4-1. It is noted that with the stated porosities and a pin axial swelling of 3.7%, the fuel does not swell radially all the way to the clad, as it is observed to do experimentally over the entire pin length at 1.9% maximum burnup. The size of the open gap ranges from 0.001 to 0.007 cm depending on the zonal configuration, particularly on how many central zone nodes are present. This gap volume corresponds to 1-5% of the total volume inside the clad.

The actual zone compositions vary with zone outer radii because the total amount of each chemical constituent is assumed conserved in each axial node. The ranges of compositions found for each zone are indicated in Table 4-2, together with corresponding ranges of solidus and liquidus temperatures for the three zones obtained from Kalimullah's correlations. Also given are fuel thermal conductivities, as obtained from Kalimullah's correlations, corresponding to the reference zonal compositions specified in Table 4-2, except that the values in the far right hand column for both conductivities and melting temperature are from Ref. 4-1.

The very low thermal conductivities calculated for the inner zone result from the high assumed porosity fraction and the high Pu and Zr contents. High Zr content also leads to high solidus and liquidus temperatures. Reduction in thermal conductivity from that for pure uranium from increasing either Pu or Zr weight percent is comparable at about 1200 K. At about 900 K the reduction for Pu addition is about half that for Zr addition, according to Kalimullah's work.

Included in the reference parameters for zone formation, as typified by those for Case 23 in Table 4-5 is an assumed fractional logging of fuel porosity of 0.2. In Kalimullah's work no sodium logging was assumed. Because the effect of sodium logging on gas volume was not taken into account in fuel extrusion calculations, it would be more consistent to regard the assumption of sodium logging as a convenient way to vary fuel thermal conductivity.

C. Calculations Performed and Results

After calculation of zone formation in the steady state, M5 transient calculations were carried out with the SAS4A code, using the EXTRUS module (Section 1) to calculate molten fuel extrusion. It was not possible to do this with the actual M5 power history because the SSCOMP calculations must be performed at normal reactor power. Therefore, an altered power history was used, given in Table 4-3, with the power starting at the level at which the fuel was irradiated in EBR-II and rising to 4.3 times normal power, corresponding to the peak power in the F2 transient. The axial maximum steady-state linear power was 39.5 kW/m, (based on cold dimensions), so that

the peak linear power was 170 kW/m, as specified by Wright, et al.[4-1] Coolant flow rate was inadvertently at 64 g/sec, instead of the 66 g/sec specified in Ref. 4-1. A recheck indicated that use of the higher flow rate reduces cavity fuel masses and extrusions by 3-4% of the tabulated values.

A further complication in applying SSCOMP to TREAT experiments arises from the difference in radial flux distribution during the EBR-II irradiation from that the pins are subjected to in the TREAT reactor. Because of this, SSCOMP parameters appropriate for the flat radial flux distribution in EBR-II will not necessarily be the same as those producing the observed zoned configuration with the TREAT radial power distribution. To study the importance of this problem, two sets of calculations were performed, one set with a flat radial flux distribution and another set using the radial flux distribution assumed in TREAT as given in Table 2-3 in Section 2. Because the pin composition is uniform before irradiation, power and flux distributions are then the same. Rearrangement of materials during zone formation alters the power distribution. In SSCOMP the flux distribution is assumed to remain constant during this process.

The effect of varying zone formation on fuel extrusion is shown in Table 4-4 for a flat radial flux distribution and in Table 4-5 for the TREAT flux distribution. In these tables the zone configuration for each axial node is shown, starting from the innermost radial node, with "C" representing central zone composition and "M" middle zone. Recall that this innermost node represents 1/18 of the total pin volume, while interior nodes are 1/9 of the total volume, with 10 radial nodes altogether, including an outermost that is again 1/18 of the total volume. Nodes not shown are understood to be of outer zone composition, except that if nothing is shown for an axial node all radial nodes are understood to be of the original fabricated composition, 15% wt Pu and 10% Zr. It is noted that in these tables the cases have been so arranged that the amount of zone formation increases from left to right for either of the two choices of radial power distribution. In Cases 22 and 29, with the TREAT radial power distribution, the as-fabricated composition has been retained.

It is seen in Tables 4-4 and 4-5 that the mass of cavity fuel and the amount of fuel extrusion do not vary much with varying zone radii for either radial power distribution. A factor that seems significant in producing this result is that zones with lower thermal conductivity tend to have higher melting temperatures. Another factor is that late in the M5 transient, when significant fuel extrusion is calculated to occur, the molten fuel cavity boundary has moved into the outer zone regardless of the zone configuration. An increase in volume of the middle zone, which has a very low Zr content, increases the Zr content of the outer zone, reducing its thermal conductivity and increasing fuel temperature, but also raising solidus and liquidus temperatures even more. As a result, although at first blush it might be expected that increasing the volume of the low melting middle zone would increase cavity fuel mass, the net result is actually to reduce this mass slightly for conditions late in the M5 transient.

The amount of molten cavity fuel calculated in EXTRUS depends on the SAS4A parameter FNMELT, Loc. 1169 in Bl. 13. FNMELT is the fraction of the heat of fusion that must be attained to include fuel in the molten pin cavity. It does not affect the actual amount of fuel melting. Increasing FNMELT decreases the amount of cavity fuel and therefore the amount of extrusion, since in EXTRUS all the porosity and retained gas of fuel entering the cavity is assumed to be released. Molten fuel outside the cavity is not taken into account. FNMELT in most cases, including Case 23 referred to above, was set at 0.3, which seemed to be reasonable in earlier TREAT experiment analyses. With this value of FNMELT the amount of cavity fuel exceeds the amount of molten fuel. Some cases were run with higher values of FNMELT. In one such case, Case 29 in Table 4-5, an increase in FNMELT to 0.50 has reduced the cavity fuel nearly to the molten fuel mass with a significant reduction in fuel extrusion from that in the original Case 22.

In addition to the amount of fuel melting, another important factor in determining the amount of fuel extrusion is the amount of fission gas retained in fuel closed porosity. This retained gas was in most cases set at 5 μmol/gm, as recommended by Sevy for U-5 Fs fuel,[4-8] and also assumed by Wright, et al.[4-1] in M5 analysis. Measurements on the U-19 Pu-10 Zr fuel at 1.9% peak burnup[4-4] show values mainly between 3.0 and 4.0 μmols/gm. Calculations have been performed mainly with 5.0 μmols/gm, as in Case 23, with

Cases 24, 30, and 31 in Table 4-6 representing variations to 3.0, 0.8, and 0.2 μmols/gm, respectively. The amount of retained gas in μmols/gm is specified in Loc. 61 in Bl. 65 in the special version of SAS4A containing EXTRUS. Case 31 corresponds to essentially zero retained gas. Because of the radial variation in retained gas suggested by Gruber's calculations[4-9] the cavity gas could be less than what would correspond to an axial node average, and it was of interest to see how extrusion decreased with decreasing retained gas. The 2.1% extrusion obtained in Case 31 with essentially zero retained gas is caused by the expansion of open porosity gas assumed trapped in the fuel at the start of the transient because of the rise in fuel temperature during the transient.

Finally, in Table 4-7 extreme assumptions about fuel melting and gas retention have been combined to produce a minimum amount of extrusion. In Case 32, a combination of an increase in FNMELT to 0.55, plus an increase in assumed fractional Na logging to 0.4, which increases effective fuel thermal conductivity by about 10-15% in the middle and outer zones and about 30% in the central zone, have been combined to obtain a sharp reduction in cavity fuel. In addition, in Case 33 the assumed retained gas has been reduced to essentially zero, reducing the calculated extrusion to 1.1%. A summary of the cases given in Tables 4-4 to 4-7 together with additional parameters used in the extrusion calculations is given in Table 4-8. The total cavity gas including the open porosity gas in μmols/gm for the various cases is given in Table A1 in the Appendix.

A further parametric variation from the reference cases that decreases fuel extrusion is an increase in the fraction of total porosity assumed to be closed. The closed porosity volumes in the cases listed in Tables 4-4 to 4-8 have been based on the assumption that this porosity traps the retained gas in bubbles having a pressure of 200 atm at steady-state temperatures.[4-8] This leads to a closed porosity fraction of 9% of the total porosity for 5 μmols/gm retained fission gas. On the same basis, this fraction decreases to 5% of the total porosity for 3 μmols/gm retained gas and 2% for 1 μmol/gm. An increase in this fraction for a given amount of retained gas represents a lowering of bubble pressure and therefore of potential for fuel extrusion.[4-8] The effect of such an increase on fuel extrusion is discussed in a later section.

D. Consequences of Assumption that Open Porosity Gas is not Trapped in Fuel

Because it was found to be very difficult to calculate the observed fuel extrusion in M5 with the current EXTRUS modelling particularly with any significant amount of retained gas in the fuel, the consequences of abandoning the assumption that the open porosity gas is trapped in the fuel during the transient were investigated. It should be noted that fuel extrusion models generally assume that whatever gas was present in the fuel at the start of a transient remains trapped during the transient.

At a retained gas content of 5.0 μmols/gm, extrusion results with the new assumption are about the same as with the original EXTRUS modeling. However, there is a reduction in extrusion with the revised modeling at lower gas contents, so that it is possible to calculate the low M5 extrusion with a retained gas content that is low but greater than zero. Applications of this assumption to the M6 experiment was not helpful in explaining the results of that experiment, as discussed in Section 5.

E. Effect of Increasing Closed Porosity Fraction

The effect of increasing the fraction of the total fuel porosity assumed to be closed for a given gas retention is to reduce the amount of released gas present in the fuel, since the split of released plus fill gas between the open porosity and plenum, calculated at steady state in EXTRUS, depends on their respective volumes, inversely weighted with steady-state temperatures. This increase in closed porosity results in a decrease in the total cavity gas in the transient, MGCT in Eq. 6 in Section 1, and an increase in the plenum gas, MGP, thereby reducing the extruded volume ΔV. The total cavity gas volume prior to equilibration at a given time, VGCT, remains the same. The only change is in the fractions coming from open and closed porosity when the cavity forms. The resulting decrease in percent fuel extrusion at 16.05 sec. for a number of cases with different retained gas, assumed uniform over the pin, and closed porosity fraction is shown in Table 4-9. Also shown are the pressures in fuel cavity and plenum prior to equilibration, and the equilibration pressure. The differences between the first two of these pressures represent the potential for fuel extrusion, which becomes less as the closed porosity volume increases and also as the retained gas decreases.

It is seen that implausible large increases in closed porosity fraction are necessary to reduce extrusion to the level observed in M5 without a drastic reduction in assumed retained gas fraction, which is more effective in reducing calculated extrusion. In any case, a large closed porosity volume appears to be inconsistent with a small retained gas content,[4-8] although some increase is possible if there are some large closed pores.[4-10]

F. Conclusions

Taking account of the three zones that develop in the irradiated ternary alloy used in the M5 experiments does not have much effect on calculated fuel melting and extrusion in the transient. Reducing the assumed retained fission gas below 5 μmols/gm of fuel, which is probably reasonable, is effective in reducing extrusion, although a reduction to zero retained gas is necessary to calculate the extrusion measured in M5. A further reduction in calculated extrusion was achieved with a parametric reduction in the calculated amount of cavity fuel. Another approach to reducing the amount of fuel extrusion is to abandon or modify the assumption that open porosity gas is trapped in the fuel from the start of the transient.

Another possible way of reducing calculated fuel extrusion is to reduce the open porosity at the expense of closed porosity. The change required seems implausibly large, however.

Because less fuel melting is being calculated at peak power in M5 F2 than in earlier M-series experiments (Section 2) it is possible that extrusion is being inhibited by frozen material at the top of the pin. Such blockage is not accounted for in the EXTRUS modeling and did not seem to play an important role in the earlier experiments even at lower melt fractions of the order of the peak values attained in M5 F2.

G. References

4-1. A. E. Wright, T. H. Bauer, and W. R. Robinson, unpublished information (1986).

4-2. Kalimullah, et al., "Advancements in the Modeling of Metallic and Oxide Fuels in the SAS4A Code," ANL/RAS 85-19 (October 1985).

4-3. W. F. Murphy, et al., "Postirradiation Examination of U-Pu-Zr Fuel Elements Irradiated in EBR-II to 4.5 Atomic Percent Burnup," ANL-7602 (November 1969).

4-4. R. G. Pahl, et al., "Postirradiation Examinations of U-Pu-Zr Fuel Elements from Subassemblies X419 and X419A," ANL-IFR-55 (October 1986).

4-5. M. C. Billone, et al., "Status of Fuel Element Modeling Codes for Metallic Fuels," ANS/AIME/DOE International Conference on Reliable Fuels for Liquid Metal Reactors, Tucson, AZ (September 7-11, 1986).

4-6. M. C. Billone, unpublished information (1986).

4-7. M. C. Billone, private communication (November 1986).

4-8. R. H. Sevy, unpublished information (1986).

4-9. E. E. Gruber, "The STARS Model for Fission-Gas Behavior: I. Steady State Behavior," ANL-IFR-58 (October 1986).

4-10. J. M. Kramer, T. H. Hughes, and E. E. Gruber, "Validation of Models for the Transient Behavior of Metallic Fast Reactor Fuel," ANL-1FR-66 (April 1987).

TABLE 4-1. Data Used in SSCOMP Parameter Adjustment and Input Preparation for U-19 Pu-10 Zr Pin Irradiated to 1.9% Peak Burnup

Zone	Central	Middle	Outer
Fractional Outer Radius			
Pin Bottom	0.50	0.65-0.70	1.00
Midplane	0.30	0.45-0.50	1.00
Top	0.20	0.35-0.40	1.00
Wt % Pu	26.0	21.0	17.0
Wt % Zr	25.0	2.0	11.0
Porosity	0.40	0.19	0.25
Fractional Sodium Logging	0.20	0.20	0.20

TABLE 4-2. Properties of Zones

Zone	Central	Middle	Outer	As Fabricated	Wright et al.[4-1]
Porosity	0.40	0.19	0.25	0.25	0.28
Fraction Na Log.	0.20	0.20	0.20	0.20	0.20
Wt % Pu					
Reference	26.	22.	17.	19.	19.
Range in Calc.	22-27	21-24	15-19		
Wt % Zr					
Reference	25.	2.	11.	10.	10.
Range in Calc.	20-29	2	9-14		
Thermal Conductivity for Reference Zone Compositions, Watts/m-K					
T,K					
600	5.3	13.0	11.2	10.9	
700	6.3	15.3	12.9	12.6	13.0
800	7.2	17.2	14.5	14.2	
900	8.2	18.8	16.0	15.6	14.0
100	9.1	20.0	17.4	16.9	
1100	10.0	20.7	18.6	18.1	15.0
1200	10.9	21.2	19.9	19.1	
1300	11.8	21.2	21.0	20.0	16.0
1400	12.7	21.0	22.0	20.8	
1500	19.4	25.9	23.8	23.8	17.0
Range of Solidus Temp, K	1434-1526	1225-1255	1356-1393	1348	1360
Range of Liquidus Temp, K	1705-1779	1345-1376	1593-1649	1583	1560

TABLE 4-3. Power History Used in Transient Calculations

Time, sec.	Normalized Power
4.3	1.0
8.5	1.5
10.0	1.83
13.0	2.87
16.0	4.30

TABLE 4-4. Effect of Varying Zone Formation and Retained Gas on Fuel Extrusion for Flat Radial Flux Distribution

Case	15[a]	20	27	16
TCM, K	955	935	935	920
TMO, K	920	905	905	890
CPCM	0.868	0.800	0.800	0.868
CPMO	0.670	0.670	0.670	0.670
CZCM	9.43	8.50	8.50	9.43
CZMO	4.57	4.57	4.57	4.57
Retained Gas, μmol/gm fuel	5.0	5.0	3.0	5.0
FNMELT	0.3	0.3	0.3	0.3
	Zone Configuration by Axial Node			
15	M	CMM	CMM	CCMM
14	MM	CM	CM	CCMM
13	MM	CCMM	CCMM	CCMM
12	M	CMM	CMM	CCMM
11	M	CMM	CMM	CCMM
10	M	CCMM	CCMM	CCMM
9	MM	CCM	CCM	CCM
8	M	CMM	CMM	CCMM
7		CM	CM	CM
6		MM	MM	CM
5		M	M	MM
4				M
Gms Cavity Fuel @ 16.05 sec.	34.1	36.4	36.4	35.6
% Cavity Fuel @ 16.05 sec.	41.0	43.8	43.8	42.8
% Molten Fuel @ 16.05 sec.	31.9	35.6	35.6	33.1
Extrusion Volume @ 16.05 sec.	0.74	0.76	0.50	0.75
% Extrusion @ 16.05 sec.	10.4	10.6	7.0	10.5

[a] Na log fraction 0.4

TABLE 4-5. Effect of Varying Zone Formation on Fuel Extrusion for TREAT Radial Flux Distribution

Case	22[a]	29[a]	23	18
TCM,K			912	920
TMO,K			895	890
CPCM			0.800	0.755
CPMO			0.670	0.670
CZCM			9.00	7.61
CZMO			4.51	4.51
Retained Gas, μmols/gm fuel	5.0	5.0	5.0	5.0
FNMELT	0.30	0.50	0.30	0.30
Zone Configuration by Ax. Node				
15			CM	MMM
14			CMM	CMMM
13			CM	CMMM
12			CCM	CCMM
11			CCM	CMMM
10			CMM	CMM
9			CM	CMM
8			CM	MM
7			M	MM
Gms Cavity Fuel @ 16.05 sec.	32.9	24.0	30.4	28.9
% Cavity Fuel @ 16.05 sec.	39.6	28.8	36.6	34.8
% Molten Fuel @ 16.05 sec.	26.4	26.4	25.3	29.3
Extruded Volume @ 16.05 sec., cc	0.70	0.56	0.66	0.64
% Extrusion @ 16.05 sec.	9.8	7.8	9.2	9.0

[a]As fabricated composition.

TABLE 4-6. Effect of Varying Retained Gas Content on Fuel Extrusion for TREAT Radial Flux Distribution

Case	23	24[a]	30[a]	31[a]
Retained Gas, μmols/gm fuel	5.0	3.0	0.8	0.2
Extruded Volume @ 16.05 sec., cc	0.66	0.43	0.20	0.15
% Extrusion	9.2	6.0	2.8	2.1

[a]Other parameters as for Case 23

Table 4-7. Effect of Variations in Amount of Cavity Fuel and Retained Gas on Fuel Extrusion for TREAT Radial Flux Distribution

Case	32	33	23
Retained Gas, μmols/gm fuel	5.0	0.01	5.0
FNMELT	0.55	0.55	0.30
Fraction Na Logging	0.40	0.40	0.20
Zone Configuration by Axial Node[a]			
15	M	M	CM
14	MM	MM	CMM
13	CM	CM	CCM
12	CM	CM	CCM
11	CM	CM	CCM
10	CM	CM	CMM
9	M	M	CM
8			CM
7			M
Gms Cavity Fuel @ 16.05 sec.	16.8	16.8	30.4
% Cavity Fuel @ 16.05 sec.	20.2	20.2	36.6
% Molten Fuel @ 16.05 sec.	22.4	22.4	25.3
Extruded Vol. @ 16.05 sec., cc	0.43	0.08	0.66
% Extrusion @ 16.05 sec.	6.0	1.1	9.2

[a]Zone formation parameters same as for Case 23

Table 4-8. Summary of Pin Conditions at 16.05 Seconds for Tabulated Cases.

Case	FNMELT	Fraction Na Logging	Retained Gas, µmols/gm	MFC, Gms	MGCC, µmols	VGCT, cc	MGCT. µmols	Cavity Gas	Total MGTO, Gas, µmols/gm	MGP, µmols	TF2 K	ΔV, cc	EXTRUS % Extrusion	EXTRUS P, Bar
							Flat Radial Flux Distribution							
15	0.30	0.20	5.0	34.1	171	0.58	290	8.5	1174	874	1566	0.74	10.4	28.5
20	0.30	0.20	5.0	36.4	182	0.69	322	8.8	1174	862	1570	0.76	10.6	29.0
27	0.30	0.20	3.0	36.4	109	0.69	274	7.5	1341	974	1570	0.50	7.0	30.1
16	0.30	0.20	5.0	35.6	182	0.73	331	9.3	1174	845	1548	0.75	10.5	28.8
							TREAT Radial Flux Distribution							
22	0.30	0.20	5.0	32.9	165	0.57	282	8.6	1174	872	1518	0.70	9.8	28.0
29	0.50	0.20	5.0	24.0	120	0.42	205	8.5	1174	872	1546	0.56	7.8	26.7
23	0.30	0.20	5.0	30.4	155	0.59	275	9.0	1174	854	1516	0.66	9.2	27.7
18	0.30	0.20	5.0	28.9	145	0.49	242	8.4	1174	873	1547	0.64	9.0	27.5
24	0.30	0.20	3.0	30.4	91	0.59	236	7.8	1341	965	1516	0.43	6.0	29.3
30	0.30	0.20	0.8	30.4	24	0.59	193	6.3	1524	1084	1516	0.20	2.8	30.7
31	0.30	0.20	0.2	30.4	6	0.59	182	6.0	1573	1116	1516	0.15	2.1	31.1
32	0.55	0.40	5.0	16.8	84	0.27	140	8.3	1174	864	1538	0.43	6.0	25.7
33	0.55	0.40	0.01	16.8	0	0.27	83	4.9	1589	1140	1538	0.08	1.1	30.6

TABLE 4-9. Effect of Variation in Closed Porosity on Fuel Extrusion for Varying Retained Gas at 16.05 sec. with EXTRUS Model

Retained Gas, μmols/gm	Closed Porosity, Percent of Total Porosity	Total Cavity Gas, μmols MGCT	Total Cavity Gas, μmols/gm Fuel	Plenum Gas, μmols	% Extrusion	Cavity, Initial	Pressures, bars Plenum, Initial	Equilibrium
5.0	9[a]	275	9.0	854	9.2	66.7	22.8	27.7
	50	230	7.6	974	5.6	55.7	26.1	29.2
	100	155	5.0	1174	0.4	37.6	31.4	31.7
3.0	5[b]	236	7.8	965	6.0	57.2	25.8	29.3
	50	178	6.3	1112	1.9	43.1	29.8	31.0
1.0	2	193	6.3	1074	2.9	46.7	28.8	30.5
	25	164	5.4	1151	1.0	39.7	30.7	31.3

[a] Identical with Case 23 in Table 4-5 and 4-8. Zone formation parameters for all cases the same as for Case 23.
[b] Identical with Case 24 in Tables 4-6 and 4-8.

5. ANALYSIS OF M6 EXPERIMENT

A. Introduction

The application of the SSCOMP module[5-1] of SAS4 to analysis of the M5 experiment was discussed in Section 4. This module makes possible the calculation of formation of the three radial zones observed in irradiated U-19 Pu-10 Zr pins. Prefailure fuel extrusion was calculated with EXTRUS (Section 1). In this section similar calculations have been carried out for M6, in which the observed prefailure axial expansion was found to be 3-5% (including 1% solid fuel expansion),[5-2] a result easier to reproduce by analysis than the 1-2% observed in M5. Because the peak power was higher in M6, more fuel extrusion is to be expected than in M5, but this alone does not explain the difference in results for the two experiments.

B. Calculation Methods and Data

Application of the SSCOMP module to calculation of zone formation was carried out as discussed in Section 4, with EXTRUS again applied to calculation of prefailure fuel extrusion. Parallel calculations were carried out with zone formation, using a prototypical steady-state power, and also with the actual TREAT power history. In the latter case no zone formation occurs because of low fuel temperatures at the very low initial power level. It was desired to study the effects of zone formation on prefailure fuel extrusion by comparing the results of these two sets of calculations. Several points had to be considered, however, to assure consistency in this comparison, as follows:

1. For prototypical steady-state power the steady-state fuel temperature will be higher than the plenum temperature. This causes the fraction of total free gas contained in the open pores of the fuel instead of in the plenum to be less than for the TREAT power history, in which these temperatures are the same.

2. Experimentally the U-19 Pu-10 Zr fuel is found to be swollen out to the clad along the entire length of the pin. It is desirable to compare the

cases with and without zone formation on this basis to assure that consistent assumptions are made for fuel porosity, which affects fuel extrusion. There is always some open gap for axial nodes with swelling less than the maximum, which is adjusted so that fuel having maximum swelling just reaches the clad. However, it is not possible to obtain uniform radial swelling with zone formation with SSCOMP because of the axial variation in zone formation, the three zones differing in porosity.

3. Because of the differing initial conditions in the two cases, it seemed possible that pin thermal conditions late in the transient might differ.

The first point was dealt with by recalculating the distribution of free gas between fuel open porosity and plenum assuming they were initially at the same temperature. The second point was addressed by increasing the fuel open porosity in the cases with zone formation by the amount of the fuel-clad gap. With regard to the third point, a study of heat balances over the pins showed that pin thermal conditions for the two power histories were very close after about 7.0 seconds into the transient, at a time when TREAT power had reached 44% of its maximum. No fuel melting had yet occurred at this time.

In addition to the adjustments to EXTRUS cases with zone formation described above, an additional adjustment had to be made to the fuel pin cavity gas volume in each case because of a spurious reduction in transient cavity porosity caused by an inconsistency in fuel density calculations discussed in Sections 2 and 4 arising from the inability at present to use SSCOMP and DEFORM simultaneously in SAS4A.

Pin failure in EXTRUS corresponds to 1% plastic clad strain as calculated by the method of Di Melfi and Kramer,[5-3] which is assumed appropriate for the D9 cladding on the M6 pins. Rapid eutectic attack is assumed to occur when the average of the outer fuel and inner clad temperature exceeds 1353 K. Since the undamaged clad is still fairly strong at this temperature, failure tends not to occur before this temperature is reached and fairly soon afterward, with about 50% of the clad thickness removed at the time of failure.

Experimentally the axial swelling during steady-state irradiation in the U-19 Pu-10 Zr fuel does not exceed about 3%.[5-4] It is now possible in SSCOMP to specify a limit on percentage axial swelling in Loc. 104 in Bl. 63. This limit was specified for the Pin 2 calculations as 3.0%. In practice what was obtained was an axial swelling of 3.9%. For Pin 1 the axial swelling obtained was 3.6% without specifying a limit.

C. Calculations Performed and Results

Two pins were used in the M6 experiment. Pin 1 had a peak burnup of 1.9% and Pin 2 had 5.3%. It was assumed that the average burnup was 10% less than the peak, with 1.727% for Pin 1 and 4.82% for Pin 2. For each of the parallel cases with and without zone formation, two cases involving variation of pin power and coolant flow were run for each pin. For Pin 1, for Case 1 the TREAT power coupling factor (PCF) in watts/gm/MW TREAT power was set at 4.9 and the sodium flow rate per pin at 85 gms/sec. For Case 2 the PCF was set at 5.2 and the flow at 91 gms/sec. For Pin 2, in Case 1 the PCF was set at 4.9 and the flow at 87 gms/sec/pin, while in Case 2 the PCF was set at 5.2 and the flow at 91. These parameter selections follow suggestions by Bauer,[5-5] except that he suggested a PCF of 5.1 instead of 5.2 for Pin 2 Case 2. The TREAT radial power distribution given in Table 2-3 of Section 1 was used in all calculations for this section.

Normalized power histories for the cases without and with zone formation are given in Table 5-1. For the actual TREAT power the tabulated numbers are the TREAT power in megawatts. For the cases with zone formation, the normalized powers are related to a steady-state power axial peak power of 197.6 watts/gm (14.2 kW/ft) for the case having the same peak transient power density as the TREAT power history case with PCF = 4.9, and to 209.7 watts/gm (15.1 kW/ft) for the TREAT power history case with PCF = 5.2.

The zone configurations obtained with various steady-state parameter assumptions for the cases with zone formation are shown in Table 5-2. The scheme followed in this display is the same as that described in Section 4, again with ten radial pin mesh intervals or nodes for each axial node which are of equal volume except that the innermost and outermost have half the

volume of the interior nodes. Properties of the zones and the significance of associated parameters were discussed in Section 4. At the far right-hand side of Table 5-2 is given the range of zonal configurations obtained from PIE, showing a conical shape for the central zone not reproducible by SSCOMP, as discussed in Section 4.

In Table 5-2 are shown the porosity fractions for each zone as input to SSCOMP. Also shown is the fuel porosity averaged over all the axial nodes as calculated in EXTRUS. This is less than what is obtained by summing up the zonal porosities input to SSCOMP because of the solid fission product swelling assumed in EXTRUS as 2.2% of the fabricated fuel volume per percent average fuel burnup. The effect of removing this reduction in porosity is shown in the values given in parentheses. Also shown in Table 5-2 are the volume of the fuel/clad gap obtained for the various zonal configurations. In calculating fuel extrusion, the pin fuel porosities were augmented by this amount, and the part of the fuel cavity gas volume before equilibration coming from open porosity in the original unmelted fuel was increased proportionally to the total fuel open porosity. This results in a total fuel porosity of about 0.280 if the solid fission product swelling is removed.

Three values for fission gas retained in closed porosity were used for each of the cases: 0.01 μmols/gm fuel (essentially zero), 1.0 μmols/gm, and 3.0 μmols/gm. A single case was also calculated for Pin 1 at 4.0 μmols/gm and a case for Pin 2 was calculated at 5 μmols/gm. With the zero value, all fuel extrusion is obtained by the expansion of open porosity gas, assumed trapped in the fuel after the start of the transient. Values of 3-4 μmols/gm were found in examination of U-19Pu - 10Zr fuel at 1.9% peak burnup.[5-4] In all calculations the FNMELT parameter, which corresponds to the fraction of the latent heat of fusion attained by fuel entering the pin cavity, was set at 0.5. With this choice, the mass of cavity fuel is approximately the same as the total molten fuel mass. The plenum gas volume was set at 3.5 cc for Pin 1 and at 3.3 cc for Pin 2, as suggested by Bauer.[5-5] Higher values for retained gas were found at 5.4% burnup.[5-6]

With the assumed steady-state powers and radial power distribution, reasonable agreement with the observed zonal configuration in the upper part

of the pin was obtained by setting TCM = 880 K and TMO 865 or 855 K, as shown in Table 5-2. These parameters are defined in Section 4. Both of these values of TMO were used for Pin 1 Case 1, with no difference in the fuel extrusion obtained.

Results obtained for fuel extrusion for the various cases mentioned are shown in Table 5-3. More details concerning these calculations are given in Table 5-4 for cases with no zone formation and in Table 5-5 for cases with zone formation. Several important points are evident from these results, as follows:

1. Zone formation does not have much effect on fuel extrusion, as also found for M5 (Section 4). Extrusion tends to be slightly higher for the cases with no zone formation.

2. Best agreement is obtained with the measured extrusions with zero retained gas, as also found by Bauer.[5-5] This is particularly true for Pin 1, in which the calculated extrusions quickly become much larger than the measured one as the retained gas content increases.

3. Extrusion is slightly larger for the higher power, higher flow rate case, particularly for Pin 1.

Factors that could cause a difference in calculated fuel extrusion between the zoned and non-zoned cases are differences in cavity porosity, in pin heat transfer, and in fuel melting temperatures. Because of the assumption made in calculating fuel extrusion that the fuel is swelled to the clad in both cases, the average fuel porosity should be the same. Volume changes in mixing components to form zonal compositions could affect this, but these are in general not known and have been neglected in Kalimullah's fuel density corrections.[5-1] There is a radial variation in porosity in the zoned cases, so that the original porosity of the fuel in the cavity, which is present in the interior part of the pin, will in general differ from the average fuel porosity. The average cavity porosity fractions in the present calculations at steady state were 0.01-0.06 greater than the corresponding average steady state total fuel porosity fractions, which range from 0.18 to

0.24, so that averaging porosities over the zones in the cavity gave a result not too much different from the average fuel porosity. There could be more disparity with different choices of the zonal porosities, which are not very well known. The disparity found here is not large enough to have a great effect on fuel extrusion.

The cavity fuel temperatures for the zoned and non-zoned cases did not differ significantly, as can be seen by comparing the values given in Tables 5-4 and 5-5. Cavity fuel masses were a few percent larger in the non-zoned cases, which is probably the main reason that fuel extrusion was found to be a little larger in these cases.

With regard to the variation of extrusion with retained gas content, it is not immediately obvious why best agreement with experiment is obtained with zero retained gas. It is possible that a strong radial variation in retained gas[5-7] could cause the retained gas in the cavity to be much less than the average over the entire fuel radius at a given axial location, but for Pin 1 the required effect seems rather extreme. For Pin 2, not such an extreme reduction in closed porosity gas content is required because of the smaller effect of closed porosity gas relative to that of open porosity gas at higher burnup. Even in this case, however, use of the measured radially averaged gas content at a given axial location gives calculated extrusions outside the measured range.

Another possible explanation for overprediction of extrusion with the measured retained gas is that part of this gas is trapped in large pores[5-7]. In the calculation method currently used when applying FPIN2[5-7], this gas is not effective in causing extrusion, so that this large pore gas is subtracted from the total retained gas while keeping the division between open and closed porosity the same. When taking account of this large pore gas in the EXTRUS method, the total retained gas stays the same, but the closed porosity volume is increased at the expense of the open porosity volume. This can be viewed as reducing the extrusion potential of the closed porosity gas through a reduction in its pressure.[5-8] The way it affects the application of Eq. 6, Section 1, is that a reduction in open porosity volume VGFO reduces the fraction of total free gas in the fuel open porosity at steady state while

correspondingly increasing the fraction of this gas in the plenum. This then leads to a reduction in the total cavity gas MGCT and a reduction in extrusion. For Pin 1 Case P125 in Table 5-4, with 3.0 μmols/gm retained gas and PCF = 2.49, reducing the open porosity to 0.75 of its original value with a corresponding increase in closed porosity reduces calculated extrusion from 8.8 to 5.9%.

In Section 4, in order to calculate the extremely low extrusions measured in M5 an alternate model was studied in which the extrusion obtained from heating of open porosity gas trapped in the fuel was eliminated by allowing this gas to expand into the plenum. Some reduction in this trapping effect seems reasonable, at least up to the beginning of fuel melting. For Pin 2 the alternate model gives about the right extrusion with the measured retained gas. However, for Pin 1 the alternate model still gives a fuel extrusion of 7-9% at the measured retained gas content, a reduction of only 1-2% from the original EXTRUS model, not of much help in reducing the discrepancy between calculation and experiment. The smaller effectiveness of this approach for the lower burnup fuel arises from the smaller amount of open porosity gas present for a given concentration of closed porosity gas and a reduced total amount of fission gas.

As an alternative to the pin cavity model used in EXTRUS as well as in several other codes modeling fuel pin behavior, Bauer[5-5] is currently using a model in which extrusion is produced by expansion of gas in the total fuel open porosity, assumed trapped in the fuel at the start of the transient. Closed porosity gas is assumed ineffective in producing extrusion. Aside from not defining a pin cavity, this model is similar to those used in EXTRUS and in FPIN2. Application of this model, with zero assumed retained closed porosity gas, gives extrusions slightly less than those with the cavity model but still in good agreement with experiment. Although the larger gas volume undergoing expansion tends to increase extrusion, this is offset by the lower average gas temperature compared to that of the cavity model. Results from this model are given in Table 5-6. Extrusions are seen to be slightly less than those obtained with the cavity model with zero retained gas as given in Table 5-3.

Failure in Pin 2, which occurred experimentally, was calculated to occur only for PCF = 5.2. For PCF = 4.9, peak fuel-clad interface temperatures tend to be 5-10 K lower, and as a result, an interface temperature of 1353 K is not quite attained and rapid eutectic attack of clad does not occur. For Pin 1, pressures are much lower and calculated clad strains are small consistent with the experimental nonfailure of Pin 1. Because of a number of uncertainties in the clad failure calculations, these calculations probably do not provide an unambiguous basis for selecting PCF = 5.2 instead of 4.9.

D. Conclusions

The fuel extrusion measured in M6 is calculated reasonably well with EXTRUS assuming no retained fission gas, with the force producing extrusion provided by expansion of open porosity gas trapped in the fuel as the fuel is heated. Using the measured retained gas gives far too much extrusion, particularly for Pin 1. Possible explanations of this discrepancy are radial variation of the retained fission gas and retention of part of the gas in large closed pores. An alternate model for reducing extrusion by allowing expansion of open porosity gas into the plenum during the transient was not helpful in removing the discrepancy for Pin 1. The extrusion results were nearly the same regardless of whether or not the formation of radial zones was taken into account.

An alternate fuel extrusion model in which open porosity gas in the entire fuel pin undergoes expansion, with closed porosity gas not considered, gave satisfactory results with calculated extrusions slightly less than those using EXTRUS with zero retained gas.

E. References

5-1. Kalimullah, et al., "Advancements in the Modeling of Metallic and Oxide Fuels in the SAS4A Code," ANL/RAS 85-19 (October 1985).

5-2. Y. I. Chang, "Integral Fast Reactor Program Quarterly Progress Report for the Period January - March 1987," ANL-IFR-68 (1987).

5-3. J. M. Kramer, unpublished information (1985).

5-4. R. G. Pahl, et al., "Postirradiation Examination of U-Pu-Zr Fuel Elements from Subassemblies X419 and X419A," ANL-IFR-55 (October 1986).

5-5. T. H. Bauer, private communication (March 5, 1987).

5-6. Y. I. Chang, "Integral Fast Reactor Program Quarterly Progress Report for the Period January - March 1987," ANL-IFR-68 (1987).

5-7. J. M. Kramer, T. H. Hughes, and E. E. Gruber, "Validation of Models for the Transient Behavior of Metallic Fast Reactor Fuel," ANL-IFR-66 (April 1987).

5-8. R. H. Sevy, unpublished information (1986).

TABLE 5-1. Power Histories used in M6 Calculations

Time, Sec.	No Zone Formation TREAT Power MW	Zone Formation Relative Power
3.6	1.0	1.00
4.2	6.2	1.00
4.75	32.0	1.20
5.0	61.5	1.53
5.5	74.0	1.84
6.0	79.0	1.96
7.0	89.4	2.22
7.5	94.2	2.34
8.0	101.0	2.50
9.0	114.6	2.84
10.0	128.2	3.18
10.5	136.5	3.38
11.0	148.0	3.67
11.5	158.6	3.94
12.0	170.0	4.22
12.5	182.5	4.53
13.0	196.4	4.81
13.25	203.1	5.04
13.35	119.5	2.97
13.45	37.6	0.94

TABLE 5-2. Zone Configurations for M6 Calculations for Cases with Prototypical Steady-State Power

Steady-State Power, watts/gm	197.6	197.6	197.6	209.7	209.7	Observed Zonal Configuration Range		
Coolant Flow, kg/sec/pin	0.085	0.085	0.087	0.091	0.091			
TCM,K	880	880	880	880	880			
TMO,K	865	855	855	865	855			
Axial node[a]			Zonal Map					
15		M	MM	M	CM	CMM	CM	CMM
14		CM	CMM	CMM	CCM	CCM	CM	CMM
13		CCM	CCMM	CCM	CCM	CMM	CM	CMM
12		CCM	CMM	CCMM	CCM	CCMM	CM	CMM
11		CCM	CMM	CMM	CCM	CCMM	CM	CCMM
10		CCM	CMM	CCMM	CCM	CCM	CM	CCMM
9		CCM	CCM	CCM	CCM	CCM	CM	CCMM
8		CM	CCM	CM	CCM	CCM	CM	CCMM
7		CM	CMM	CM	CCM	CCM	CM	CCMM
6		CM	CM	CM	CM	CM	CCMM	
5			M	M		MM	CCMM	CCMM
4						CCMM	CCCMM	
3						CCMM	CCCMM	
2						CCCMM	CCCMM	
1						CCCMM	CCCMM	
Zonal Porosity Fraction								
Center	0.40	0.40	0.40	0.40	0.40			
Middle	0.19	0.19	0.19	0.19	0.19			
Outer	0.26	0.26	0.25	0.26	0.25			
Swollen Fuel Vol, cc		7.10	7.05	6.99	7.05	7.04		
Fuel/Clad Gap Vol. cc	0.167	0.224	0.293	0.120	0.251			
Average Fuel Porosity Fraction								
1.9% Max BU	0.239 (0.263)[b]	0.233 (0.257)		0.244 (0.268)				
5.3% Max Bu			0.177 (0.246)		0.181 (0.251)			

[a]Height of each axial node as fabricated is 2.307 cm, giving a total height of 34.60 cm. Inner clad radius 0.254 cm, outer 0.292 cm.

[b]Values in parentheses include volume of solid fission products.

TABLE 5-3. Summary of Fuel Extrusion for M6 at Peak Power

		No Zone Formation		Zone Formation					
	Retained Gas, µmol/gm	0.01	1.0	3.0	0.01	1.0	3.0	4.0	5.0
PCF	Na Flow, gms/sec/pin	Fuel Extrusion, Percent							
				Pin 1 (1.9% max BU)					
4.9	85	4.2	5.9	9.4	3.9	5.5	8.8	10.6	
5.2	91	5.1	6.9	10.8	4.5	6.1	9.6		
				Pin 2 (5.3% max BU)					
4.9	87	3.5	4.1	5.2	3.8	4.3	5.2	6.2	
5.2	91	3.8	4.5	5.7	3.9	4.3	5.2		

TABLE 5-4. Results of M6 Extrusion Calculations at Peak Power with Zone Formation

Case	Max BU,%	Steady State Power, watts/gm	Equivalent PCF, watts/ gm/MW	Coolant Flow, gms/ pin/sec	TCM, K	TMO, L	Retained Δ Gas, μ μmols/ gm	TF2, K	TP2, K	VGP, cc	MFC, gms	MGP, μmols	MGCT, μmols	P bars	VGCT, cc	V, cc	% Extrusion
P129	1.9	197.6	4.9	85	880	865	0.01 1605	1165	3.5	36.8	1019	260	30.6	0.857	0.276	3.9	
P124					1.0			971	281	30.2		0.385	5.5				
P125					3.0			873	324	29.3		0.617	8.8				
P128	1.9	197.6	4.9	85	880	855	0.01 1625	1165	3.5	36.5	1020	246	30.6	0.808	0.276	3.9	
P130					1.0			971	276	30.2		0.386	5.5				
P126					3.0			874	310	29.3		0.618	8.8				
P119	1.9	209.7	5.2	91	880	865	0.01 1612	1150	3.5	40.0	1019	289	30.6	0.948	0.317	4.5	
P118					1.0			971	310	30.2		0.427	6.1				
P117					3.0			813	357	29.5		0.673	9.6				
P238	5.3	197.6	4.9	87	880	855	0.01 1609	1148	3.3	36.4	2736	596	86.1	0.660	0.266	3.8	
P242					1.0			2693	615	85.7		0.300	4.3				
P237					3.0			2607	650	84.8		0.366	5.2				
P243	5.3	209.7	5.2	91	880	855	0.01 1629	1159	3.3	39.0	2737	655	87.1	0.747	0.272	3.9	
P227					1.0			2696	672	86.7		0.303	4.3				
P229					3.0			2608	705	85.7		0.367	5.2				

TABLE 5-5. Result of M6 Extrusion Calculations at Peak Power with No Zone Formation

Case	Max BU,%	PCF, watts/ gm/MW	Coolant Flow, gms/ pin/sec	Retained Gas, µmol/ gm fuel	Input Fuel Porosity	TF2, K	TP2, K	VGP, c	MFC, cc	MGP, gm.	MGCT, µmols	VGCT, µmols	δV, cc	% Extrusion
P122	1.9	4.9	85	0.01	0.288	1627	1162	3.5	38.3	1013	258	0.851	0.293	4.2
P121				1.0						964	281		0.410	5.9
P120				3.0						865	328		0.658	9.4
P113	1.9	5.2	91	0.01	0.288	1640	1160	3.5	43.2	1013	291	0.958	0.355	5.1
P112				1.0						964	317		0.489	6.9
P111				3.0						865	328		0.757	10.8
P240	5.3	4.9	87	0.01	0.285	1629	1146	3.3	37.4	2747	571	0.655	0.241	3.5
P236				1.0						2102	597		0.290	4.1
P234				3.0						2609	640		0.367	5.2
P231	5.3	5.2	91	0.01	0.285	1647	1158	3.3	43.2	2781	658	0.753	0.267	3.8
P241				1.0						2703	682		0.317	4.5
P233				3.0						2609	732		0.403	5.7

TABLE 5-6. Results of Extrusion by Bauer Model, Zero Retained Gas

Case	PCF PCF	TF2, K	TP2, K	VGFO, cc	Δ V, cc	% Extrusion
Pin 1, nonzoned	4.9	1438	1162	1.886	0.269	3.8
	5.2	1460	1160	1.886	0.290	4.1
Pin 1, zoned	4.9	1421	1165	1.863	0.248	3.5
	5.2	1418	1150	1.864	0.262	3.7
Pin 2, nonzoned	4.9	1433	1146	1.506	0.240	3.4
	5.2	1466	1158	1.506	0.254	3.6
Pin 2, zoned	4.9	1419	1148	1.527	0.230	3.3
	5.2	1439	1160	1.526	0.233	3.3

6. CLAD FAILURE AND FUEL EXTRUSION IN METAL FUEL

A. Introduction

The M5 experiment, using irradiated prototypical metal fuel, showed unexpectedly low fuel extrusion but also indicated that pin failure might not occur in a transient overpower (TOP) accident before a considerable power rise had taken place.[6-1] In this section fuel extrusion and clad failure conditions in a full-length prototypical pin are calculated using a three-zone calculation based on the SSCOMP model,[6-2] taking account of differing thermal-hydraulic conditions at different burnup stages. The SAFR design has been used as a basis for the calculations, but PRISM conditions would not actually be too much different. TOP calculations have been carried out for single subassemblies using an assumed power history typical of a 10¢/sec transient. The EXTRUS model (Section 1) has been used to calculate prefailure fuel extrusion.

B. Calculation Methods and Parameter Choices

The pin geometric and thermal-hydraulic pin parameters chosen here are given in Table 6-1. Fuel properties, including density, heat capacity and heat of fusion, thermal conductivity, and solidus and liquidus temperatures are calculated in SSCOMP using correlations as functions of composition and temperature developed by Kalimullah.[6-2] The sodium flow rate was adjusted to give a sodium outlet temperature of 813 K (1003 F) for fresh fuel, which was assumed to have a peak linear power (based on fabricated dimensions) of 14.1 kW/ft. This peak power is consistent with discrete cycle studies on SAFR metal-fueled cores.[6-3] Peak powers assumed at later stages of the fuel cycle, assumed to contain four stages with a peak burnup of 14.8%, are also shown in Table 6-1. The peak coolant and clad temperatures shown are consistent with SAFR specifications.[6-4] These temperatures fall as the burnup cycle proceeds because subassembly power falls while coolant flow remains constant.

The peak linear powers shown for various burnup stages correspond to a core average for beginning-of-equilibrium cycle (BOEC) of 12.6 kW/wt, and to an end-of-equilibrium cycle (EOEC) average of 11.6 kW/ft.

The normalized power history used for the 10¢/sec TOP calculations is given in Table 6-2. The axial power distribution assumed is that given in Table 3-2, Section 3. The SSCOMP methodology is described in Ref. 6-2. Parameter choices for application of SSCOMP were discussed in Section 4. The parameters used here, given in Table 6-3, are those for M5 Case 27 in Table 4-4, in Section 4. TCM and TMO determine the location of zone outer radii, while CPCM, CPMO, CZCM, and CZMO determine zone compositions. Zone formation will be somewhat different in the present case with these parameters because of different fuel temperatures. In the present calculations, 11 equal volume radial nodes are used, with the 9 interior nodes each 1/10 of the total volume, and with inner and outer nodes 1/20 of the total. Zone formation is depicted in Table 6-4 in the manner described in Section 4. For each axial node, starting from the center of the pin, the number of radial nodes in the center zone is denoted by "C" and the number of middle zone nodes by "M". The remaining nodes up to the total of 11 are understood to be outer nodes. If nothing is shown for an axial node, it is understood to have the as-fabricated composition. The core axial nodes extend from node 3 at the bottom to node 22 at the top, with each node having a length in the preirradiated condition of 4.57 cm.

Gas pressures generated during a slow TOP calculation for metal fuel are usually too low to cause clad failure before extensive clad thinning from eutectic penetration has occurred. The time scale of events is too short for appreciable thinning to occur before rapid penetration starts. In the present calculations, rapid penetration is assumed to start when the fuel/clad interface reaches a temperature of 1353 K, as in previous sections of this report. Clad failure is calculated to occur in the present cases about 1.0 second after the start of rapid penetration, by which time almost complete penetration has occurred. This is because the temperature for rapid penetration is reached only for lower burnup cases, for which gas pressures are low.

Two parametric cases have been studied for fuel extrusion. In one of these the retained fission gas was set at the low value of 0.8 μmol/gm fuel and the FNMELT parameter at 0.3. This parameter combination gave calculated fuel extrusions slightly larger than measured in the M5 experiment

(Section 4). In the other case the retained gas was set at 0.01 μmol/gm, essentially zero, and FNMELT was set at 0.5, reducing cavity fuel and extrusion somewhat. This combination was found to give extrusion results well within the range of the M5 measurements, (Section 4) and probably represents a lower limit for extrusion.

It was found necessary to make an estimated correction to the calculated extrusion results because of an inconsistency in transient fuel porosity calculations created by the impossibility of using DEFORM in conjunction with SSCOMP in the current version of SAS4A as discussed in Section 4. In the present cases the overestimate in extrusion from this inconsistency was in the range of 25 to 50% of the calculated values of extrusion.

C. Results of Calculations

Calculations have been carried out for three burnup stages, corresponding to the initial and final burnups during an equilibrium cycle of the first two batches of the four-batch scheme. The first batch goes from 0.0 to 3.7% peak burnup and the second batch from 3.7 to 7.4%. The effect of burnup in the two later stages was not considered because the power would be too low for clad failure to be a problem before it had already occurred in the earlier stages, and there would be too little fuel melting to produce any fuel extrusion.

In applying the SSCOMP module, it has been assumed that zone formation continually follows the equilibrium assumptions of the model. This means that, as shown in Table 6-4, the volumes of central and middle zones will decrease as irradiation proceeds because of the lower power and fuel temperatures. Whether this will actually happen in practice is not really known, but it is not a very critical item because transient clad temperatures and fuel extrusion are not very sensitive to zone configuration (Sections 4 and 5).

Because SSCOMP is an equilibrium model, it does not take any account of time-dependent processes. According to SSCOMP, zone formation is most extensive in freshly-loaded fuel because subassembly power and fuel temperatures are then at a maximum. However, there is evidence that zone

formation has not yet taken place at very low burnups.[6-5] To explore the importance of this question, the zero burnup case was run both with zone formation allowed (Case 12 in Tables 6-4 and 6-5) and with the as-fabricated composition retained (Case 13). No significant difference in peak transient clad temperatures was evident. It was found that in either case the fuel/clad interface temperature of 1353 K at which rapid eutectic attack on clad was assumed to start was reached at a transient time of about 16.20 seconds, corresponding to a normalized power of 3.6. Complete penetration of clad, producing clad failure, occurred at 17.25 seconds, at a normalized power of 3.9.

The swollen core length in the irradiated cases is about 11% greater than the fabricated one, excessive for this type fuel. These calculations were performed before the input limitation on swollen core height discussed in Section 4 was available.

At the end of an equilibrium cycle for the Batch 1 fuel, the peak linear power is assumed to have fallen to 13.1 kW/ft. In this case, rapid eutectic attack for this fuel does not start until a normalized power of 3.9 has been attained, as indicated in Table 6-5. At EOEC for Batch 2 fuel, with a peak linear power of 12.1 kW/ft, rapid eutectic attack does not occur before clad failure would have occurred in the Batch 1 fuel.

Results for fuel extrusion and the accompanying reactivity feedback are given in Table 6-5. No results for extrusion of nearly fresh fuel have been given in this table. For completely fresh fuel no extrusion was observed in M4.[6-6] It is expected that for low burnups of up to at least a few tenths of a percent, there would be a large amount of extrusion, because all fission gas is trapped in the fuel and plenum pressure is low. This was indeed found to be the case in M2 and M3 for 0.3% burnup fuel.[6-7] However, in M5 extrusion was found to be low for 0.8% burnup fuel.[6-1] Although the peak transient power at which clad damage occurs is lowest for fresh fuel, there does seem to be the potential for a large prefailure negative feedback from fuel extrusion for low burnup fuel. This cannot really be evaluated until the M5 results are satisfactorily explained, however.

At higher burnup, Cases 17 and 19 in Table 6-5 correspond for 3.7 and 7.4% maximum burnup respectively to parameter choices of 0.8 μmol/gm retained gas and FNMELT = 0.3. Cases 20 and 18 correspond to the choices of retained gas of 0.01 μmol/gm and of FNMELT = 0.5 for the 3.7 and 7.4% cases. Calculated feedbacks are based on the assumption of 25 subassemblies in each fuel batch, and on a feedback per subassembly, of -0.5¢ per subassembly per gram fuel per pin extruded, typical for SAFR.

To avoid clad damage to the Batch 1 fuel early in the cycle, the power would need to peak at 3.6 times normal, the value attained at 16.20 sec. The feedback available from the Batches 2 and 3 fuel at BOEC (or 1 and 2 at EOEC) to accomplish this totals -74¢ for the first set of parameter choices and -36¢ for the second. Feedback for Batch 3 at EOEC or for Batch 4 has been neglected because of the assumed low subassembly power. Feedback from Batch 1 fuel early in the cycle has been neglected, although as discussed above, this fuel might provide considerable negative feedback at a few tenths percent burnup. Late in the cycle, when the power in the Batch 1 subassemblies is approaching 13.1 kW/ft, the permissible feedback before clad damage occurred would rise to the 17.25 second values, amounting to a total for Batch 1 and Batch 2 fuel of -$1.57 for the first parameter choices and -63¢ for the second.

Thus it seems that even with the disappointing fuel extrusion results in M5, some appreciable prefailure reactivity effect should be available from this source. The question of how much prefailure fuel extrusion will occur in prototypical fuel cannot be definitely answered yet, pending satisfactory explanation of why so little extrusion was observed in the M5 experiment. Early results from M6[6-8] indicate extrusions several times those found in M5, implying a significant prefailure feedback.

D. References

6-1. A. E. Wright, T. H. Bauer, and W. R. Robinson, unpublished information (1986).

6-2. Kalimullah, et al., "Advancements in the Modeling of Metallic and Oxide Fuels in the SAS4A Code," ANL/RAS 85-19 (October 1985).

6-3. H. Khalil, et al., "Discrete Fuel Management Studies of the SAFR Metal and Oxide Cores," ANL-SAFR-6 (January 1986).

6-4. D. J. Malloy, private communication (February 1987).

6-5. Y. I. Chang, "Integral Fast Reactor Program Quarterly Progress Report for January - March 1987," ANL-IFR-68 (1987).

6-6. E. A. Rhodes, "Fuel Motion in TREAT Test M4: Preliminary Analysis of Hodoscope Data" (May 1986).

6-7. W. R. Robinson, et al., "IFR Safety Tests M2 and M3 in TREAT: Data and Analysis," ANL-IFR-18 (June 1985).

6-8. Y. I. Chang, Integral Fast Reactor Program Quarterly Progress Report for January - March 1987," ANL-IFR-68 (1987).

TABLE 6-1. Pin Parameters

Clad ID	0.3061 cm
Clad OD	0.3619 cm
Fabricated Core Height	91.44 cm
Fabricated Volume Inside Clad	26.92 cm^3
Fuel Mass	323.85 g
Fabricated Density	15.57 g/cc
Fabricated Smear Density	12.03 g/cc
Sodium Flow Rate	0.1512 kg/sec
Sodium Inlet Temperature	630 K

Fabricated Composition: U-15 wt % Pu-10 wt % Zr

Case	Ave. % Burnup	Max. % Burnup	Peak Linear Power, kW/ft[a]	Steady State Subassembly Outlet Temp. K	Steady State Subassembly Outlet Temp. F	Steady State Peak Clad Temp. K	Steady State Peak Clad Temp. F
12,13	0.0	0.0	14.1	813	1003	845	1061
14	3.06	3.7	13.1	800	980	830	1034
15	6.12	7.4	12.1	787	957	815	1007
	9.18	11.1	11.0				
	12.2 (Discharge)	14.8	10.0				

[a]Based on fabricated length.

TABLE 6-2. Normalized Power History Assumed in Transient Calculation

Time, Sec.	Normalized Power
0.0	1.00
6.0	1.48
9.0	1.89
12.0	2.50
15.0	3.25
16.20	3.59
16.80	3.77
17.25	3.90
18.00	4.15

TABLE 6-3. Zone Formation Parameters

Parameters	SAS4A Locations	Value
TCM,K	81, Bl. 63	935
TMO,K	80, Bl. 63	905
CPCM	1287, Bl. 13	0.800
CPMO	1288, Bl. 13	0.670
CZCM	1289, Bl. 13	8.50
CZMO	1290, Bl. 13	4.57
Fr. Na Logging Zone Porosity	93-103, Bl. 13	0.20
Center	92, Bl. 63	0.40
Middle	91, Bl. 63	0.19
Outer	90, Bl. 63	0.25

TABLE 6-4. Zone Formation for Full-Length Prototypical Pins

Case		13	12	14	15,16
Max. Burnup, %		0.0	0.0	3.7	7.4
Max. Linear Power, kW/ft		14.1	14.1	13.1	12.1
Batch Correspondence	BOEC	1	1	2	3
	EOEC			1	2
		Zone Configuration by Axial Node			
Axial Node					
22		As Fabricated	CCMMMM	CMM	MM
21			CCCMM	CCMM	CMM
20			CCCMMM	CCMMM	CMMM
19			CCCMMM	CCMMM	CMMM
18			CCCMMM	CCMMM	CMMM
17			CCCMM	CCMMM	CM
16			CCCMM	CCMMM	CM
15			CCCMM	CCMM	CM
14			CCCMM	CCMM	CMM
13			CCCM	CMM	CMM
12			CCMM	CCMM	CM
11			CCM	CM	MM
10			CMM	CMM	M
9			CM	M	
8			CM	M	
7			M		
6			M		

TABLE 6-5. Results for Clad Failure and Fuel Extrusion for 10¢/sec TOP Accident for Full-Length Prototypical Pin

Case	Time, Sec.	Max. % Burnup	Fuel Batch BOEC	Fuel Batch EOEC	Peak Linear Power kW/ft	Normalized Power	Retained Fission Gas µmols/gm	FMELT	Peak Clad/Fuel Interface Temperature, K	% Fuel Extrusion	Fuel Reactivity in Cents for 25 Subassemblies
13[a]	16.20	0.0	1	-	14.1	3.59			1349[b]		
	16.80					3.77			1370		
	17.25					3.90			1381[c]		
12	16.20	0.0	1	-	14.1	3.59			1352[b]		
	16.80					3.77			1370		
	17.25					3.90			1380[c]		
17	16.20	3.7	2	1	13.1	3.59	0.8	0.3	1301	1.2	-49
	16.80					3.77			1334	2.0	-81
	17.25					3.90			1359[b]	2.8	-114
20	16.20	3.7	2	1	13.1	3.59	0.01	0.5	1301	0.6	-23
	16.80					3.77			1334	0.6	-25
	17.75					3.90			1359[b]	1.0	-43
18	16.20	7.4	3	2	12.1	3.59	0.8	0.3	1250	0.6	-25
	16.80					3.77			1281	0.8	-34
	17.25					3.90			1305	1.1	-43
19	16.20	7.4	3	2	12.1	3.59	0.01	0.5	1250	0.3	-13
	16.80					3.77			1281	0.5	-20
	17.25					3.90			1305	0.5	-20

[a]As fabricated composition.
[b]Start of rapid clad penetration by eutectic.
[c]Clad failure.

8/82

Blank Page

Appendix: EXTRUS Input and Output

Input specially required for EXTRUS in the special version of SAS4A in which it is available is as follows, all in Block 65:

Location

54 Average fuel atom percent burnup.

55 Na bond factor. This factor times the total volume inside the pin clad is the sodium bond volume SØDVØL. The volume available for gas in the plenum, VGP in this report (PGSVØL in the code) is calculated from

VGP = VFGPLN + GAPVØL - SODVØL

where VFGPLN is the total plenum volume, calculated from the plenum length PLENL, loc. 53 in Bl 61 and the inside clad radius, and GAPVØL is the fuel/clad gap volume over the total core height, calculated by the code.

57 Temperature, K, at which closed porosity gas is at 200 atm pressure (see Section 1). Default is steady state temperatures calculated by the code.

58 Temperature, K, at or above which rapid eutectic attack occurs (see Section 1). This must be input.

61 Retained gas in μgm-mols/gm fuel.

The EXTRUS output edit is not labeled and must be interpreted according to the keys given here. There is a steady-state output, given once immediately after the regular SAS steady-state output, and a transient output given every main SAS time step. The EXTRUS transient output edit immediately precedes the corresponding power and reactivity time step edit.

The key to the steady-state output is given in Table A1 and that for the transient output is given in Table A2. Four different blocks of data are listed in Table A2, labeled "A", "B", "C", and "D". Within each block a number of variables are listed and labeled with numbers. The FORTRAN variable name of each of these is listed at the right. The items in Table A2 are mostly self-explanatory except for the following:

Item 2 in Block C is the fuel worth after extrusion has taken place, and item 4 is the worth before extrusion, both on a thermally expanded scale. Item 5 is the original fuel worth on the original mesh. Item 3 is meaningless.

In block D, item 6 applies to HT-9 clad and so is not relevant for M6, in which the clad was D9. Items 11-13 are defined in Ref. A1. Item 9 shows the extent of eutectic attack on the clad.

A sample output is given here for Case M6P13O, with the transient output given for 13.2996 sec. Note that all SAS input and output data follow the SI system of units except as specifically noted. The EXTRUS input specifications for this case in Block 65 are as follows:

Location	Value
54	1.727
55	0.2107
58	1353.
61	1.00

The plenum length PLENL, loc. 53 in Block 61, is 24.6 cm, which with the clad inner radius of 0.254 cm gives a plenum volume of 4.986 cc. The swollen core height in this case was 34.605 x 1.0361 = 35.654 cm, given a volume inside this clad of 7.267 cc. This volume multiplied by the bond factor, 0.2107, gave a bond volume of 1.531 cc. The gap volume of 0.313 cc added to the plenum volume of 4.986 cc, minus the bond volume of 1.531 cc gives a plenum gas volume of 3.768 cc.

The JCL used to run problem M6P130 is given in Fig. A1, and the complete SAS4A input for this case is given in Fig. A2.

The steady-state output for case M6P130 is given in Fig. A3. Note that channel 1 is designated, and that 15 axial nodes are shown. In the table only the edit for nodes 1-2 and 14.15 is shown; nodes 3 through 13 have been omitted for the sake of bevity.

The transient output edit for case M6P130 is given in Fig. A4. Attention is called to items 23 and 24 in Block A. The difference between these two fractional cavity porosities arises from the inconsistency in calculating transient fuel porosity mentioned in Sections 4 and 5 arising from the inability to use DEFORM simultaneous with SSCOMP. In single-zone calculations in which DEFORM could be used, it was found that the transient fractional cavity porosity was about 0.01 less than for the same fuel at steady-state. Accordingly, in approximately correcting for the inconsistency, it was assumed that the correct fractional cavity porosity was 0.01 less than that calculated at steady state.

A. References

A1. J. M. Kramer, unpublished information (1985).

```
//M6P130   JOB ('11642850-0001646,B01646  ,  ,F01646  '),'B01646',     *
// CLASS=X,MSGLEVEL=(1),REGION=2300K,TIME=(2),USER=B01646
//*MAIN LINES=49                                                        3.
//*MAIN CARDS=0                                                         4.
//*MAIN ORG=LOCAL                                                       5.
//*FORMAT PR,DDNAME=JESMSG,DEST=3800                                    6.
//*FORMAT PR,DDNAME=JESJCL,DEST=3800                                    7.
//*FORMAT PR,DDNAME=SYSMSG,DEST=3800                                    8.
//*FORMAT PR,DDNAME=SYSPRINT,DEST=3800                                  9.
//*FORMAT PR,DDNAME=FT06F001,DEST=3800                                 10.
//*FORMAT PR,DDNAME=SYSLOUT,DEST=3800                                  11.
//*FORMAT PR,DDNAME=FT10F001,DEST=3800                                 12.
//*FORMAT PR,DDNAME=JESMSG,DEST=ANLVM.FICHE                            13.
//*FORMAT PR,DDNAME=JESJCL,DEST=ANLVM.FICHE                            14.
//*FORMAT PR,DDNAME=SYSMSG,DEST=ANLVM.FICHE                            15.
//*FORMAT PR,DDNAME=SYSPRINT,DEST=ANLVM.FICHE                          16.
//*FORMAT PR,DDNAME=FT06F001,DEST=ANLVM.FICHE                          17.
//*FORMAT PR,DDNAME=SYSLOUT,DEST=ANLVM.FICHE                           18.
//*FORMAT PR,DDNAME=FT10F001,DEST=ANLVM.FICHE                          19.
//STEP1 EXEC PGM=LOADER                                                20.
//SYSLIN DD DISP=SHR,DSN=C112.AAS.UTILITY.LOAD(UPDAT)                  21.
//SYSLOUT DD SYSOUT=A                                                  22.
//FT01F001 DD DISP=SHR,DSN=B32490.SAS4A.DEC85.COMMON                   23.
//FT02F001 DD DISP=SHR,DSN=B32490.SASCORE.RELEASE1.ONE.SOURCE(MAIN),   24.
//            LABEL=(,,,IN)                                            25.
// DD DISP=SHR,DSN=B32490.SASCORE.RELEASE1.ONE.SOURCE(FAILUR)          26.
// DD DISP=SHR,DSN=B32490.SAS4A.RELEASE1.ONE.SOURCE(DELOPS)            27.
// DD DISP=SHR,DSN=B32490.SAS4A.RELEASE1.ONE.SOURCE(FSHELL)            28.
// DD DISP=SHR,DSN=B32490.SAS4A.RELEASE1.ONE.SOURCE(CSIGMA)            29.
// DD DISP=SHR,DSN=B32490.SAS4A.RELEASE1.ONE.SOURCE(ALPHF)             30.
// DD DISP=SHR,DSN=B32490.SASCORE.RELEASE1.ONE.SOURCE(FEEDBK)          31.
// DD DISP=SHR,DSN=B32490.SAS4A.RELEASE1.ONE.SOURCE(DFORM3)            32.
// DD DISP=SHR,DSN=B32490.SASCORE.RELEASE1.ONE.SOURCE(RESTAR)          33.
// DD DISP=SHR,DSN=B22053.SOURCE.S3COMP3                               33.1
//FT04F001 DD DISP=(NEW,PASS),UNIT=SASCR,SPACE=(CYL,(10,1)),           34.
//       DSN=&&SOURCE,DCB=(RECFM=FB,LRECL=80,BLKSIZE=2000)             35.
//FT05F001 DD DSN=B15753.PINFAILY,DISP=SHR                             36.
//FT06F001 DD SYSOUT=A                                                 37.
//FT08F001 DD DSN=&&OPLIST,DISP=(NEW,DELETE),UNIT=SASCR,               38.
//     DCB=(RECFM=FB,LRECL=80,BLKSIZE=2000),SPACE=(TRK,(10,10,1),RLSE) 39.
//STEP2 EXEC FTXCP,OPTIONS='OPT=2'                                     40.
//FTX.SYSPRINT DD DUMMY                                                41.
//FTX.SYS03J  DD DSN=&&PREA,DISP=(NEW,PASS),UNIT=SASCR,                42.
//   DCB=(RECFM=FB,LRECL=80,BLKSIZE=3200),SPACE=(TRK,(5,5),RLSE)       43.
//FTX.SYSIN DD DISP=(OLD,DELETE),DSN=*.STEP1.FT04F001                  44.
//STEP3 EXEC FTXEG,                                                    45.
// E1RCOM='(CYL,(6,1))',                                               46.
// LDRCOM='(CYL,(6,1,1))',                                             47.
// EDTOPTS=MAP,LSIZE='(1550K,24K)'                                     48.
//SYSLIB DD DSN=B23970.SAS4A.DEC85.LOAD,DISP=SHR                       49.
//       DD DSN=B23970.SASCORE.DEC85.LOAD,DISP=SHR                     50.
//       DD DSN=SYS1.ANDLIB,DISP=SHR                                   51.
//       DD DSN=SYS1.FORTLIB,DISP=SHR                                  52.
//       DD DSN=SYS1.PLOTUTL,DISP=SHR                                  53.
//       DD DSN=SYS1.ANDLIBX,DISP=SHR                                  54.
//EDT.PINFIL DD DISP=(OLD,DELETE),                                     55.
// DSN=*.STEP2.FTX.SYSLIN                                              56.
//EDT.LABFIL DD DISP=SHR,LABEL=(,,,IN),                                57.
// DSN=B23970.SASSYS.DEC85.LOAD                                        58.
//EDT.CCRFIL DD DISP=SHR,LABEL=(,,,IN),                                59.
```

Fig. A1. JCL for Case M6P130, Provided by WYLBUR Data Set B01646.M2R.CNTL

```
      // LDROOM='(CYL,(6,1,1))',                                              47.
      // EDTOPTS=MAP,LSIZE='(1550K,24K)'                                      48.
33    XX        PROC EDITOR=IEWL,                                            04/14/86
      XX             E1ROOM='(CYL,(1,4))',                                   04/14/86
      XX             EDTOPTS=,LSIZE='(8192K,64K)',EDTREGN=256K,              04/14/86
      XX             PRELIB='SYS1.DUMMYLIB',POSTLIB='SYS1.DUMMYLIB',         04/14/86
      XX             PLOTUTL='SYS1.PLOTUTL',                                 04/14/86
      XX             AMDLIBX='SYS1.AMDLIBX',                                 04/14/86
      XX             AMDLIB='SYS1.AMDLIB',LIBRARY='SYS1.FORTLIB',            04/14/86
      XX             LOAD='&G(G)',LDUNIT=SASCR,                              04/14/86
      XX             LDROOM='(CYL,(1,4,1))',LDDISP='(MOD,PASS)',             04/14/86
      XX             GOIF='(5,LT,EDT)',GOREGN=100K                           04/14/86
34    XXEDT     EXEC PGM=&EDITOR,PARM='DCBS,LIST,MAP,&EDTOPTS,SIZE=&LSIZE',  04/14/86
      XX             REGION=&EDTREGN                                         04/14/86
35    //SYSLIB DD DSN=B23970.SAS4A.DEC85.LOAD,DISP=SHR                        49.
      X/SYSLIB   DD  DISP=SHR,DSN=&PRELIB                                    04/14/86
36    //        DD DSN=B23970.SASCORE.DEC85.LOAD,DISP=SHR                     50.
      X/          DD  DISP=SHR,DSN=&AMDLIB                                   04/14/86
37    //        DD DSN=SYS1.AMDLIB,DISP=SHR                                   51.
      X/          DD  DISP=SHR,DSN=&LIBRARY                                  04/14/86
38    //        DD DSN=SYS1.FORTLIB,DISP=SHR                                  52.
      X/          DD  DISP=SHR,DSN=&POSTLIB                                  04/14/86
39    //        DD DSN=SYS1.PLOTUTL,DISP=SHR                                  53.
      X/          DD  DISP=SHR,DSN=&PLOTUTL                                  04/14/86
40    //        DD DSN=SYS1.AMDLIBX,DISP=SHR                                  54.
      X/          DD  DISP=SHR,DSN=&AMDLIBX                                  04/14/86
41    XXSYSLIN   DD  DDNAME=SYSIN                                            04/14/86
42    XXSYSLMOD  DD  DSNAME=&LOAD,UNIT=&LDUNIT,SPACE=&LDROOM,DISP=&LDDISP,   04/14/86
      XX             DCB=BLKSIZE=6144                                        04/14/86
43    XXSYSPRINT DD  SYSOUT=*,DCB=(LRECL=121,BLKSIZE=1210)                   04/14/86
44    XXSYSUT1   DD  SPACE=&E1ROOM,UNIT=(SASCR,SEP=(SYSLIN,SYSLMOD))         04/14/86
45    //EDT.PINFIL DD DISP=(OLD,DELETE),                                      55.
      // DSN=*.STEP2.FTX.SYSLIN                                             56.
46    //EDT.LADFIL DD DISP=SHR,LABEL=(,,,IN),                                 57.
      // DSN=B23970.SASSYS.DEC85.LOAD                                       58.
47    //EDT.CORFIL DD DISP=SHR,LABEL=(,,,IN),                                 59.
      // DSN=B23970.SASCORE.DEC85.LOAD                                      60.
48    //EDT.SYSIN DD *,DCB=BLKSIZE=80                                         61.
49    XXGO      EXEC PGM=*.EDT.SYSLMOD,COND=&GOIF,REGION=&GOREGN             04/14/86
50    //GO.FT05F001 DD DISP=SHR,                                              67.
      //  DSN=B01646.M6PIN1.DATA05                                           68.
      X/FT05F001 DD  DDNAME=SYSIN                                            04/14/86
51    //GO.FT06F001 DD SYSOUT=*                                               69.
      X/FT06F001 DD  SYSOUT=*,DCB=(RECFM=FBA,LRECL=133,BLKSIZE=1596)         04/14/86
52    //GO.FT07F001 DD SYSOUT=B                                               70.
      X/FT07F001 DD  SYSOUT=B                                                04/14/86
      ***  THIS PROCEDURE IS DOCUMENTED IN TM-400, "BATCH PROCESSING AT ANL" 04/14/86
      ***                          AND IN TM-336, "GUIDE TO COMPUTING AT ANL" 04/14/86
53    //GO.FT10F001 DD SYSOUT=*                                               71.
54    //GO.FT26F001 DD DUMMY                                                  72.
55    //GO.FT12F001 DD DUMMY                                                  73.
56    //GO.FT13F001 DD DUMMY                                                  74.
57    //GO.FT14F001 DD DUMMY                                                  75.
58    //GO.FT15F001 DD DUMMY                                                  76.
59    //GO.FT18F001 DD DUMMY                                                  77.
60    //GO.FT17F001 DD DUMMY                                                  78.
61    //GO.FT20F001 DD DUMMY                                                  82.
62    //GO.FT11F001 DD DUMMY                                                  83.
```

Fig. A1. JCL for Case MyP130, Provided by WYLBUR Data Set B01646.M2R.CNTL (Contd.)

```
// DSN=B23970.SASCORE.DEC85.LOAD                                          60.
//EDT.SYSIN DD *                                                          61.
//GO.FT05F001 DD DISP=SHR,                                                67.
//  DSN=B01646.M6PIN1.DATA05                                              68.
//GO.FT06F001 DD SYSOUT=*                                                 69.
//GO.FT07F001 DD SYSOUT=B                                                 70.
//GO.FT10F001 DD SYSOUT=*                                                 71.
//GO.FT26F001 DD DUMMY                                                    72.
//GO.FT12F001 DD DUMMY                                                    73.
//GO.FT13F001 DD DUMMY                                                    74.
//GO.FT14F001 DD DUMMY                                                    75.
//GO.FT15F001 DD DUMMY                                                    76.
//GO.FT18F001 DD DUMMY                                                    77.
//GO.FT17F001 DD DUMMY                                                    78.
//GO.FT20F001 DD DUMMY                                                    82.
//GO.FT11F001 DD DUMMY                                                    83.
/*                                                                        84.
/* END OF FILE                                                            85.
    1     //M6P130   JOB ('11642850-0001646,B01646  ,  ,F01646  '),'B01646',     *
          // CLASS=X,MSGLEVEL=(1),REGION=2300K,TIME=(2),USER=B01646
    2     //STEP1 EXEC PGM=LOADER                                                  20.
    3     //SYSLIN DD DISP=SHR,DSN=C112.AAS.UTILITY.LOAD(UPDAT)                    21.
    4     //SYSLOUT DD SYSOUT=A                                                    22.
    5     //FT01F001 DD DISP=SHR,DSN=B32490.SAS4A.DEC85.COMMON                     23.
    6     //FT02F001 DD DISP=SHR,DSN=B32490.SASCORE.RELEASE1.ONE.SOURCE(MAIN),     24.
          //            LABEL=(,,,IN)                                            25.
    7     // DD DISP=SHR,DSN=B32490.SASCORE.RELEASE1.ONE.SOURCE(FAILUR)           26.
    8     // DD DISP=SHR,DSN=B32490.SAS4A.RELEASE1.ONE.SOURCE(RELGAS)             27.
    9     // DD DISP=SHR,DSN=B32490.SAS4A.RELEASE1.ONE.SOURCE(FSHELL)             28.
   10     // DD DISP=SHR,DSN=B32490.SAS4A.RELEASE1.ONE.SOURCE(CSIOMA)             29.
   11     // DD DISP=SHR,DSN=B32490.SAS4A.RELEASE1.ONE.SOURCE(ALFHF)              30.
   12     // DD DISP=SHR,DSN=B32490.SASCORE.RELEASE1.ONE.SOURCE(FEEDBK)           31.
   13     // DD DISP=SHR,DSN=B32490.SAS4A.RELEASE1.ONE.SOURCE(DFORMS)             32.
   14     // DD DISP=SHR,DSN=B32490.SASCORE.RELEASE1.ONE.SOURCE(RESTAR)           33.
   15     // DD DISP=SHR,DSN=B22853.SOURCE.SSCOMP3                                33.1
   16     //FT04F001 DD DISP=(NEW,PASS),UNIT=SASCR,SPACE=(CYL,(10,1)),           34.
          //       DSN=&&SOURCE,DCB=(RECFM=FB,LRECL=80,BLKSIZE=2000)             35.
   17     //FT05F001 DD DSN=B15758.PINFAILY,DISP=SHR                             36.
   18     //FT06F001 DD SYSOUT=A                                                 37.
   19     //FT08F001 DD DSN=&&OPLIST,DISP=(NEW,DELETE),UNIT=SASCR,               38.
          //     DCB=(RECFM=FB,LRECL=80,BLKSIZE=2000),SPACE=(TRK,(10,10,1),RLSE)  39.
   20     //STEP2 EXEC FTXCP,OPTIONS='OPT=2'                                     40.
   21     XXFTXCP   PROC REGN=240K,OPTIONS=,COMPILE=IFEAAB,                    05/13/85
          XX             STEPLIB='SYS1.FORTHX'                                 05/13/85
   22     XXFTX     EXEC PGM=&COMPILE,REGION=&REGN,PARM='NOTERM,&OPTIONS'      05/13/85
   23     XXSTEPLIB  DD  DISP=SHR,DSN=&STEPLIB                                 05/13/85
   24     XXSYSINDEX DD  SYSOUT=*                                              05/13/85
   25     XXSYSLIN   DD  DDNAME=SYSOBJ                                         05/13/85
   26     //FTX.SYSPRINT DD DUMMY                                                41.
          X/SYSPRINT DD  SYSOUT=*,DCB=(RECFM=VBA,LRECL=137,BLKSIZE=1511)       05/13/85
   27     XXSYSPUNCH DD  SYSOUT=B,DCB=(RECFM=F,BLKSIZE=80)                     05/13/85
   28     XXSYSUT1   DD  SPACE=(TRK,(0,19)),UNIT=(SASCR),DCB=BLKSIZE=2940      05/13/85
   29     XXSYSUT2   DD  SPACE=(TRK,(0,19)),UNIT=(SASCR,SEP=(SYSUT1))          05/13/85
          ***  THIS PROCEDURE IS DOCUMENTED IN TM-400, "BATCH PROCESSING AT ANL" 05/13/85
          ***                          AND IN TM-336, "GUIDE TO COMPUTING AT ANL" 05/13/85
   30     //FTX.SYSOBJ  DD DSN=&&PREA,DISP=(NEW,PASS),UNIT=SASCR,                42.
          //   DCB=(RECFM=FB,LRECL=80,BLKSIZE=3200),SPACE=(TRK,(5,5),RLSE)      43.
   31     //FTX.SYSIN DD DISP=(OLD,DELETE),DSN=*.STEP1.FT04F001                  44.
   32     //STEP3 EXEC FTXEG,                                                    45.
          // E1ROOM='(CYL,(6,1))',                                               46.
```

Fig. A1. JCL for Case M6P130, Provided by WYLBUR Data Set B01646.M2R.CNTL (Contd.)

```
        SAS4A 0.0  FNM .5,1.25X SS PWR.,CORR. RHOCG,TREAT RAD PR,PCF 4.9
                   COOLANT.085,BU 1.727,RET GAS 1.0,TCM 880,TMO 855,ALFO 0.260,BOND F..2107
FNM .5,1.25X SS PWR.,CORR. RHOCG,TREAT RAD PR,PCF 4.9
COOLANT.085,BU 1.727,RET GAS 1.0,TCM 880,TMO 855,ALFO 0.260,BOND F..2107
  1  0  0  0
INPCOM     1     0     0
    1    10     1     0     5     1     0     0     0     1     1     0
   11    10  1000    10    10     0     0     6     0    20     3     0
   21    10     0     2     0    11     0     0     0     0     0     0
   31    10     0     0     0     0     0     0     0     0    -5     0
   41    10     0     0     0     0     0     0     0     0     1     0
   -1
OPCIN     11     0     0
    1     5 1.000000D-02 1.000000D-03 1.000000D-05 1.000000D-05 1.500000D-01
    6     5 1.000000D-02 1.345000D+01 1.000000D-03 1.000000D+01 5.000000D+01
   11     5 3.000000D+01 5.273150D+03 1.000000D+01 1.000000D+01 0.0
   -1
POWINA     12     0     0
    1     5 1.073800D+03 3.690000D-07 9.000000D+08 7.977200D-05 7.120600D-04
    6     5 6.260500D-04 1.217500D-03 5.623900D-04 1.823100D-04 1.290400D-02
   11     5 3.141800D-02 1.356900D-01 3.465000D-01 1.370300D+00 3.761900D+00
   26     5 0.0          0.0          0.0          1.000000D+00 1.000300D+00
   31     5 1.200000D+00 1.530000D+00 1.840000D+00 1.930000D+00 2.220000D+00
   36     5 2.340000D+00 2.500000D+00 2.810000D+00 3.100000D+00 3.300000D+00
   41     5 3.670000D+00 3.940000D+00 4.220000D+00 4.530000D+00 4.870000D+00
   46     5 5.040000D+00 2.970000D+00 9.400000D-01 3.600000D+00 4.200000D+00
   51     5 4.750000D+00 5.000000D+00 5.500000D+00 6.000000D+00 7.000000D+00
   56     5 7.500000D+00 8.000000D+00 9.000000D+00 1.000000D+01 1.050000D+01
   61     5 1.100000D+01 1.150000D+01 1.200000D+01 1.250000D+01 1.300000D+01
   66     5 1.325900D+01 1.335000D+01 1.345000D+01 9.250000D-01 3.062000D-01
   71     5 4.190000D+00 2.100000D-05-8.600000D+00 0.0          2.040000D+04
   76     5 2.670000D+03 1.360000D+01-1.541000D+02 7.000000D-01 0.0
  256     5 0.0          0.0          0.0          0.0          2.204720D-02
  261     5 1.764170D-02 2.413130D-02 1.000000D-06 1.000000D-06 1.000000D-06
  286     5 0.0          0.0          0.0          0.0          1.009460D-01
  291     5 5.167910D-03 1.565370D-04 7.620000D-05 9.725000D-06 8.875000D-07
  321     5 0.0          0.0          0.0          0.0          1.000000D+00
  361     5 0.0          0.0          0.0          0.0          1.000000D+00
  401     5 0.0          0.0          0.0          0.0          1.300000D+00
  411     5 0.0          0.0          0.0          2.000000D-05 1.400000D-05
  416     5 2.750000D+02 0.0          0.0          0.0          0.0
   -1
PMATCM     13     0     0
    1     5 1.580000D+04 6.800000D-05 0.0          0.0          0.0
   11     5 2.450000D+01 2.490000D+01 2.540000D+01 2.590000D+01 2.630000D+01
   16     5 2.680000D+01 2.720000D+01 2.760000D+01 2.800000D+01 3.050000D+01
   71     5 2.940000D+02 3.730000D+02 4.730000D+02 5.730000D+02 6.730000D+02
   76     5 7.730000D+02 8.730000D+02 9.730000D+02 1.073000D+03 1.700000D+03
   91     5 1.580000D+04 1.571500D+04 1.563300D+04 1.555200D+04 1.547200D+04
   96     5 1.539200D+04 1.533300D+04 1.519200D+04 1.501600D+04 1.495300D+04
  101     5 1.486700D+04 1.477900D+04 1.477070D+04 1.465200D+04 0.0
  111     5 1.580000D+04 1.571500D+04 1.563300D+04 1.555200D+04 1.547200D+04
  116     5 1.539200D+04 1.533300D+04 1.519200D+04 1.501600D+04 1.495300D+04
  121     5 1.486700D+04 1.477900D+04 1.477070D+04 1.465200D+04 0.0
  131     5 1.580000D+04 1.571500D+04 1.563300D+04 1.555200D+04 1.547200D+04
  136     5 1.542700D+04 1.532300D+04 1.501300D+04 1.491100D+04 1.481200D+04
  141     5 1.453200D+04 1.436400D+04 0.0          0.0          0.0
  151     5 1.580000D+04 1.571500D+04 1.563300D+04 1.555200D+04 1.547200D+04
  156     5 1.542700D+04 1.532300D+04 1.501300D+04 1.491100D+04 1.481200D+04
  161     5 1.453200D+04 1.436400D+04 0.0          0.0          0.0
```

Fig. A2. SAS4A Input for Case M6P130, Provided by WYLBUR Data Set B01646.M6P1N1.DATA05

```
      SAS4A 0.0  FNM .5,1.25X SS PWR.,CORR. RHOCG,TREAT RAD PR,PCF 4.9
                 COOLANT.035,BU 1.727,RET GAS 1.0,TCM 855,TMD 855,ALFD 0.250,BOND F..2107
171     5 9.20700D+02 8.73600D+02 8.25000D+02 7.77500D+02 7.29100D+02
176     5 6.80700D+02 6.32700D+02 5.83900D+02 5.30700D+02 4.71000D+02
251     5 3.00000D+02 4.00000D+02 5.00000D+02 6.00000D+02 7.00000D+02
256     5 8.00000D+02 8.68000D+02 9.32000D+02 1.00000D+03 1.10000D+03
261     5 1.20000D+03 1.30000D+03 1.38500D+03 1.50000D+03 0.0
271     5 3.00000D+02 4.00000D+02 5.00000D+02 6.00000D+02 7.00000D+02
276     5 8.00000D+02 8.68000D+02 9.32000D+02 1.00000D+03 1.10000D+03
281     5 1.20000D+03 1.30000D+03 1.38500D+03 1.50000D+03 0.0
291     5 3.00000D+02 4.00000D+02 5.00000D+02 6.00000D+02 7.00000D+02
296     5 8.00000D+02 9.00000D+02 1.00000D+03 1.10000D+03 1.20000D+03
301     5 1.48300D+03 1.65300D+03 0.0         0.0         0.0
311     5 3.00000D+02 4.00000D+02 5.00000D+02 6.00000D+02 7.00000D+02
316     5 8.00000D+02 9.00000D+02 1.00000D+03 1.10000D+03 1.20000D+03
321     5 1.48300D+03 1.65300D+03 0.0         0.0         0.0
331     5 4.00000D+02 6.00000D+02 8.00000D+02 1.00000D+03 1.20000D+03
336     5 1.40000D+03 1.60000D+03 1.80000D+03 2.00000D+03 2.20000D+03
416     5 0.0         0.0         0.0         3.0015D+02  1.1400D+01
421     5 1.34000D+01 1.55000D+01 1.77000D+01 2.01000D+01 2.25000D+01
426     5 2.51000D+01 2.78000D+01 3.06000D+01 3.65000D+01 4.39000D+01
436     5 0.0         0.0         0.0         0.0         7.00000D+00
441     5 8.20000D+00 9.50000D+00 1.09000D+01 1.23000D+01 1.38000D+01
446     5 1.54000D+01 1.70000D+01 1.88000D+01 2.24000D+01 2.69000D+01
456     5 0.0         0.0         0.0         0.0         1.80000D+01
461     5 2.01000D+01 2.24000D+01 2.49000D+01 2.76000D+01 3.02000D+01
466     5 3.36000D+01 3.68000D+01 4.03000D+01 4.77000D+01 6.00000D+01
476     5 0.0         0.0         0.0         0.0         1.10000D+01
481     5 1.23000D+01 1.38000D+01 1.53000D+01 1.69000D+01 1.87000D+01
486     5 2.06000D+01 2.26000D+01 2.47000D+01 2.92000D+01 4.00000D+01
496     5 0.0         0.0         0.0         0.0         8.60000D+01
501     5 8.10000D+01 7.60000D+01 7.10000D+01 6.60000D+01 6.20000D+01
506     5 5.80000D+01 5.40000D+01 5.00000D+01 4.20000D+01 3.20000D+01
576     5 0.0         0.0         0.0         0.0         5.70000D+02
581     5 4.73000D+02 5.73000D+02 6.73000D+02 7.73000D+02 8.73000D+02
586     5 9.73000D+02 1.0730D+03  1.1730D+03  1.3730D+03  1.6730D+03
596     5 0.0         0.0         0.0         0.0         1.31000D+02
601     5 2.56000D-01 1.97000D+02 6.00000D-01 2.50000D+00 0.0
606     5 1.33200D+02 1.46300D+02 1.59000D+02 1.72200D+02 1.85400D+02
611     5 1.98000D+02 2.07800D+02 1.60000D+02 1.69000D+02 1.82400D+02
616     5 1.95100D+02 2.08300D+02 2.21000D+02 2.46300D+02 0.0
626     5 1.33200D+02 1.46300D+02 1.59000D+02 1.72200D+02 1.85400D+02
631     5 1.98000D+02 2.07800D+02 1.69000D+02 1.69200D+02 1.82400D+02
636     5 1.95100D+02 2.08300D+02 2.21000D+02 2.46300D+02 0.0
646     5 1.50700D+02 1.53200D+02 1.69200D+02 1.91200D+02 2.16100D+02
651     5 2.42000D+02 2.61400D+02 2.74700D+02 1.79000D+02 1.79000D+02
656     5 1.79000D+02 1.79000D+02 1.79000D+02 1.79000D+02 0.0
666     5 1.50700D+02 1.53200D+02 1.69800D+02 1.91200D+02 2.16100D+02
671     5 2.42000D+02 2.61400D+02 2.74700D+02 1.79000D+02 1.79000D+02
676     5 1.79000D+02 1.79000D+02 1.79000D+02 1.79000D+02 0.0
686     5 1.41200D+03 1.36980D+03 1.32800D+03 1.29520D+03 1.27200D+03
691     5 1.25900D+03 1.25500D+03 1.25500D+03 1.25900D+03 1.27200D+03
696     5 1.29300D+03 1.32600D+03 1.36600D+03 1.47500D+03 0.0
766     5 2.98000D+02 4.00000D+02 5.00000D+02 6.00000D+02 7.00000D+02
771     5 8.00000D+02 8.73000D+02 9.23000D+02 1.00000D+03 1.10000D+03
776     5 1.20000D+03 1.30000D+03 1.40000D+03 1.60000D+03 0.0
786     5 1.37900D+03 1.37900D+03 1.48700D+03 1.48700D+03 1.48700D+03
791     5 0.0         0.0         0.0         1.5380D+03  1.5830D+03
796     5 1.65700D+03 1.65700D+03 1.65700D+03 0.0         0.0
801     5 0.0         9.17000D+04 9.17000D+04 9.02000D+04 9.02000D+04
```

Fig. A2. SAS4A Input for Case M6P130, Provided by WYLBUR Data Set BO1646.M6P1N1.DATA05 (Contd.)

```
      SAS4A 0.0  FNM .5,1.25X SS PWR.,CORR. RHOCG,TREAT RAD FR,PCF 4.9
                 COOLANT.085,BU 1.727,RET GAS 1.0,TCM 850,TMO 855,ALFO 0.260,BOND F..2107
  806     5 1.00000D+00 0.0          0.0          0.0          1.69015D+03
  811     5 0.0         0.0          1.71015D+03 0.0          0.0
  816     5 2.68300D+05 0.0          0.0          4.49100D+02 4.82500D+02
  821     5 5.21500D+02 5.63400D+02 6.15400D+02 6.84700D+02 7.85000D+02
  826     5 8.66100D+02 1.02150D+03 1.21000D+03 8.69300D+02 7.49000D+02
  876     5 0.0         0.0          0.0          2.94000D+02 3.73900D+02
  831     5 4.73000D+02 5.73000D+02 6.73000D+02 7.73000D+02 8.73000D+02
  836     5 9.23000D+02 9.73000D+02 9.93000D+02 1.02300D+03 1.07300D+03
  906     5 0.0         0.0          0.0          0.0          6.20000D+08
  911     5 6.20000D+08 6.10000D+08 5.90000D+08 5.40000D+08 4.20000D+08
  916     5 2.60000D+08 1.20000D+08 4.00000D+07 1.00000D+00 0.0
  966     5 0.0         0.0          0.0          0.0          3.00000D+02
  971     5 4.00000D+02 5.00000D+02 6.00000D+02 7.00000D+02 8.00000D+02
  976     5 9.00000D+02 1.00000D+03 1.10000D+03 2.00000D+03 0.0
  986     5 0.0         0.0          0.0          0.0          3.42500D+06
  991     5 3.73600D+06 4.02400D+06 4.33100D+06 4.71200D+06 5.22000D+06
  996     5 5.95900D+06 6.56000D+06 7.71900D+06 9.13400D+06 6.54700D+06
 1001     5 5.62700D+06 0.0          0.0          0.0          0.0
 1046     5 0.0         0.0          0.0          0.0          2.94000D+02
 1051     5 3.73000D+02 4.73000D+02 5.73000D+02 6.73000D+02 7.73000D+02
 1056     5 8.73000D+02 9.23000D+02 9.73000D+02 9.92000D+02 1.02300D+03
 1061     5 1.07300D+03 0.0          0.0          0.0          0.0
 1081     5 0.0         0.0          2.07040D+01 4.52810D+05 1.50000D+00
 1086     5 8.31434D+00 1.00000D+00 5.00000D+04 5.65065D+04 1.71700D+10
 1091     5 3.87000D+05 1.45556D-08 2.67000D+05 2.23000D-03 6.33750D+04
 1096     5 9.46900D+01 3.13000D+03 5.00000D-06 2.50000D-06 0.0
 1101     5 1.66000D+00 1.04400D+09 1.00300D+00 1.50000D-01 8.05900D-01
 1106     5 1.98000D+00 5.67000D-08 9.00000D-01 8.00000D-01 6.92000D+03
 1111     5 3.39500D+01 3.38000D-01 1.43000D+04 9.5750D+00 2.00000D-05
 1116     5 8.33000D+03 3.00000D-01 2.30000D-01 1.00000D+00 3.77000D+05
 1121     5 0.0         0.0          0.0          6.36200D+01 0.0
 1126     5 0.0         2.10000D+03 2.00000D-02 0.0          0.0
 1136     5 0.0         0.0          0.0          2.50000D+02 4.40000D+01
 1141     5 0.0         0.0          0.0          0.0          7.30000D-05
 1146     5 0.0         0.0          1.50000D-01 0.0          0.0
 1151     5 2.24000D+05 0.0          0.0          0.0          3.00000D-03
 1156     5 0.0         6.00000D-01 0.0          0.0          0.0
 1161     5 2.50000D+05 6.50000D-03 0.0          0.0          1.95200D-02
 1166     5 1.00000D+00 0.0          0.0          5.00000D-01 1.66700D+01
 1186     5 2.00000D-01 0.0          6.00000D-11 0.0          0.0
 1196     5 0.0         0.0          0.0          0.0          1.47070D+04
 1201     5 6.00000D-05 0.0          0.0          0.0          0.0
 1206     5 0.0         0.0          0.0          0.0          1.00000D+06
 1211     5 1.27000D+06 7.50000D+02 0.0          0.0          0.0
 1221     5 0.0         1.58000D-03 7.20000D-05 7.50000D-01 4.00000D+00
 1226     5 3.00000D-03 0.0          0.0          0.0          0.0
 1256     5 0.0         0.0          1.00000D+00 2.00000D-01 0.0
 1261     5 0.0         6.00000D-01 1.00000D+00 0.0          0.0
 1266     5 1.00000D-02 5.00000D-01 8.00000D-01 5.00000D-02 2.00000D-02
 1271     5 1.00000D-02 5.35000D+00 7.33000D+00 3.85330D+04 2.00000D-01
 1276     5 2.50000D+04 2.00000D-05 0.0          5.00000D-02 0.0
 1281     5 1.07000D+00 5.40000D-03 6.25000D+00 0.0          0.0
 1286     5 1.00000D+00 8.00000D-01 6.70000D-01 9.00000D+00 4.57000D+00
 1291     5 4.48000D-01 5.86600D-01 1.00000D-06 1.00000D-03 0.0
   -1
PRIMIN    14    0    0
    1     5 3.43400D+05 0.0          0.0          0.0          1.00000D+00
    6     5 1.00000D+00 1.00000D+00 0.0          0.0          0.0
```

Fig. A2. SAS4A Input for Case M6P130, Provided by WYLBUR Data Set B01646.M6P1N1.DATA05 (Contd.)

```
      SAS4A 0.0  FNM .5,1.25X SS PWR.,CORR. RHOCG,TREAT RAD PR,PCF 4.9
                 COOLANT.005,BU 1.727,RET GAS 1.0,TCM 836,TMD 855,ALFC 0.260,BOND F..2107
   26     5 1.00000D+00 3.00000D+01 0.0          0.0          0.0
   41     5 0.0         0.0         0.0          0.0          5.03000D+02
   46     5 5.83000D+02 0.0         0.0          0.0          0.0
   66     5 1.00000D+02 0.0         0.0          0.0          0.0
   81     5 0.0         0.0         0.0          0.0          1.10000D+03
   86     5 0.0        -1.89350D+00 1.03645D+00 0.0          1.00000D-01
   91     5 2.50000D-01 0.0         5.92500D-03 1.07870D-02 1.00000D+00
   -1
PLOTDA    4     0     0
   -1
INPMR4    3     0     0
    1    10     5     4     0     8     4     0     2     0     0    28
   11    10     1     7     9     8     4     9     4     4     4     0
   41    10     0     0     0     0     0     0     0     0     1     2
   51    10     2     2     2     2     2     3     2     3     3     3
   61    10     6     3     3     5     3     3     3     3     5     3
   71    10     3     7     3     8     3     3     0     0     0     0
  181    10     0     0     0     0     0     0     0     0     1     2
  191    10     1     2     1     2     1     2     2     3     3     4
  201    10     4     5     5     1     9     7     7     8     8     9
  211    10     9     6     0     0     0     0     0     0     0     0
  261    10     0     0     0     0     0     0     0     0     2     3
  271    10     3     4     0     0     0     0     0     0     0     0
  321    10     0     0     0     0     1     3     3     3     1     3
  331    10     1     4     2     4     2     1     0     0     0     0
  361    10     0     0     0     0     1     2     5     8    11    12
  371    10    15    16    20    22    26    28     0     0     0     0
  401    10     0     0     0     0     2    16    21     0     0     0
  461    10     0     0     0     0     0     0     0     0     0     1
  471    10     0     0    13     0     0     0     0     0     0     0
  481    10    24     0     0     0     0     0     0     0     0     0
  511    10     0    21     6     6     6     6     6     6     4     6
  521    10     4     4     4    40     4     4    10    60    30    40
  531    10     2    80    10     0     0     0     0     0     0     0
  611    10     0     0     2     3     4     5     6     7     8     9
  621    10    10    11    12    13    14    15    16    20    22    25
  631    10    26    27    28     0     0     0     0     0     0     0
  711    10     0     0     2     3     4     5     6     7     8     9
  721    10    10    11    12    13    14    15    19    21    23    25
  731    10    26    27    28     0     0     0     0     0     0     0
  811    10     0     0     7     6     6     6     6     6     6     6
  821    10     0     1     1     1     1     1     1     1     0     2
  831    10     3     4     5     6     7     9     0     0     1    26
  851    10     0     1     0     0     0     0     0     0     0     0
  861    10     0     0     0     2     0     0     0     0     0     0
  881    10     0     0     0     0     0     0     0     0     0  1000
  961    10     0     0     0     0     1     0     0     0     0     0
  991    10     0     0     0     0     0     0     0     0     0     2
 1001    10     0     0     0     1     0     0     0     0     0     0
   -1
PMR4IN   18     0     0
    1     5 0.0         4.11050D+03 2.32780D+02 1.09720D+02 1.33340D+02
    6     5 1.14660D+03 1.14660D+03 2.29320D+03 2.29320D+03 2.27800D+03
   11     5 1.13900D+03 2.27800D+03 0.0         0.0         0.0
   41     5 0.0        -1.96900D+00-1.96900D+00-1.96900D+00-1.96900D+00
   46     5 6.50000D+00 6.50000D+00 3.44000D+00 5.66000D+00 1.96900D+01
   51     5 2.34200D+01 2.10600D+01 1.96900D+01 0.0         0.0
   81     5 0.0         1.00000D+00 1.00000D+00 1.00000D+00 1.00000D+00
```

Fig. A2. SAS4A Input for Case M6P130, Provided by WYLBUR Data Set B01646.M6P1N1.DATA05 (Contd.)

```
      SAS4A 0.0  FNM .5,1.25X SS FWR.,CORR. RHOCG,TREAT RAD FR,PCF 4.9
                 COOLANT.035,BU 1.727,RET GAS 1.0,TCM 850,TMD 855,ALFO 0.260,BOND F..2107
  86     5 1.000000D+00 1.000000D+00 1.000000D+00 1.000000D+00 4.000000D+00
  91     5 1.000000D+00 1.000000D+00 4.000000D+00 2.000000D+00 1.000000D+00
  96     5 1.000000D+00 2.000000D+00 1.000000D+00 1.000000D+00 2.000000D+00
 101     5 2.000000D+00 1.000000D+00 1.000000D+00 1.000000D+00 1.000000D+00
 181     5 0.0          3.150000D+00 0.0          1.120000D+00 3.150000D+00
 186     5 0.0          1.120000D+00 3.150000D+00 0.0          1.120000D+00
 171     5 3.150000D+00 6.500000D+00 5.530000D+00 2.290000D-01-1.194000D+00
 176     5 4.510000D+00 5.660000D+00 1.000000D+00-1.939000D+00-1.969000D+00
 181     5 2.200000D+01 2.342000D+01 5.560000D+00 2.290000D-01 5.560000D+00
 186     5 2.106000D+01-2.410000D+00 1.939000D+01 2.342000D+01 0.0
 301     5 0.0          5.112000D+00 1.969000D+00 1.120000D+00 2.030000D+00
 306     5 1.969000D+00 1.120000D+00 2.030000D+00 1.969000D+00 1.120000D+00
 311     5 2.030000D+00 1.590000D+00 9.398000D-01 5.334000D+00 1.770000D+00
 316     5 1.070000D+00 1.575000D+00 3.060000D+00 3.920000D+00 1.340000D+00
 321     5 2.390000D+00 1.575000D+00 2.327000D+01 5.334000D+00 5.334000D+00
 326     5 3.211000D+01 2.347000D+01 2.504000D+01 9.144000D+00 0.0
 441     5 0.0          0.0          1.146500D-01 1.146500D-01 1.146500D-01
 446     5 6.879000D-02 6.879000D-02 6.879000D-02 4.085000D-01 4.085000D-01
 451     5 4.085000D-01 5.100000D-01 2.744000D+00 9.059000D-01 4.010000D-01
 456     5 4.314000D-01 8.090000D-01 3.550000D-01 3.020000D-01 6.030000D+00
 461     5 2.740000D-01 8.090000D-01 1.500000D-01 1.830000D-01 1.647000D+00
 466     5 1.510000D-01 1.770000D+00 2.740000D-01 4.350000D-02 0.0
 501     5 0.0          0.0          2.450000D-03 2.450000D-03 2.450000D-03
 506     5 2.450000D-03 2.450000D-03 2.450000D-03 1.471000D-02 1.471000D-02
 591     5 1.471000D-02 8.070000D-01 2.850000D+00 2.310000D-02 7.130000D-01
 596     5 7.410000D-01 1.010000D+00 3.360000D-01 4.350000D-01 2.950000D+00
 601     5 5.910000D-01 1.010000D+00 4.350000D-01 4.020600D-01 3.620000D-02
 606     5 4.380000D-01 5.200000D-02 5.910000D-01 2.350000D-01 0.0
 721     5 0.0          1.000000D-05 1.000000D-05 1.000000D-05 1.000000D-05
 726     5 1.000000D-05 1.000000D-05 1.000000D-05 1.000000D-05 1.000000D-05
 731     5 1.000000D-05 1.000000D-05 1.000000D-05 1.000000D-05 1.000000D-05
 736     5 1.000000D-05 1.000000D-05 1.000000D-05 1.000000D-05 1.000000D-05
 741     5 1.000000D-05 1.000000D-05 1.000000D-05 1.000000D-05 1.000000D-05
 746     5 1.000000D-05 1.000000D-05 1.000000D-05 1.000000D-05 0.0
 876     5 0.0          0.0          0.0          1.000000D+00 0.0
 881     5 0.0          0.0          6.000000D+00 0.0          0.0
 886     5 2.000000D+00 0.0          5.000000D+00 3.000000D+00 0.0
1021     5 4.800000D-02 0.0          5.300000D-01 2.600000D-01 1.711000D+02
1026     5 0.0          3.434000D+02 4.400000D-01 0.0          0.0
1141     5 0.0          5.000000D-01 0.0          0.0          0.0
1146     5 0.0          0.0          0.0          0.0          1.550000D+07
1151     5 0.0          1.550000D+07 2.350000D+05 3.180000D+06 0.0
1156     5 2.190000D+06 1.087000D+05 4.587000D+06 1.830000D+05 1.104000D+05
1161     5 1.050000D+07 8.224000D+04 4.666000D+06 6.135000D+04 3.620000D+05
1166     5 0.0          6.135000D+04 0.0          8.224000D+04 3.265000D+04
1236     5 0.0          0.0          0.0          0.0          4.780000D+03
1291     5 0.0          4.780000D+03 1.800000D+04 2.000000D+03 0.0
1296     5 1.300000D+03 4.140000D+03 1.653000D+02 4.525000D+03 4.525000D+03
1301     5 7.600000D+02 5.946000D+03 1.653000D+02 5.946000D+03 4.460000D+03
1306     5 0.0          5.946000D+03 0.0          5.946000D+03 6.110000D+03
1421     5 0.0          0.0          7.870000D+00 4.640000D+01 1.081500D+02
1426     5 5.270000D+02 1.000000D+00 2.098000D+01 1.000000D+00 1.000000D+00
1431     5 1.000000D+00 0.0          0.0          0.0          0.0
1461     5 0.0          1.038000D+05 1.038000D+05 1.038000D+05 0.0
1466     5 1.047700D+05 0.0          0.0          0.0          0.0
1496     5 0.0          0.0          0.0          2.000000D-08 2.000000D-08
1501     5 2.000000D-08 2.000000D-08 2.000000D-08 2.000000D-08 2.000000D-08
1506     5 2.000000D-08 2.000000D-08 0.0          0.0          0.0
```

Fig. A2. SAS4A Input for Case M6P130, Provided by WYLBUR Data Set B01646.M6P1N1.DATA05 (Contd.)

```
      SAS4A 0.0  FNM .5,1.25X SS PWR.,CORR. RHOCG,TREAT RAD FR,PCF 4.9
                 COOLANT.085,BU 1.727,RET GAS 1.0,TCH 880,TMD 855,ALFO 0.260,BOND F..2107
1571     5 0.0          0.0          0.0          0.0         -1.969000+00
1576     5 3.150000+00 6.500000+00 3.150000+00 5.660000+00 2.342000+01
1581     5 2.342000+01 2.106000+01 1.969000+01 0.0          0.0
1611     5 0.0          0.0          1.000000+00 9.000000+00 2.263000+01
1616     5 1.431000+01 1.000000+00 6.590000+00 1.000000+00 1.000000+00
1621     5 1.000000+00 0.0          0.0          0.0          0.0
1626     5 0.0          0.0          0.0          1.600000+00 2.070000+03
1691     5 1.900000-05 2.730000+02 1.000000+00 1.000000+00 0.0
1721     5 1.000000+00 1.000000+00 0.0          0.0          0.0
1746     5 0.0          0.0          0.0          4.000000+00 1.000000+00
1751     5 1.000000+00 4.000000+00 0.0          0.0          0.0
1801     5 0.0          0.0          0.0          0.0          1.000000+00
1806     5 1.000000+00 0.0          0.0          0.0          0.0
1831     5 0.0          0.0          1.000000-05 1.000000-05 0.0
1861     5 1.000000+01 1.000000+01 1.000000+01 1.000000+01 1.000000+01
1866     5 1.000000+01 1.000000+01 1.000000+01 1.000000+01 0.0
1981     5 0.0          0.0          1.000000+00 1.000000+00 3.682000-01
1986     5 1.948000-01 1.215000-01 8.370000-02 8.090000-02 6.820000-02
1991     5 5.080000-02 4.120000-02 3.290000-02 2.540000-02 1.550000-02
1996     5 1.310000-02 8.300000-03 7.100000-03 4.700000-03 3.900000-03
2001     5 2.900000-03 1.800000-03 1.000000+00 1.000000+00 3.682000-01
2006     5 1.948000-01 1.215000-01 8.370000-02 8.090000-02 6.820000-02
2011     5 5.080000-02 4.120000-02 3.290000-02 2.540000-02 1.550000-02
2016     5 1.310000-02 8.300000-03 7.100000-03 4.700000-03 3.900000-03
2021     5 2.900000-03 1.800000-03 0.0          0.0          0.0
2221     5 0.0          0.0          0.0          1.000000+03 1.002000+03
2226     5 1.004000+03 1.006000+03 1.008000+03 1.010000+03 1.012000+03
2231     5 1.040000+03 1.060000+03 1.080000+03 1.100000+03 1.150000+03
2236     5 1.200000+03 1.250000+03 1.300000+03 1.400000+03 1.450000+03
2241     5 1.550000+03 1.750000+03 0.0          1.000000+03 1.002000+03
2246     5 1.004000+03 1.006000+03 1.008000+03 1.010000+03 1.012000+03
2251     5 1.040000+03 1.060000+03 1.080000+03 1.100000+03 1.150000+03
2256     5 1.200000+03 1.250000+03 1.300000+03 1.400000+03 1.450000+03
2261     5 1.550000+03 1.750000+03 0.0          0.0          0.0
2461     5 0.0          0.0          9.783500+00 2.130000-10 2.130000-10
2466     5 2.130000-10 2.130000-10 2.130000-10 2.130000-10 2.130000-10
2471     5 2.130000-10 2.130000-10 0.0          0.0          0.0
2501     5 0.0         -2.800000-04-2.800000-04-2.800000-04-2.800000-04
2506    5-2.800000-04-2.800000-04-2.800000-04-2.800000-04-2.800000-04
2536     5 0.0          0.0          0.0          0.0          8.440000+02
2541     5 8.440000+02 8.440000+02 8.440000+02 8.440000+02 8.440000+02
2546     5 8.440000+02 8.440000+02 8.440000+02 0.0          0.0
2576     5 0.0          0.0          6.100000+03 3.000000+03 3.100000+03
2581     5 5.700000+02 3.000000+03 7.430000+02 5.440000+03 5.940000+03
2586     5 5.946000+03 0.0          0.0          0.0          0.0
2616     5 1.210000+02 5.330000+01 9.610000+01 3.110000+02 5.290000+01
2621     5 4.230000+01 1.000000+00 1.000000+00 1.000000+00 0.0
2651     5 0.0          0.0          0.0          5.130000+06 4.620000+06
2656     5 9.000000+06 1.250000+08 6.870000+06 1.552000+07 6.800000+05
2661     5 6.800000+05 6.800000+05 0.0          0.0          0.0
2691     5 0.0          0.0          0.0          1.600000-02 8.600000-01
2696     5 4.550000+00 2.474000+01 1.690000+01 8.880000+00 2.474000+01
2701     5 1.690000+01 8.880000+00 2.172000+01 0.0          0.0
2711     5 0.0          0.0          2.650000+01 2.650000+01 2.650000+01
2716     5 2.650000+01 2.650000+01 2.650000+01 2.505000+01 0.0
2726     5 0.0          0.0          0.0          2.650000+01 2.650000+01
2731     5 2.650000+01 2.650000+01 2.650000+01 2.650000+01 2.365000+01
2736     5 0.0          2.490000-03 2.490000-03 2.490000-03 2.490000-03
```

Fig. A2. SAS4A Input for Case MyP130, Provided by WYLBUR Data Set BO1646.M6P1N1.DATA05 (Contd.)

```
        SAS4A 0.0  FNM .5,1.25X SS PWR.,CORR. RHOCG,TREAT RAD FR,FCF 4.9
                   COOLANT.085,BU 1.727,RET GAS 1.0,TCN 880,TND 855,ALFO 0.260,BOND F..2107
2741     5 2.49000D-03 2.49000D-03 8.72000D-03 0.0         5.59000D-04
2746     5 5.59000D-04 5.59000D-04 5.59000D-04 5.59000D-04 5.59000D-04
2751     5 5.59000D-04 0.0         3.64000D-03 3.64000D-03 3.64000D-03
2756     5 3.64000D-03 3.64000D-03 3.64000D-03 9.07000D-03 0.0
2761     5 4.02000D+06 3.35000D+06 1.80000D+06 4.02000D+06 3.35000D+06
2766     5 1.80000D+06 4.50000D+06 0.0         0.0         0.0
2776     5 0.0         4.95000D+06 4.95000D+06 4.95000D+06 4.95000D+06
2781     5 4.95000D+06 4.95000D+06 4.25000D+06 0.0         0.0
2791     5 0.0         0.0         4.95000D+06 4.95000D+06 4.95000D+06
2796     5 4.95000D+06 4.95000D+06 4.95000D+06 4.69000D+06 0.0
2806     5 0.0         0.0         1.10500D-01 1.76400D-01 2.24300D-01
2811     5 2.21400D-01 1.68800D-01 9.86000D-02 0.0         0.0
2826     5 0.0         0.0         0.0         1.11800D-01 1.75000D-01
2831     5 2.23700D-01 2.20900D-01 1.67500D-01 1.01100D-01 0.0
2841     5 0.0         0.0         1.11800D-01 1.75000D-01 2.23700D-01
2846     5 2.20900D-01 1.67500D-01 1.01100D-01 0.0         0.0
2856     5 0.0         0.0         0.0         0.0         4.12000D-02
2866     5 0.0         0.0         0.0         1.97000D-02 0.0
2871     5 0.0         0.0         0.0         0.0         1.41000D-02
2901     5 0.0         0.0         0.0         0.0         1.00000D+00
2906     5 1.00000D+00 1.00000D+00 1.00000D+00 1.00000D+00 1.00000D+00
2911     5 1.00000D+00 0.0         0.0         0.0         0.0
2921     5 1.58600D+02 1.58600D+02 1.58600D+02 9.51500D+01 9.51500D+01
2926     5 9.51500D+01 2.74630D+02 0.0         1.48700D+01 1.48700D+01
2931     5 1.48700D+01 8.92000D+00 8.92000D+00 8.92000D+00 8.92100D+01
2936     5 0.0         1.00000D+00 1.00000D+00 0.0         0.0
3101     5 0.0         0.0         0.0         0.0         1.05300D+01
3106     5 1.05300D+01 0.0         0.0         0.0         0.0
3271     5 0.0         0.0         0.0         1.00000D+10 0.0
3441     5 1.00000D-03 0.0         0.0         0.0         7.70000D+05
3451     5 0.0         0.0         0.0         0.0         1.00000D+00
3456     5 1.00000D+00 1.00000D+00 1.00000D+00 1.00000D+00 1.00000D+00
3461     5 1.00000D+00 1.00000D+00 1.00000D+00 1.00000D+00 1.00000D+00
3466     5 1.00000D+00 1.00000D+00 1.00000D+00 1.00000D+00 1.00000D+00
3471     5 1.00000D+00 1.00000D+00 1.00000D+00 1.00000D+00 1.00000D+00
3476     5 1.00000D+00 1.00000D+00 1.00000D+00 1.00000D+00 1.00000D+00
3481     5 1.00000D+00 1.00000D+00 1.00000D+00 1.00000D+00 1.00000D+00
3486     5 1.00000D+00 1.00000D+00 1.00000D+00 1.00000D+00 1.00000D+00
3491     5 1.00000D+00 1.00000D+00 1.00000D+00 1.00000D+00 1.00000D+00
3496     5 1.00000D+00 1.00000D+00 1.00000D+00 1.00000D+00 1.00000D+00
3501     5 1.00000D+00 1.00000D+00 1.00000D+00 1.00000D+00 1.00000D+00
3506     5 1.00000D+00 1.00000D+00 1.00000D+00 1.00000D+00 1.00000D+00
3511     5 1.00000D+00 1.00000D+00 1.00000D+00 1.00000D+00 1.00000D+00
3521     5 0.0         0.0         0.0         1.57300D+02 0.0
3531     5 0.0         1.72800D+02 0.0         0.0         0.0
3546     5 0.0         0.0         1.14300D-03 0.0         0.0
3561     5 0.0         0.0         0.0         4.58000D+06 0.0
3571     5 0.0         2.92400D+01 0.0         0.0         0.0
3576     5 0.0         0.0         0.0         0.0         2.92400D+01
3586     5 0.0         0.0         1.00000D+09 0.0         0.0
3596     5 1.00000D+09 0.0         0.0         0.0         0.0
3601     5 0.0         0.0         0.0         1.00000D+00 0.0
3611     5 0.0         0.0         8.31000D+00 1.93700D+01 2.62000D+01
3616     5 0.0         9.60000D+00 0.0         0.0         0.0
3646     5 0.0         0.0         0.0         0.0         1.60000D-02
3651     5 8.60000D-01 4.55000D+00 1.60000D-02 8.60000D-01 4.55000D+00
3931     5 0.0         0.0         0.0         1.12000D+06 2.26000D+02
3936     5 1.97500D+07 0.0         1.00000D+00 2.34700D+01 1.16600D-02
```

Fig. A2. SAS4A Input for Case M6P130, Provided by WYLBUR Data Set B01646.M6P1N1.DATA05 (Contd.)

```
      SAS4A 0.0  FNM .5,1.25X SS PWR.,CORR. RHOCG,TREAT RAD PR,FCF 4.9
                 COOLANT.085,BU 1.727,RET GAS 1.0,TCN 850,TND 855,ALFC 0.260,BOND F..2107
 3941     5 1.588000D-02 5.000000D-02 7.000000D-04 1.952000D+00 2.500000D+03
 3946     5 1.975000D+07 6.537900D+02 6.772100D+02 1.407000D+00 2.422000D+03
 3951     5 2.804000D+06 1.531000D+03 0.0          1.000000D+00 0.0
 3956     5 0.0          0.0          1.000000D+00 9.600000D-01 8.000000D-01
 3971     5 2.500000D-01 2.200000D-01 1.200000D-01 0.0          3.000000D-01
 3976     5 7.000000D-01 8.000000D+00 2.500000D+01 9.000000D+01 0.0
 4231     5 0.0          2.000000D-01 0.0          0.0          0.0
   -1
INPCHN    51     1     0
    1     10     0     0     1     6     1     1     5    21     4     2
   11     10     0     0     0    10     2     5     1     0    31     1
   21     10     1     0     0     0     1     1     0     0     0     0
   31     10     4     0     0     0     0     0     1     1     0     0
   41     10     0     0     0     0     0    12    14     0     0     0
   51     10     1     0     0     0     0     0     0     0     0     0
   71     10     1     0     0     2     0     0     0     0     0     0
   81     10     0     0     0     0     1     8     0     0     0     0
   91     10     0     0     0     0     3     0     0     0     0     0
  111     10     0     0     0     0     0     0     0     1   100     0
  181     10     0     0    24     0     0     0     0     0     2     1
  201     10     0     0     1     0     0     0     0     0     0     0
   -1
GEOMIN    61     1     0
    1      5 3.000000D-05 2.299600D-05 2.299600D-05 2.299600D-05 0.0
    6      5 0.0          0.0          2.307000D-02 2.307000D-02 2.307000D-02
   11      5 2.307000D-02 2.307000D-02 2.307000D-02 2.307000D-02 2.307000D-02
   16      5 2.307000D-02 2.307000D-02 2.307000D-02 2.307000D-02 2.307000D-02
   21      5 2.307000D-02 2.307000D-02 0.0          0.0          0.0
   31      5 0.0          1.000000D-01 3.229150D-03 3.229150D-03 3.229150D-03
   36      5 0.0          0.0          0.0          2.370000D-02 4.691610D-03
   41      5 4.691610D-03 4.691610D-03 0.0          0.0          0.0
   46      5 1.000000D-05 1.000000D-05 1.000000D-05 1.000000D-05 0.0
   51      5 0.0          0.0          2.490000D-01 2.510000D-03 0.0
   76      5 0.0          0.0          2.920000D-03 0.0          0.0
  101      5 0.0          2.540000D-03 2.920000D-03 1.000000D-06 1.000000D-06
  106      5 1.000000D-06 1.000000D-06 1.000000D-06 1.000000D-06 1.000000D-06
  111      5 1.000000D-06 1.000000D-06 1.000000D-06 1.000000D-06 1.000000D-06
  116      5 1.000000D-06 1.000000D-06 1.000000D-06 1.000000D-06 1.000000D-06
  121      5 1.000000D-06 1.000000D-06 1.000000D-06 1.000000D-06 1.000000D-06
  126      5 1.000000D-06 1.000000D-06 2.160000D-03 0.0          0.0
  151      5 0.0          1.587500D+00 3.810000D-01 2.317750D+00 8.310500D-01
  156      5 0.0          0.0          0.0          1.200000D-03 1.822300D-03
  161      5 1.822830D-03 1.822830D-03 0.0          0.0          0.0
  166      5 6.415330D-05 0.0          0.0          1.000000D-05 1.649600D-03
  171      5 5.588000D-04 1.622700D-03 0.0          0.0          0.0
  176      5 0.0          0.0          0.0          0.0          2.540000D-03
  181      5 2.920000D-03 1.000000D-05 2.274200D-02 2.274200D-02 2.274200D-02
  186      5 0.0          0.0          0.0          1.000000D-05 1.000000D-05
  191      5 1.000000D-05 1.000000D-05 0.0          0.0          0.0
   -1
POWINC    62     1     0
    1      5 0.0          7.800000D-03 0.0          4.800000D-03 1.140000D-02
    6      5 6.607000D-01 7.457000D-01 8.283000D-01 8.959000D-01 9.444000D-01
   11      5 9.760000D-01 9.940000D-01 1.000000D+00 9.940000D-01 9.760000D-01
   16      5 9.444000D-01 8.959000D-01 8.283000D-01 7.457000D-01 6.607000D-01
   26      5 0.0          0.0          0.0          0.0          6.200000D-01
   31      5 6.600000D-01 7.100000D-01 7.900000D-01 8.300000D-01 9.600000D-01
   36      5 1.040000D+00 1.230000D+00 1.500000D+00 1.750000D+00 1.000000D+00
```

Fig. A2. SAS4A Input for Case M6P130, Provided by WYLBUR Data Set B01646.M6P1N1.DATA05 (Contd.)

```
      SAS4A 0.0  FNM .5,1.25X SS PWR.,CORR. RHOCG,TREAT RAD PR,PCF 4.9
                 COOLANT.085,BU 1.727,RET GAS 1.0,TCM 830,TMO 855,ALFC 0.260,BOND F..2107
   41     5 0.0          0.0           0.0           0.0           1.000000D+00
   46     5 1.000000D+00 0.0           0.0           0.0           0.0
   51     5 0.0          0.0           8.640000D+02 4.200000D+02 0.0
   61     5 1.000000D+15-1.199930D-04-7.830540D-05 0.0           0.0
   66     5 5.390540D-02 4.549030D-02 4.520720D-02 4.771270D-02 4.939640D-02
   71     5 5.321340D-02 5.627730D-02 5.886490D-02 5.973220D-02 6.027350D-02
   76     5 5.994730D-02 5.815000D-02 5.643990D-02 5.353301D-02 4.927940D-02
   81     5 4.402730D-02 4.119050D-02 3.674510D-02 3.373070D-02 3.540100D-02
  111     5 0.0          2.833660D-06 2.113550D-06 6.134030D-06 1.847460D-05
  116     5 3.087060D-05 4.324720D-05 5.495000D-05 6.511810D-05 7.301000D-05
  121     5 8.059410D-05 8.514500D-05 8.707740D-05 8.639940D-05 8.319460D-05
  126     5 7.733320D-05 6.945710D-05 5.991270D-05 4.918370D-05 3.717310D-05
  131     5 2.475380D-05 1.249650D-05-2.816250D-08-4.036650D-06-2.402260D-06
  156     5 0.0          0.0           0.0           0.0           6.886110D-07
  161     5 1.642550D-06-5.541510D-07-5.124170D-06-9.592100D-06-1.393600D-05
  166     5-1.788170D-05-2.131800D-05-2.426560D-05-2.655330D-05-2.804400D-05
  171     5-2.867910D-05-2.844610D-05-2.735920D-05-2.544060D-05-2.276070D-05
  176     5-1.951500D-05-1.586840D-05-1.179450D-05-7.408210D-06-2.966550D-06
  181     5 1.713470D-06 3.909680D-06 2.533010D-06 0.0           0.0
  206     5 0.0          0.0           2.166390D-05 2.770940D-05 3.554880D-05
  211     5 4.305970D-05 5.101530D-05 5.890310D-05 6.214100D-05 6.845330D-05
  216     5 7.377260D-05 7.785280D-05 7.877920D-05 7.909760D-05 7.947970D-05
  221     5 7.754360D-05 7.622490D-05 7.142640D-05 6.549720D-05 5.871200D-05
  226     5 5.519120D-05 4.712390D-05 3.921540D-05 3.207720D-05 2.437450D-05
  231     5 1.765010D-05 0.0           0.0           0.0           0.0
  256     5 1.695940D+00 0.0           0.0           0.0           0.0
   -1
PMATCH    63     1     0
    1     5 0.0          0.0           0.0           0.0           1.000000D+06
    6     5 1.000000D+06 3.000000D-02 0.0           0.0           0.0
   11     5 2.700000D+01 2.700000D+01 2.700000D+01 2.700000D+01 0.0
   16     5 0.0          0.0           2.700000D+01 2.700000D+01 2.700000D+01
   21     5 2.700000D+01 0.0           0.0           0.0           4.810000D-05
   26     5 1.000000D-05 1.013250D+05 2.700000D+01 2.700000D+01 2.700000D+01
   31     5 2.700000D+01 0.0           0.0           0.0           7.760000D+03
   36     5 8.500000D+02 5.500000D+06 5.500000D+06 5.500000D+06 5.500000D+06
   41     5 0.0          0.0           0.0           5.500000D+06 5.500000D+06
   46     5 5.500000D+06 5.500000D+06 0.0           0.0           0.0
   51     5 5.500000D+06 5.500000D+06 5.500000D+06 5.500000D+06 0.0
   56     5 0.0          0.0           6.530000D+03 3.000000D-02 0.0
   61     5 0.0          0.0           0.0           8.000000D-01 1.000000D+00
   66     5 0.0          0.0           0.0           1.000000D-08 1.000000D-08
   71     5 2.000000D-03 1.580000D+04 1.800000D-05 1.400000D-05 1.050000D+11
   76     5 1.900000D+11 0.0           0.0           1.000000D+00 8.550000D+02
   81     5 8.800000D+02 0.0           0.0           0.0           0.0
   86     5 0.0          0.0           0.0           0.0           2.600000D-01
   91     5 1.900000D-01 4.000000D-01 2.000000D-01 2.000000D-01 2.000000D-01
   96     5 2.000000D-01 2.000000D-01 2.000000D-01 2.000000D-01 2.000000D-01
  101     5 2.000000D-01 2.000000D-01 2.000000D-01 0.0           0.0
   -1
COOLIN    64     1     0
    1     5 0.0          0.0           1.440000D-02 8.600000D-01 4.480000D+00
    6     5 0.0          0.0           6.400000D+01 0.0           0.0
   46     5 0.0          8.500000D-02 1.836000D+01 0.0           0.0
   56     5 1.836000D+01 0.0           0.0           0.0           0.0
   61     5 0.0          0.0           0.0           0.0           1.860000D+00
   66     5 7.160000D+00 5.000000D-01 5.000000D-01 1.500000D+01 5.000000D+01
   71     5 1.000000D-01 6.300000D+04 2.000000D-02 0.0           1.000000D-04
```

Fig. A2. SAS4A Input for Case M6P130, Provided by WYLBUR Data Set BO1646.M6P1N1.DATA05 (Contd.)

```
          SAS4A 0.0  FNM .5,1.25X SS PWR.,CORR. RHOCG,TREAT RAD FR,FCF 4.9
                     COOLANT.CC5,EU 1.727,RET GAS 1.0,TCH 880,TMO 855,ALFO 0.260,DOND F..2107
      76     5 1.000000D-04 1.500000D-04 0.0          0.0          0.0
      81     5 0.0          0.0          0.0          1.500000D-04 0.0
     161     5 0.0          0.0          0.0          5.000000D+00 1.000000D+01
     171     5 1.000000D-06 1.000000D-07 1.000000D-07 0.0          0.0
     176     5 0.0          1.000000D-06 1.000000D-05 0.0          0.0
      -1
  FUELIN    65     1     0
       1     5 0.0          2.000000D-01 0.0          0.0          0.0
      21     5 0.0          1.100000D+00 5.000000D-01 1.530000D+04 7.100000D-01
      26     5 1.900000D-01 1.000000D-01 0.0          0.0          0.0
      51     5 0.0          0.0          0.0          1.727000D+00 2.107000D-01
      56     5 0.0          0.0          1.353000D+03 0.0          0.0
      61     5 1.000000D+00 0.0          0.0          0.0          0.0
     126     5 0.0          0.0          0.0          1.000000D+00 1.000000D+00
     131     5 6.500000D-01 6.000000D-01 5.500000D-01 5.000000D-01 4.500000D-01
     136     5 4.000000D-01 3.500000D-01 3.000000D-01 2.500000D-01 2.000000D-01
     141     5 1.500000D-01 1.000000D-01 1.200000D-01 1.400000D-01 1.600000D-01
     146     5 1.800000D-01 2.000000D-01 2.200000D-01 2.400000D-01 2.600000D-01
     151     5 1.000000D+00 1.000000D+00 0.0          0.0          0.0
      -1
  ENDJOB    -1

FUEL MELTING POINT IS NOT IN THE DENSITY TABLE.

FUEL MELTING POINT IS NOT IN THE DENSITY TABLE.

FUEL MELTING POINT IS NOT IN THE DENSITY TABLE.

FUEL MELTING POINT IS NOT IN THE DENSITY TABLE.

FUEL MELTING POINT IS NOT IN THE DENSITY TABLE.
```

Fig. A2. SAS4A Input for Case M6P130, Provided by WYLBUR Data Set BO1646.M6P1N1.DATA05 (Contd.)

Fig. A3. EXTRUS Steady-State Output Edit for Case M6P130

```
SAS4A 0.0  FNM .5,1.25X SS PWR.,CORR. RHOCG,TREAT RAD PR,PCF 4.9                    5/04/87  19.49.25  PAGE  32
                COOLANT.085,BU 1.727,RET GAS 1.0,TCM 880,TMO 855,ALFO 0.260,BOND F..2107
    1    1 0.21933D-02 0.39204D+05 0.81499D-01 0.17875D-03
    1    1 0.16650D-02 0.54332D-02 0.10000D+01 0.23839D-01 0.0
7.67342D+02 7.57121D+02 7.44327D+02 7.30650D+02 7.16098D+02 7.00736D+02 6.84206D+02 6.66419D+02 6.46940D+02 6.25320D+02
1.00571D-06 5.87207D-04 1.01707D-03 1.31303D-03 1.55360D-03 1.76162D-03 1.94754D-03 2.11720D-03 2.27424D-03 2.42111D-03
2.49130D-03 2.54000D-03
    1    1 0.71338D-06 0.71338D-06 0.83327D-05
3.96324D-08 7.92649D-08 7.92649D-08 7.92649D-08 7.92649D-08 7.92649D-08 7.92649D-08 7.92649D-08 7.92649D-08 3.96324D-08
3.01846D-04 6.03693D-04 6.03693D-04 6.03693D-04 6.03693D-04 6.03693D-04 6.03693D-04 6.03693D-04 6.03693D-04 3.01846D-04
    1    2 0.18788D-02 0.54332D-02 0.10000D+01 0.47684D-01 0.23839D-01
7.93696D+02 7.82502D+02 7.68472D+02 7.53461D+02 7.37478D+02 7.20588D+02 7.02394D+02 6.82789D+02 6.61287D+02 6.37371D+02
1.00592D-06 5.87329D-04 1.01728D-03 1.31331D-03 1.55392D-03 1.76198D-03 1.94795D-03 2.11764D-03 2.27471D-03 2.42162D-03
2.49182D-03 2.54000D-03
    1    2 0.71338D-06 0.71338D-06 0.94944D-05
3.96324D-08 7.92649D-08 7.92649D-08 7.92649D-08 7.92649D-08 7.92649D-08 7.92649D-08 7.92649D-08 7.92649D-08 3.96324D-08
3.01846D-04 6.03693D-04 6.03693D-04 6.03693D-04 6.03693D-04 6.03693D-04 6.03693D-04 6.03693D-04 6.03693D-04 3.01846D-04


    1   14 0.18724D-02 0.54332D-02 0.10000D+00 0.33462D+00 0.31069D+00
8.85868D+02 8.78404D+02 8.68299D+02 8.54196D+02 8.38359D+02 8.22280D+02 8.05274D+02 7.87417D+02 7.68213D+02 7.47268D+02
1.01208D-06 6.57141D-04 1.03346D-03 1.30524D-03 1.54884D-03 1.75887D-03 1.94623D-03 2.11694D-03 2.27473D-03 2.42214D-03
2.49250D-03 2.54000D-03
    1   14 0.71338D-06 0.71338D-06 0.94600D-05
3.02163D-08 9.09293D-08 9.09293D-08 7.71244D-08 7.71244D-08 7.71244D-08 7.71244D-08 7.71244D-08 7.71244D-08 3.85622D-08
2.30132D-04 6.92531D-04 6.92531D-04 5.87391D-04 5.87391D-04 5.87391D-04 5.87391D-04 5.87391D-04 5.87391D-04 2.93695D-04
    1   15 0.16592D-02 0.54332D-02 0.12000D+00 0.35854D+00 0.33462D+00
8.85650D+02 8.76218D+02 8.61911D+02 8.47193D+02 8.32527D+02 8.17653D+02 8.02119D+02 7.85791D+02 7.68280D+02 7.49235D+02
1.01098D-06 5.64699D-04 9.77091D-04 1.28465D-03 1.53151D-03 1.74362D-03 1.93245D-03 2.10428D-03 2.26297D-03 2.41111D-03
2.48180D-03 2.54000D-03
    1   15 0.71338D-06 0.71338D-06 0.83015D-05
4.54561D-08 9.09123D-08 7.69354D-08 7.69354D-08 7.69354D-08 7.69354D-08 7.69354D-08 7.69354D-08 7.69354D-08 3.84677D-08
3.46201D-04 6.92401D-04 5.85951D-04 5.85951D-04 5.85951D-04 5.85951D-04 5.85951D-04 5.85951D-04 5.85951D-04 2.92976D-04
    1    1 0.10701D-04 0.16803D-03 0.59870D-01 0.94013D+00 0.17873D-03
    1    1 0.25955D+03 0.10637D-02
1.56778D+04 1.56862D+04 1.56967D+04 1.57079D+04 1.57199D+04 1.57326D+04 1.57462D+04 1.57609D+04 1.57771D+04 1.57950D+04
9.84782D-01 9.85011D-01 9.85297D-01 9.85601D-01 9.85923D-01 9.86261D-01 9.86622D-01 9.87009D-01 9.87430D-01 9.87894D-01
1.52179D-02 1.49887D-02 1.47031D-02 1.43991D-02 1.40773D-02 1.37393D-02 1.33776D-02 1.29907D-02 1.25696D-02 1.21056D-02
6.01564D-09 1.20525D-08 1.20790D-08 1.21074D-08 1.21375D-08 1.21693D-08 1.22035D-08 1.22403D-08 1.22805D-08 6.16260D-09
9.15452D-11 1.80652D-10 1.77599D-10 1.74335D-10 1.70863D-10 1.67198D-10 1.63254D-10 1.59010D-10 1.54362D-10 7.46017D-11
    1    1 0.75752D-13 0.10945D-06 0.10793D-06 0.15134D-08
5.92410D-09 1.18718D-08 1.19014D-08 1.19330D-08 1.19666D-08 1.20021D-08 1.20403D-08 1.20813D-08 1.21262D-08 6.08799D-09
    1    1 0.19662D-10 0.10288D+01
1.53762D-06 3.08138D-06 3.08906D-06 3.09727D-06 3.10599D-06 3.11520D-06 3.12510D-06 3.13575D-06 3.14740D-06 1.58016D-06
1.56562D+04 1.56653D+04 1.56769D+04 1.56892D+04 1.57023D+04 1.57162D+04 1.57312D+04 1.57474D+04 1.57652D+04 1.57850D+04
9.84040D-01 9.84296D-01 9.84616D-01 9.84956D-01 9.85316D-01 9.85694D-01 9.86099D-01 9.86532D-01 9.87004D-01 9.87525D-01
1.59597D-02 1.57038D-02 1.53844D-02 1.50444D-02 1.46844D-02 1.43062D-02 1.39013D-02 1.34678D-02 1.29957D-02 1.24748D-02
5.93301D-09 1.18893D-08 1.19126D-08 1.19498D-08 1.19831D-08 1.20182D-08 1.20560D-08 1.20967D-08 1.21413D-08 6.09546D-09
9.46893D-11 1.86707D-10 1.83360D-10 1.79778D-10 1.75965D-10 1.71935D-10 1.67593D-10 1.62916D-10 1.57785D-10 7.60394D-11
    1    2 0.75799D-13 0.10808D-06 0.10652D-06 0.15568D-08
5.83833D-09 1.17026D-08 1.17352D-08 1.17700D-08 1.18071D-08 1.18463D-08 1.18884D-08 1.19338D-08 1.19835D-08 6.01942D-09
    1    2 0.19674D-10 0.10325D+01
1.51536D-06 3.03747D-06 3.04592D-06 3.05497D-06 3.06458D-06 3.07475D-06 3.08569D-06 3.09747D-06 3.11038D-06 1.56237D-06
```

Fig. A3. EXTRUS Steady-State Output Edit for Case M6P130

```
 1.18395D+04 1.78557D+04 1.78902D+04 1.51053D+04 1.51979D+04 1.52107D+04 1.52242D+04 1.52334D+04 1.52538D+04 1.52705D+04
 9.93496D-01 9.69077D-01 9.69563D-01 9.83903D-01 9.84194D-01 9.84490D-01 9.84800D-01 9.85126D-01 9.85478D-01 9.85860D-01
 6.50356D-03 3.09229D-02 3.04367D-02 1.60263D-02 1.58053D-02 1.55999D-02 1.52001D-02 1.48735D-02 1.45223D-02 1.41399D-02
 1.23395D-03 7.77524D-09 7.80357D-09 1.23193D-03 1.23140D-03 1.23072D-03 1.22994D-03 1.22907D-03 1.22810D-03 6.13463D-09
 8.05761D-11 2.40433D-10 2.37667D-10 1.98312D-10 1.94634D-10 1.90034D-10 1.85952D-10 1.82307D-10 1.78349D-10 8.67429D-11
   1  14 0.76909D-13 0.10792D-06 0.10614D-06 0.17774D-03
 1.23090D-03 7.53481D-09 7.57091D-09 1.21215D-03 1.21194D-03 1.21163D-03 1.21125D-03 1.21079D-03 1.21026D-03 6.04789D-09
   1  14 0.19983D-10 0.10324D+01
 3.19434D-06 1.95569D-06 1.96506D-06 3.14619D-06 3.14564D-06 3.14485D-06 3.14335D-06 3.14266D-06 3.14129D-06 1.56976D-06
 1.73120D+04 1.70645D+04 1.51419D+04 1.51533D+04 1.51652D+04 1.51770D+04 1.51894D+04 1.52023D+04 1.52163D+04 1.52315D+04
 9.69475D-01 9.69690D-01 9.83992D-01 9.84262D-01 9.84524D-01 9.84791D-01 9.85070D-01 9.85363D-01 9.85679D-01 9.86021D-01
 3.05246D-02 3.03100D-02 1.60034D-02 1.57333D-02 1.54756D-02 1.52089D-02 1.49301D-02 1.46356D-02 1.43214D-02 1.39788D-02
 3.97009D-09 7.91125D-09 1.24691D-08 1.24666D-08 1.24537D-08 1.24507D-08 1.24422D-08 1.24334D-08 1.24238D-08 6.20639D-09
 1.21185D-10 2.39790D-10 1.99611D-10 1.96202D-10 1.92806D-10 1.89361D-10 1.85764D-10 1.81982D-10 1.77927D-10 8.67581D-11
   1  15 0.76813D-13 0.10523D-06 0.10346D-06 0.17714D-08
 3.84890D-09 7.67146D-09 1.22695D-08 1.22704D-08 1.22659D-08 1.22613D-08 1.22565D-08 1.22514D-08 1.22459D-08 6.11963D-09
   1  15 0.19937D-10 0.10287D+01
 9.98992D-07 1.99116D-06 3.18461D-06 3.18482D-06 3.18366D-06 3.18247D-06 3.18122D-06 3.17990D-06 3.17848D-06 1.58838D-06
   1   1 0.16380D-05 0.16124D-05 0.25572D-07 0.98439D+00 0.15612D-01
```

Fig. A4. Transient Output Edit for EXTRUS Case M6P130 at 13.2996 sec.

```
A  3.05934D+06 2.29531D-04 1.16529D+03 3.76756D-06 9.95877D-07 1.62504D+03 7.54839D-07 1.26408D+03 2.25497D-04 3.65202D-02
   4.49783D-02 2.02443D-04 1.53115D-06 3.12710D-07 3.15297D-06 4.98600D-06 2.55602D-06 3.98927D-07 6.68275D-01 5.96950D-07
   9.11917D-05 1.06371D-03 1.89330D-01 2.34816D-01 3.15297D-06 2.41260D-06
   1.00000D-10 0.0         0.0         0.0         0.0         5.43323D-03 0.0         9.04607D-06 2.16689D-05
   1.00000D-10 0.0         0.0         0.0         0.0         5.43323D-03 0.0         1.02077D-05 2.77094D-05
   1.00000D-10 0.0         0.0         0.0         0.0         5.43323D-03 0.0         1.13359D-05 3.55480D-05
   8.68850D-08 5.34352D-06 1.49750D+03 7.76227D-08 6.10692D-08 4.52770D-03 9.05539D-04 1.22584D-05 4.30597D-05
   1.45909D-07 8.60185D-06 1.55231D+03 1.28361D-07 1.02104D-07 3.88894D-03 1.54429D-03 1.28953D-05 5.10153D-05
   2.13050D-07 1.33485D-05 1.55746D+03 1.84992D-07 1.43007D-07 3.29698D-03 2.13526D-03 1.33190D-05 5.89031D-05
   2.64506D-07 1.57072D-05 1.60042D+03 2.32432D-07 1.84331D-07 2.64326D-03 2.78998D-03 1.35657D-05 6.21410D-05
B  2.93163D-07 2.00778D-05 1.53371D+03 2.49510D-07 1.84137D-07 2.75133D-03 2.68190D-03 1.36435D-05 6.84533D-05
   3.53161D-07 2.37821D-05 1.59704D+03 3.01942D-07 2.25299D-07 2.13992D-03 3.29331D-03 1.35585D-05 7.37726D-05
   3.23833D-07 1.92455D-05 1.68271D+03 2.84797D-07 2.26377D-07 2.05537D-03 3.37737D-03 1.33157D-05 7.78528D-05
   3.83539D-07 2.29658D-05 1.67224D+03 3.37000D-07 2.67359D-07 1.46048D-03 3.96476D-03 1.28834D-05 7.87792D-05
   3.83424D-07 2.31125D-05 1.67737D+03 3.36963D-07 2.67440D-07 1.46048D-03 3.96476D-03 1.22217D-05 7.98976D-05
   4.05139D-07 2.67757D-05 1.63431D+03 3.49734D-07 2.66026D-07 1.50426D-03 3.92397D-03 1.12954D-05 7.94797D-05
   3.83642D-07 2.36609D-05 1.63678D+03 3.36834D-07 2.66790D-07 1.46042D-03 3.96476D-03 1.01733D-05 7.75436D-05
   3.77099D-07 2.28753D-05 1.61791D+03 3.32776D-07 2.66451D-07 1.46400D-03 3.96836D-03 9.01435D-06 7.62249D-05
C  REAC DEBUG     1 0.46574D-05 0.46226D-06 0.49554D-05 0.49554D-05-0.29796D-06 0.15000D+00 0.99579D-01 0.99579D-01
   ********PIN FAIL DATA   1    1 0.0          7.17145D+02 1.56825D-14 3.70565D-13 7.81907D+02 3.79424D-12 2.54000D-03 2.92000D-03
    1.77096D+07 3.00352D-02 2.21370D+07 2.31452D+11 1.72952D-14 7.86336D+02 7.77445D+02 9.95791D-02 1.50000D-01 1.33500D+01
   ********PIN FAIL DATA   1    2 0.0          7.67060D+02 4.13473D-13 8.01450D-12 8.39593D+02 4.29927D-11 2.54000D-03 2.92000D-03
    1.77096D+07 3.47779D-02 2.21370D+07 2.26313D+11 5.21423D-13 8.44635D+02 8.34560D+02 9.95791D-02 1.50000D-01 1.33500D+01
   ********PIN FAIL DATA   1    3 3.94506D-02 8.20215D+02 9.23425D-12 1.47852D-10 3.99754D+02 3.87903D-10 2.54000D-03 2.92000D-03
    1.77096D+07 4.14151D-02 2.21370D+07 2.20341D+11 1.25754D-11 9.05310D+02 8.94190D+02 9.95791D-02 1.50000D-01 1.33500D+01
   ********PIN FAIL DATA   1    4 1.32651D-01 8.74657D+02 1.52461D-10 2.01492D-09 9.59647D+02 2.63573D-09 2.54000D-03 2.92000D-03
    1.77097D+07 4.99664D-02 2.21371D+07 2.15237D+11 2.22019D-10 9.65536D+02 9.53657D+02 9.95791D-02 1.50000D-01 1.33500D+01
   ********PIN FAIL DATA   1    5 2.30361D-01 9.27379D+02 1.75130D-09 1.94833D-08 1.01518D+03 1.27286D-08 2.54001D-03 2.92000D-03
    1.77101D+07 5.99328D-02 2.21376D+07 2.09809D+11 2.62633D-09 1.02141D+03 1.00395D+03 9.95791D-02 1.50000D-01 1.33500D+01
   ********PIN FAIL DATA   1    6 3.56991D-01 9.80021D+02 1.54242D-08 1.45752D-07 1.06974D+03 5.09858D-08 2.54005D-03 2.92000D-03
    1.77116D+07 7.15556D-02 2.21395D+07 2.04390D+11 2.40135D-08 1.07612D+03 1.06335D+03 9.95791D-02 1.50000D-01 1.33500D+01
   ********PIN FAIL DATA   1    7 4.39096D-01 1.03345D+03 1.07186D-07 8.66746D-07 1.12518D+03 1.82011D-07 2.54015D-03 2.92000D-03
    1.77161D+07 8.50455D-02 2.21451D+07 1.92889D+11 1.82401D-07 1.13131D+03 1.11856D+03 9.95791D-02 1.50000D-01 1.33500D+01
D  ********PIN FAIL DATA   1    8 4.80812D-01 1.08162D+03 5.89637D-07 4.13156D-06 1.17135D+03 4.79031D-07 2.54041D-03 2.92000D-03
    1.77278D+07 9.26703D-02 2.21590D+07 1.93930D+11 9.66413D-07 1.17775D+03 1.16496D+03 9.95791D-02 1.50000D-01 1.33500D+01
   ********PIN FAIL DATA   1    9 5.53754D-01 1.12936D+03 2.67682D-06 1.63634D-05 1.21305D+03 1.18312D-06 2.54101D-03 2.92001D-03
    1.77539D+07 1.13707D-01 2.21922D+07 1.83964D+11 4.50523D-06 1.22433D+03 1.21172D+03 9.95791D-02 1.50000D-01 1.33500D+01
   ********PIN FAIL DATA   1   10 6.81057D-01 1.17532D+03 3.15442D-06 5.41373D-05 1.26218D+03 2.61431D-06 2.54215D-03 2.92001D-03
    1.78040D+07 1.13707D-01 2.21922D+07 1.83964D+11 2.55312D-03 1.24859D+03 1.25576D+03 9.95791D-02 1.50000D-01 1.33500D+01
   ********PIN FAIL DATA   1   11 7.10572D-01 1.21818D+03 2.60092D-06 1.48973D-04 1.30169D+03 5.08033D-06 2.54399D-03 2.92001D-03
    1.78237D+07 1.13707D-01 2.21922D+07 1.83964D+11 1.28332D-07 1.30791D+03 1.29547D+03 9.95791D-02 1.50000D-01 1.33500D+01
   ********PIN FAIL DATA   1   12 7.49317D-01 1.25931D+03 2.09672D-06 3.32230D-04 1.32793D+03 7.72696D-06 2.54631D-03 2.92001D-03
    1.78380D+07 1.13707D-01 2.21922D+07 1.83964D+11 4.21551D-07 1.33372D+03 1.32208D+03 9.95791D-02 1.50000D-01 1.33500D+01
   ********PIN FAIL DATA   1   13 7.35319D-01 1.27965D+03 2.03489D-06 5.95240D-04 1.34614D+03 1.02333D-05 2.54840D-03 2.92001D-03
    1.78037D+07 1.13707D-01 2.21922D+07 1.83964D+11 1.09331D-06 1.35133D+03 1.34095D+03 9.95791D-02 1.50000D-01 1.33500D+01
   ********PIN FAIL DATA   1   14 7.33577D-01 1.28732D+03 4.62740D-06 1.28499D-03 1.35231D+03 7.53259D-06 2.63983D-03 2.92001D-03
    2.43502D+07 1.13707D-01 2.21922D+07 1.83964D+11 9.25037D-06 1.35143D+03 1.32112D+03 9.95791D-02 1.50000D-01 1.33500D+01
   ********PIN FAIL DATA   1   15 7.05434D-01 1.30355D+03 6.09402D-06 1.90818D-03 1.33614D+03 8.78248D-06 2.65353D-03 2.92002D-03
    2.62385D+07 1.13707D-01 2.21922D+07 1.83964D+11 2.24030D-05 1.34036D+03 1.33151D+03 9.95791D-02 1.50000D-01 1.33500D+01
   FEEDBACK PR    1-0.29796D-06 0.0          0.49554D-05 0.0          0.13530D+04-0.29796D-06-0.29796D-06
```

.....		TOTAL TIME	TIME STEP	NORMALIZED VALUES TOTAL POWER	DECAY POWER	TOTAL ENERGY	NET	PROGRAM	** REACTIVITIES ($) ** RADIAL SCRAM	EXPAN.	DOPPLER	DENSITY	TOTAL COOLANT	TOTAL FUEL MOTION	TOTAL CLADDING MOTION
	STEP	(SEC)	(SEC)												
SHORT	89	13.2996	0.09958	4.776	0.0	3.040D+01	-0.0143	0.0	0.0	0.0	-0.0147	0.0	0.0000	-0.0001	0.0

TABLE A1. Key to EXTRUS Steady-State Output Edit

NOTE: Items 1, 8, 9, and 19 are given once for each channel. Items 2-7 and 10-18 are given for each channel and each axial node. S1 units are used except as noted.

1. ch. no.; ch. no.; mass fission gas/mass fuel for given BU; avg. linear power, w/m; total fuel mass in pin.
2. ch. no.; ax. node; mass fission gas/mass fuel in ax. node; fuel mass in ax. node; retained gas fr. in ax. node.
3. fuel temp. for each rad. node of ax. node.
4. rad. fuel mesh for ax. node.
5. ch. no.; ax. node no.; total retained gas in ax. node; total retained gas mass in ax. node; total released gas mass in ax. node.
6. retained gas mass in each rad. node of ax. node.
7. fuel mass in each rad. node of ax. node.
8. ch. no.; ch. no.; total retained gas mass in pin;
9. ch. no.; ch. no.; gas density in gm-mols/m^3 in plenum and fuel open porosity (fill gas + fission gas); gm-mols gas in plenum.
10. theoretical density of fuel for each rad. node in ax. node.
11. open porosity fract. of total porosity by rad. node.
12. closed porosity fract. of total porosity by rad. node.
13. total porosity vol. for each rad. node in ax. node.
14. closed porosity vol. for each rad. node in ax. node.
15. ch. no.; ax. node no.; vol. of central hole; total porosity vol. in ax. node.; open porosity vol. in ax. node; closed porosity vol. in ax. node.
16. open porosity vol. for each rad. node in ax. node.
17. ch. no.; ax. node no; gm mols gas in central hole; swelling factor for solid fission products.
18. gm. mols free gas in each rad. node of ax. node.
19. ch. no.; ch. no.; total porosity vol. in pin; total open porosity vol. in pin; total closed fract. in pin; closed porosity fract. of total.

NOTE: the third items in 15 and 17 are meaningless as there is no central hole in this case. The fourth item in 17 is the factor by which the fabricated fuel volume is multiplied to account for solid fission product swelling.

TABLE A2. Key to EXTRUS Transient Output Edit

Transient Data A for Each Channel:

1.	equilibrated pressure (Pa)	PEQUIL
2.	gm-mols gas in solid fuel	SØLFGM
3.	plenum gas temp.	TGASP2
4.	vol. available for gas in plenum	PGSVØL
5.	vol. of gas in cavity after equil.	CAVFGV
6.	cavity temp.	TCAVVL
7.	ol. of gas in solid fuel	SØLFGV
8.	temp. solid fuel	TSØLVL
9.	gm-mols gas in cavity	CAVFGM
10.	fuel mass in cavity	CAVFMS
11.	fuel mass in solid fuel	SØLFMS
12.	gm-mols fill gas	HEMØLE
13.	vol. of Na bond	SØDVØL
14.	vol. of gap	GAPVØL
15.	vol. of cavity before equil.	CAVVL
16.	vol. of gas plenum in fresh pin	VFGPLN
17.	vol. of fuel in cavity	CAVFVL
18.	difference in cavity vol. before and after equil.	EXVØL
19.	ratio of (new-old) gas cavity vol. to old.	EXVØLR
20.	cavity gas vol. before equil.	CAVFGØ
21.	total released gas in current solid fuel	SØLFGO
22.	gm mols gas in plenum	PLNGGS(ICH)
23.	porosity fract. in current cavity cells before equil.	CAVPRT
24.	porosity fract. in steady state of the cells currently in cavity	CAVPRZ
25.	vol. of cells in steady state of cells currently in cavity	CAVVLS
26.	vol. of fuel in steady state of cells currently in cavity	CAVVLS

Transient Data B for Each Channel and for Each Axial Node

1.	vol. of cavity portion of cell after equilibration	EXVØLN
2.	moles of gas in cell in cavity portion	FGMASN
3.	temp. of cavity portion	TFUMSN
4.	vol. of cavity portion before equilibration	CAVVLN
5.	vol. of fuel in cavity portion	FUMVLN
6.	mass of fuel in solid portion	FUSMSN
7.	mass of fuel in cavity portion	FUMMSN

TABLE A2. Key to EXTRUS Transient Output Edit (Contd.)

8.	total gas produced in this axial node	BURNDN
9.	fuel worth Δk/kg	FUELRA(J)
	Transient Data C for Each Channel, "REAC DEBUG":	
1.	chan. no.	ICH
2.	current fuel worth on expanded meshΔk/kg	RYFU
3.	not used	
4.	current worth of unextruded fuel on a thermally expanded mesh Δk/kg	RYFUE
5.	original fuel worth at steady state Δk/kg	DFUELI(2)
6.	fuel feedback for this channel neglecting effect of axial expansion Δk/kg	DFUELI(5)
7.	initial and max time step sec	DTO
8.	heat tran time step sec	DTIME
9.	PRIMAR time step sec	DTPRI

Transient Data D for Each Channel and Each Axial Node, "PIN FAIL DATA":

1.	chan. no	ICH
2.	axial node	J
3.	fuel melt fact.	FRAC(J)
4.	clad mid-wall temp.	T2(NE,J)
5.	total of current fractional plastic strain	DFUELI(50+J)
6.	damage parameter sum	DFUELI(25+J)
7.	avg. of outer fuel and inner clad temp.	TINF
8.	eutectic penetration rate M/S	EURATE
9.	inner clad rad (M)	R(NE,J)
10.	outer clad rad (M)	R(NEP,J)
11.	σT	SIGTRU
12.	Ec (from fit in Ref. A1) E_c	ECLLAD
13.	∂s	SIGSAT
14.	Young's mod. for clad.	YNGCLD
15.	strain rate s^{-1}	STRATE
16.	outer fuel temp.	T2(NT,J)
17.	inner clad temp.	T2(NEPP,J)
18.	DEFORM time step	DTP
19.	current DEFORM time step	DT
20.	current accumulated time = Σ(DT)	DFUELI(6)